Escape

An optimization method based on crowd evacuation behaviors

Kaichen OuYang[a], Shengwei Fu[b], Yi Chen[c], Qifeng Cai[d], Ali Asghar Heidari[e], Huiling Chen[c,*]

[a]Department of Mathematics, University of Science and Technology of China, Hefei 230026, China
oykc@mail.ustc.edu.cn
[b]Key Laboratory of Advanced Manufacturing Technology, Ministry of Education, Guizhou University, Guiyang, Guizhou 550025, China
shengwei_fu@163.com
[c]Department of Computer Science, Wenzhou University, Wenzhou 325035, China
kenyoncy2016@gmail.com, chenhuiling.jlu@gmail.com, chenhuiling_jsj@wzu.edu.cn
[d]Department of Physics, University of Science and Technology of China, Hefei 230026, China
qifengcai@mail.ustc.edu.cn
[e]School of Surveying and Geospatial Engineering, College of Engineering, University of Tehran, Tehran, Iran
as_heidari@ut.ac.ir

* Corresponding author: Huiling Chen (chenhuiling.jlu@gmail.com)

Abstract: Meta-heuristic algorithms, particularly those based on swarm intelligence, are highly effective for solving black-box optimization problems. However, maintaining a balance between exploration and exploitation within these algorithms remains a significant challenge. This paper introduces a useful algorithm, called Escape or Escape Algorithm (ESC), inspired by crowd evacuation behavior, to solve real-world cases and benchmark problems. The ESC algorithm simulates the behavior of crowds during the evacuation, where the population is divided into calm,

herding, and panic groups during the exploration phase, reflecting different levels of decision-making and emotional states. Calm individuals guide the crowd toward safety, herding individuals imitate others in less secure areas, and panic individuals make volatile decisions in the most dangerous zones. As the algorithm transitions into the exploitation phase, the population converges toward optimal solutions, akin to finding the safest exit. The effectiveness of the ESC algorithm is validated on two adjustable problem size test suites, CEC 2017 and CEC 2022. ESC ranked first in the 10-dimensional, 30-dimensional tests of CEC 2017, and the 10-dimensional and 20-dimensional tests of CEC 2022, and second in the 50-dimensional and 100-dimensional tests of CEC 2017. Additionally, ESC performed exceptionally well, ranking first in the engineering problems of pressure vessel design, tension/compression spring design, and rolling element bearing design, as well as in two 3D UAV path planning problems, demonstrating its efficiency in solving real-world complex problems, particularly complex problems like 3D UAV path planning. Compared with 12 other high-performance, classical, and advanced algorithms, ESC exhibited superior performance in complex optimization problems. The source codes of ESC algorithm will be shared at https://aliasgharheidari.com/ESC.html and other websites.

Keywords: Swarm intelligence, Crowd behavior, Escape Algorithm (ESC), Engineering optimization, 3D UAV path planning

1 Introduction

With the rapid advancement of technology, solving complex optimization problems has become increasingly critical across various domains, such as engineering and economics, particularly in emerging fields like 3D UAV path planning[1-3]. These optimization problems require finding the best solution that maximizes or minimizes an objective function under specific constraints [4]. Notably, the 3D UAV path planning problem is a challenging problem characterized by its computational complexity and the significant challenge of finding optimal paths in three-dimensional space under various constraints. As the complexity of real-world problems like this continues to increase, traditional optimization methods, such as Newton's method[5] and the steepest descent method[6], have shown significant limitations. These methods often struggle with high-dimensional and constraint-heavy problems, relying heavily on the continuity of the objective function and frequently falling into local optima[7].

To address these challenges, meta-heuristic algorithms have emerged as powerful tools, offering more flexible and robust solutions to complex optimization problems. Inspired by natural phenomena and human behavior, these algorithms leverage stochastic techniques and intelligent learning strategies to effectively navigate complex solution spaces[8, 9]. Meta-heuristic algorithms have demonstrated their effectiveness across various domains, particularly in applications where traditional deterministic methods cannot show a fitting performance [10]. Their key advantages include simplicity, flexibility, the ability to avoid local optima, and independence from the specific

nature of the problem, making them suitable for a wide range of applications[11, 12].

Meta-heuristic algorithms are generally classified into four categories based on their inspiration and methodology: evolutionary algorithms, swarm intelligence algorithms, physics-based algorithms, and human behavior-based algorithms[13], **Fig.1** shows the classification of meta-heuristic algorithm. Among these, human behavior-based algorithms are particularly noteworthy for their ability to model complex decision-making processes, social interactions, and learning mechanisms. This category of algorithms has been successfully applied in various optimization problems, demonstrating significant potential for further development[14-16].

However, despite the advancements in meta-heuristic algorithms, there remains a pressing need for algorithms that can more effectively solve complex real-world optimization problems, such as the difficult problem of 3D UAV path planning, while enriching the diversity of existing meta-heuristic approaches. Recognizing this gap, we propose Escape Algorithm (ESC), a useful meta-heuristic algorithm inspired by the dynamics of crowd evacuation. The ESC algorithm stands out from existing approaches by incorporating unique behavioral models observed during emergency evacuations, such as the "leader-follower" system [17, 18] and categorizing individuals into calm, herding, and panic groups. These models allow the ESC algorithm to simulate the diverse and adaptive strategies that people use in life-threatening situations, translating them into a computational framework that can solve complex optimization problems more effectively.

The ESC algorithm is distinct in its approach by drawing on the nuanced dynamics of crowd behavior, which has not been fully explored in existing meta-heuristic algorithms. Specifically, the ESC algorithm leverages the behaviors of different crowd segments—calm, herding, and panic groups—during evacuations, integrating these behaviors into its exploration and exploitation phases. This methodology not only provides a useful way to simulate the optimization process but also enhances the algorithm's ability to avoid local optima and achieve better global solutions. Through the incorporation of these unique behavioral strategies, the ESC algorithm offers significant improvements in solving complex, real-world problems, such as the complex 3D UAV path planning problem, as demonstrated through rigorous testing on 42 benchmark functions from the CEC 2017 and CEC 2022 test suites, where it has outperformed most existing algorithms across various dimensions.

The primary motivation for this research is to develop a more effective algorithm for solving complex real-world optimization challenges, particularly those encountered in 3D UAV path planning. Additionally, this work aims to contribute to the diversification of existing optimization algorithms, providing the research community with new tools for addressing a broader array of problems. In the study and application of optimization algorithms, it is widely recognized that no single algorithm can offer the best solution for every situation. This understanding is underscored by the "No Free Lunch" (NFL) theorem [19], which asserts that the average performance of all algorithms is equal across all possible optimization problems. This aligns with the NFL theorem's principle, highlighting the need for diverse and innovative approaches like ESC.

The rest of this paper is organized as follows: Section 3 introduces the inspiration behind the

ESC algorithm and presents the mathematical model. Section 4 details the numerical experiments conducted on the ESC algorithm and analyzes the relevant results. Section 5 applies the ESC algorithm to solve four practical engineering problems and two UAV path planning problems. Finally, Section 6 summarizes the research findings and discusses potential future research directions.

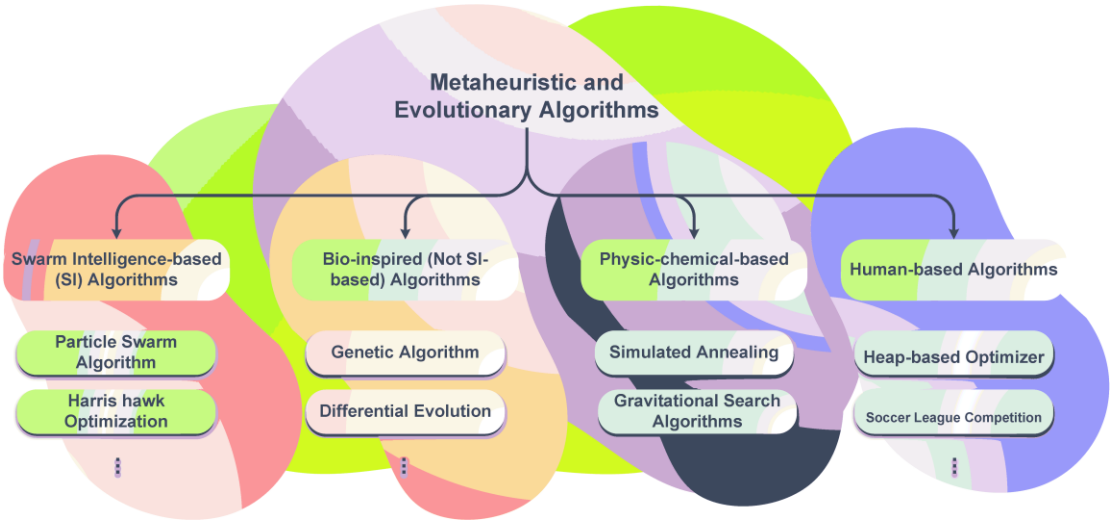

Fig. 1 The classification of meta-heuristic algorithms.

2 Related Works

This section will review the four MH (Meta- Heuristic) algorithms mentioned above. Evolutionary algorithms simulate the process of natural selection and biological evolution and search the optimal solution by simulating the mechanism of biological recombination, mutation, and selection. The most popular EA is GA[20], which mimics Darwinian evolution. The social behavior of animal groups, such as ants, bees, and birds inspire swarm intelligence algorithms. For example, Particle swarm optimization[21] (PSO) was proposed in 1995. Physics-based algorithms draw on the physical laws of nature, such as gravity and the motion of celestial bodies[22]. Finally, algorithms based on human behavior mimic human social interactions and learning processes, such as the dynamics of teaching and learning[23]. These categories reflect the diversity of meta-heuristics and their potential for a wide range of applications in solving complex optimization problems.

Of the four categories of meta-heuristic algorithms mentioned above, the particularly noteworthy ones are those based on human behavior heuristics. Human's unique thinking ability and intelligence occupy a prominent place in nature, providing a rich source of inspiration for developing new optimization algorithms. Such algorithms, which mimic human decision-making processes, social interactions and learning mechanisms, have proven effective in solving complex problems across multiple domains. The development and application of optimization algorithms based on human behavior demonstrate the great potential of human intelligence in solving

computing challenges. In the last ten years, some algorithms inspired by human behavior in the last decade are listed in **Table 1**.

In addition to the standalone meta-heuristic algorithms, hybrid optimization algorithms have gained significant attention due to their ability to combine the strengths of different approaches. Hybrid algorithms enhance performance by integrating various strategies, making them more effective in solving complex and large-scale problems. Notable examples include L-SHADE[24] and iL-SHADE[25], which are advanced variants of the Differential Evolution (DE) algorithm[26] that incorporate adaptive mechanisms to maintain diversity and prevent premature convergence. The hybrid whale optimization algorithm (WOABHC)[27] is another example, which combines WOA with β-hill climbing to enhance exploration and reduce premature convergence, improving overall optimization accuracy."

Other hybrid algorithms include the Exploratory Cuckoo Search (ECS)[28], which enhances the original Cuckoo Search algorithm by incorporating refraction learning, Gaussian perturbation, and multiple mutation strategies to improve exploration and avoid stagnation in suboptimal solutions. Similarly, the Improved Salp Swarm Algorithm (ISSA) with Highly Disruptive Polynomial Mutation (HDPM)[29] integrates advanced mutation techniques and opposition-based learning to enhance convergence rates and exploration capabilities. The Hybrid Snake Optimizer Algorithm (HSOA)[30] for solving Economic Load Dispatch Problems with Valve Point Effect enhances the original Snake Optimizer (SO) by introducing Oppositional-mutual learning in the initialization phase and dynamic polynomial mutation throughout the optimization process. These innovations improve population diversity and reduce early convergence issues. These hybrid algorithms represent the ongoing innovation in meta-heuristic optimization, offering powerful tools for addressing increasingly complex optimization challenges [31].

In summary, the landscape of meta-heuristic algorithms is rich and diverse, encompassing traditional approaches such as evolutionary, swarm intelligence, physics-based, human behavior-inspired algorithms, and innovative hybrid algorithms. By integrating multiple strategies' strengths, these hybrid methods have enhanced performance in tackling complex and large-scale optimization problems. The continuous development of both traditional and hybrid algorithms reflects the dynamic nature of optimization research and its expanding potential to solve a wide array of challenging problems across various fields.

Table 1 Some Meta-heuristic Algorithms based on Human Behavior (2013-2023)

Algorithms	Inspiration	Reference
Cultural Evolution Algorithm	The evolution of social civilization	[32]
Soccer League Competition Algorithm	The competitive behavior of teams and players	[33]
Exchange Market Algorithm	The process of trading shares on the stock market	[34]
Election Algorithm	The behavior of candidates and voters in elections	[35]
Passing Vehicle Search	The vehicle was overtaking on a two-lane highway	[36]
Social Learning Optimization	Evolution of human intelligence and social learning theory	[37]
Football Game Algorithm	Players' behavior during a game	[38]
Human Behavior-Based Optimization	Human behavior	[39]
Social Engineering Optimizer	Rules of social engineering techniques	[40]
Queuing Search Algorithm	Human queuing activity	[41]
Evolution and Learning Optimization	Human social learning behavior organized as family in social environment	[42]
Search and Rescue Optimization	Human exploration in search and rescue operations	[43]
Social Ski-Driver Optimization	Behavior in skiing	[44]
Gaining Sharing Knowledge-Based Algorithm	The process of acquiring and sharing knowledge in human life	[45]
Political Optimizer	The multi-stage process of politics	[46]
Heap-Based Optimizer	Subject to corporate hierarchy	[47]
Most Valuable Player Algorithm	A sport in which players team up	[48]
Herd Immunity Optimization	Herd immunity concept	[49]
Stock Exchange Trading Optimization	The behavior of traders and changes in stock prices in the stock market	[50]
Anti Coronavirus Optimization Algorithm	Isolation behavior in the fight against	[51]
Skill Optimization Algorithm	Human efforts to acquire and improve skills.	[52]
Chernobyl Disaster Optimizer	The nuclear reactor core explosion of Chernobyl	[53]

3. Escape Algorithm (ESC)

ESC is inspired by how people behave during emergency evacuations. This section explains the background of crowd evacuation systems and how these behaviors inspired the design of the ESC algorithm. By modeling the different responses—calm, herding, and panic—of individuals in a crowd, the ESC algorithm effectively balances exploration and exploitation in solving complex optimization problems.

3.1 Inspiration

In this section, we will introduce the crowd evacuation system's research background and explain the Escape algorithm's inspiration source.

The development of the ESC draws profound inspiration from the nuanced dynamics of human behavior during emergency evacuations[54]. In the chaotic backdrop of emergency scenarios—ranging from natural disasters to human-induced threats—individuals exhibit a spectrum of behaviors influenced by panic, environmental conditions, and the collective movement of the crowd [55-57]. These behaviors significantly impact the efficiency of evacuation processes, highlighting the importance of adaptive and strategic planning. Our algorithm encapsulates this complexity through a computational lens, translating the observed human behaviors into a meta-heuristic framework to solve optimization problems.

The ESC algorithm is particularly inspired by the "leader-follower" system[58, 59] observed in crowds, where individuals naturally assume roles that guide the collective movement. In this system, leaders (both static and dynamic) emerge to influence the direction and pace of the evacuation, while followers form the bulk of the crowd, their movement influenced by those around them. This phenomenon is mirrored in our algorithm through the division of agents into calm, herding, and panic crowd[60] in the exploration phase of the algorithm, each exhibiting distinct behaviors that collectively drive the search process towards optimal solutions.

- **Calm crowd**: The calm individuals in a crowd, who assess situations with a clear mind and make rational decisions. These agents methodically search the problem space, akin to calm individuals finding efficient paths in an evacuation, guiding others through their steady influence.
- **Herding crowd**: The herding behavior, where individuals follow the crowd without clear personal direction, is mirrored in the conforming agents of our algorithm. This behavior enhances the exploitation phase, as agents converge on promising areas of the search space, similar to how individuals in a crowd might follow others to perceived exits or safe areas.
- **Panic crowd**: The panic-stricken individuals, whose unpredictable and erratic movements can both hinder and unexpectedly aid in finding escape routes, inspire the diversification mechanisms in our algorithm. Their behavior is replicated in the panic

agents, introducing randomness and preventing premature convergence to local optima, akin to how panic in a crowd can lead to discovering unconventional exits.

Through the ESC algorithm, we harness the intrinsic wisdom of crowd behavior during emergencies, translating the interplay of calm, herding, and panic into a computational model. This approach not only offers a useful perspective on algorithm design but also underscores the potential of natural and human phenomena as sources of inspiration for developing advanced problem-solving strategies.

3.2 Algorithm and Population Initialization

ESC is designed to simulate crowd behavior during emergency evacuations, where individuals must navigate toward exits in a dynamic and uncertain environment. The ESC introduces the concept of an Elite Pool, representing the best-performing individuals who symbolize potential exits identified by the crowd. This mechanism enhances the algorithm's ability to explore the solution space thoroughly, avoiding local optima by simultaneously considering multiple directions.

The ESC algorithm begins by initializing a population of N individuals, each described by a D-dimensional vector $x_i = (x_{i,1}, x_{i,2} \ldots, x_{i,D})$ The value of the $j-th$ dimension for the $i-th$ individual is given by:

$$\boldsymbol{x}_{i,j} = lb_j + r_{i,j} \times (ub_j - lb_j), \quad r_{i,j} \sim U(0,1) \tag{1}$$

Here,lb_j and ub_j represent the lower and upper bounds of the $j-th$ dimension, ensuring that each individual's initial position is randomly distributed within the feasible space. The random variable $r_{i,j}$ is uniformly distributed between 0 and 1, reflecting the randomness in the initial cdecision-making process during an evacuation.

After initializing the population, the fitness of each individual $f_i = f(x_i)$ is evaluated using a fitness function f.The population is then sorted by fitness in ascending order, and the top individuals are stored in the Elite Pool E as Eq. (2), the parameter that represents the number of potential safety exits found by the crowd.

$$\boldsymbol{E} = \{\boldsymbol{x}_{(1)}, \boldsymbol{x}_{(2)}, \ldots, \boldsymbol{x}_{(\text{exist})}\} \tag{2}$$

These elite individuals represent the best potential solutions (exits) identified by the population and serve as reference points for subsequent iterations.

3.3 Panic Index and Iterative Process

The ESC algorithm models the iterative process to reflect the evolving behavior of the crowd as the evacuation progresses. The algorithm adjusts individual movements based on their classification into calm, conforming, or panic groups, corresponding to different behavioral responses during an evacuation.

At the start of each iteration t, the panic index $P(t)$ is calculated as follows:

$$P(t) = cos\left(\frac{\pi t}{6\mathrm{T}}\right) \tag{3}$$

The panic index reflects the overall level of panic in the crowd, with higher values indicating

more chaotic behavior. This index decreases over time as t goes from 0 to the number of iterations T, simulating the crowd's adaptation to the evacuation environment.

3.4 Exploration Phase

During the exploration phase, when $t \leq \frac{T}{2}$ (T is the maximum number of iterations of the algorithm, and t is the current number of iterations), the population is divided into calm, conforming, and panic groups based on their fitness levels. Specifically, the population is sorted in ascending order of fitness, and individuals are stratified into three groups according to the proportions,$c = 0.15$, $h = 0.35$,and $p = 0.5$ for the calm, conforming, and panic groups, respectively. This stratification reflects the varied responses of individuals in a crowd during an evacuation, where some remain calm, others conform to the group's behavior, and some panic.

3.4.1 Calm Group Update

Individuals in the calm group behave rationally, moving toward a central position C_j, which represents the collective decision of the group:

$$x_{i,j}^{\text{new}} = x_{i,j} + m_1 \times \left(w_1 \times (C_j - x_{i,j}) + v_{c,j}\right) \times P(t) \quad (4)$$

Here,$C_j$is the center of the calm group in the $j-th$ dimension, calculated as the mean of all calm individuals in that dimension. The vector $v_{c,j}$ is defined as Eq. (5), where $R_{c,j} = r_{min,j}^{c} + r_{i,j} \times (r_{max,j}^{c} - r_{min,j}^{c})$ is a randomly generated position within the calm group's bounds.$r_{min,j}^{c}$ and $r_{max,j}^{c}$ represent the minimum and maximum values of the j − th dimension for all individuals in the calm group and $\epsilon_j = \frac{z_j}{50}(z_j \sim N(0,1))$represents a slight adjustment in the individual's movement.The binary variable m_1 is determined by a Bernoulli distribution , allowing for partial updates, which simulates parts of the dimension that are not updated due to crowd congestion. Specifically, m_1 is generated such that it takes the values 0 or 1 with equal probability. w_1 is an adaptive Levy weight, calculated using a Levy distribution to simulate the step sizes in the exploration phase, which is defined in section 3.6. **Fig 2** shows the updating process of the calm group.

$$v_{c,j} = R_{c,j} - x_{i,j} + \epsilon_j \quad (5)$$

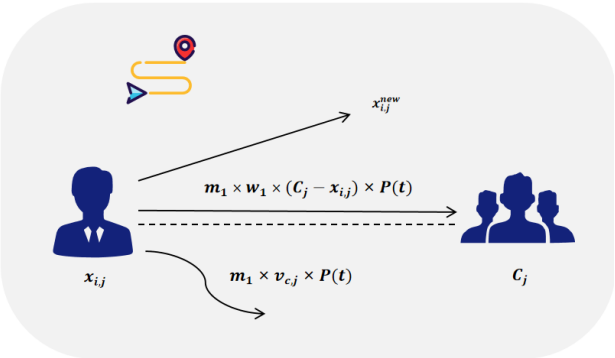

Fig. 2 Updated schematic of the Calm Group

3.4.2 Herding Group Update

Herding individuals follow the behavior of both the calm and panic groups. Their positions are updated based on influences from both:

$$x_{i,j}^{\text{new}} = x_{i,j} + m_1 \times \left(w_1 \times (C_j - x_{i,j}) + m_2 \times w_2 \times (x_{p,j} - x_{i,j}) + v_{h,j} \times P(t)\right) \quad (6)$$

In this equation,$x_{p,j}$is a randomly selected individual from the panic group, representing a potential direction of panic-driven movement.$w_2$is another adaptive Levy weight used for the conforming group, which is defined in section 3.6. The vector $v_{h,j}$is defined as Eq. (7), where $R_{h,j} = r_{min,j}^{h} + r_{i,j} \times (r_{max,j}^{h} - r_{min,j}^{h})$ is a randomly generated position within the herding group's bounds. The $r_{min,j}^{h}\ and\ r_{max,j}^{h}$ represent the minimum and maximum values of the $j-th$ dimension for all individuals in the herding group and the m_2 is a binary variable which is generated through the same mechanism as m_1. **Fig 3** shows the updating process of the herding group.

$$v_{h,j} = R_{h,j} - x_{i,j} + \epsilon_j \quad (7)$$

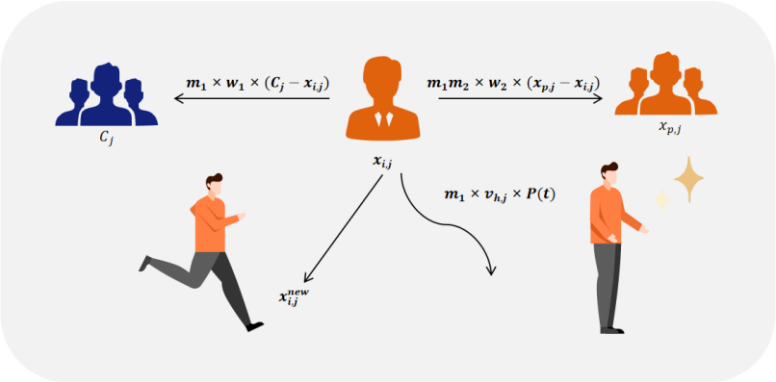

Fig. 3 Updated schematic of the herding crowd

3.4.3 Panic Group Update

Panic-driven individuals explore the solution space more erratically, influenced by potential exits (from the Elite Pool) and random directions from other individuals:

$$x_{i,j}^{\text{new}} = x_{i,j} + m_1 \times \left(w_1 \times (E_j - x_{i,j}) + m_2 \times w_2 \times (x_{\text{rand},j} - x_{i,j}) + v_{p,j} \times P(t)\right) \quad (8)$$

Here,E_j is a randomly selected individual from the Elite Pool, representing a possible exit that a panic-driven individual might head toward.$x_{rand,j}$ represents a randomly selected individual from the population, introducing an element of randomness in the panic-driven movement. The vector $v_{h,j}$is defined as Eq. (9), where $R_{p,j} = r_{min,j}^{p} + r_{i,j} \times (r_{max,j}^{p} - r_{min,j}^{p})$ is a randomly generated position within the panic group's bounds.$r_{min,j}^{p}\ and\ r_{max,j}^{p}$ represent the minimum and maximum values of the $j-th$ dimension for all individuals in the panic group. **Fig 4** shows the updating process of the panic group.

$$v_{p,j} = R_{p,j} - x_{i,j} + \epsilon_j \quad (9)$$

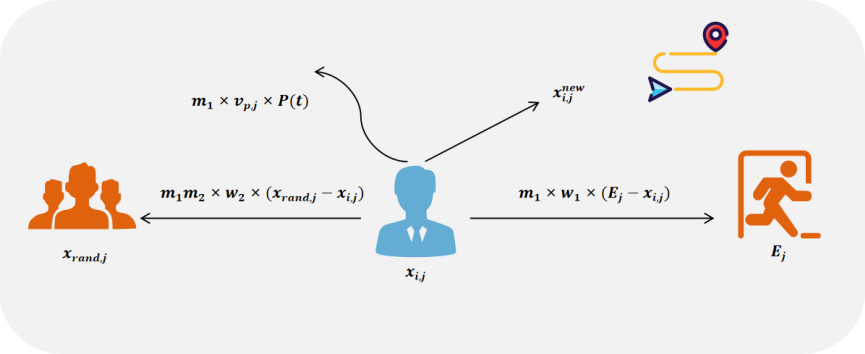

Fig. 4 Panic crowd update schematic

3.5 Exploitation Phase

As the iteration progresses beyond $\frac{T}{2}$, the algorithm transitions into the exploitation phase, where all individuals are considered calm. The focus shifts to fine-tuning positions based on the best solutions identified so far. During this phase, individuals refine their positions by moving closer to members of the Elite Pool, which represents both possible safety exits and the best solutions identified in previous iterations, as well as randomly selected individuals from the population. This process simulates the crowd's gradual convergence towards identified optimal exits. The position update during this phase is given by the Eq. (10).

$$x_{i,j}^{new} = x_{i,j} + m_1 \cdot w_1 \cdot \left(E_j - x_{i,j}\right) + m_2 \cdot w_2 \cdot \left(x_{\text{rand},j} - x_{i,j}\right) \quad (10)$$

In Eq. (10), $x_{i,j}$represents the position of the $i-th$ individual in the $j-th$ dimension.E_j is the position of a member from the Elite Pool, symbolizing both a possible safety exit and one of the best solutions identified so far. $x_{rand,j}$ is the position of a randomly selected individual from the population. This allows individuals to refine their positions by moving closer to both the Elite Pool members and randomly selected individuals, simulating the crowd's gradual convergence towards the identified optimal exits. **Fig. 5** shows the population update schematic in the exploration phase.

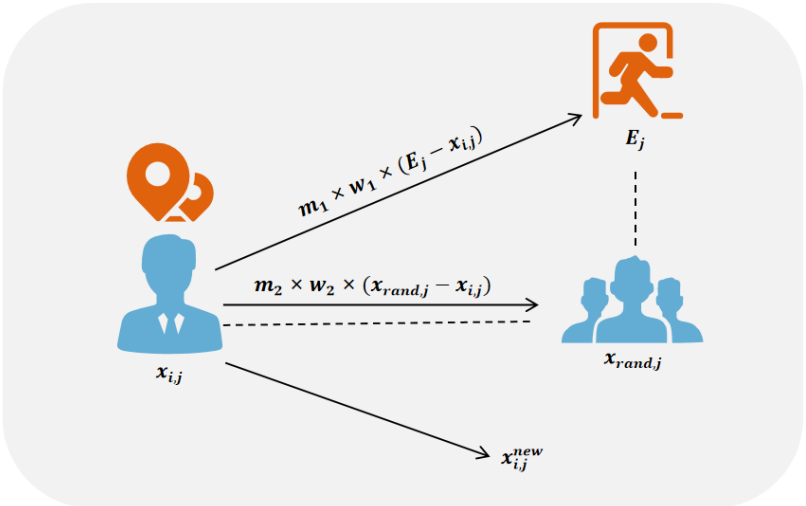

Fig. 5 Population update schematic in the exploration phase

3.6 Adaptive Levy Weights and Behavior Simulation

The step sizes of individuals are controlled by adaptive Levy weights, which simulate varying degrees of exploration and exploitation at different stages of the algorithm. The Levy weight for each dimension j is calculated as Eq. (11)

$$w_j = \frac{|u_j|}{|v_j|^{\frac{1}{\beta}}}, \quad u_j \sim N(0,\sigma^2), \quad v_j \sim N(0,1), \ \sigma = \left(\frac{\Gamma\left(\frac{1+\beta}{2}\right)\cdot\beta\cdot 2^{\frac{1}{\beta}-1}}{\Gamma(1+\beta)\cdot sin\left(\frac{\pi\beta}{2}\right)} \right)^{\frac{1}{\beta}} \tag{11}$$

where β is a parameter that dynamically adjusts as the algorithm progresses as Eq. (12) and Γ is the Gamma function.

$$\beta = \beta_{\text{base}} + 0.5 \times sin\left(\frac{\pi t}{2\text{T}}\right) \tag{12}$$

In Eq. (12), β_{base} is the initial value of β , which is same to the empirical setting used in the Harris Hawks Optimization (HHO) [61] algorithm, with a value of 1.5. This adjustment allows the algorithm to initially make larger exploratory moves (when β is smaller) and gradually transition to finer, exploitative moves (as β increases), mirroring the natural progression from panic-driven exploration to calm, rational decision-making in a crowd.

3.7 Fitness Evaluation and Elite Pool Update

At each iteration, the fitness of each updated individual is recalculated. A greedy selection process is used to retain the better solution between the old and new positions:

$$f_i^{\text{new}} = f(x_i^{\text{new}}) \tag{13}$$

The update rule for each individual can be described as:

$$x_i = \begin{cases} x_i^{\text{new}} & \text{if } f_i^{\text{new}} < f_i \\ x_i & \text{otherwise} \end{cases} \tag{14}$$

If the new fitness f_i^{new} is better (i.e., lower for a minimization problem) than the previous fitness f_i the individual's position is updated to x_i^{new} . Otherwise, the previous position x_i is retained. The Elite Pool E is updated at each iteration to ensure it contains the best solutions found so far. This pool plays a crucial role in guiding the population toward the best exits identified during the simulation.

3.8 Computational Complexity

In this section, we describe the general computational complexity of the ESC (Escape) algorithm. The computational complexity of ESC primarily depends on two components: the initialization of the population and the main iterative process of the algorithm, which includes calculating the fitness functions, sorting, and updating the solutions. Assume that the number of search agents is N, T denotes the maximum number of iterations, and D represents the dimensionality of the problem. The computational complexity of initializing the population, where each individual is represented by a D-dimensional vector, is $O(N \times D)$. The fitness evaluation for the entire population also requires $O(N \times D)$ operations. Sorting the population by fitness values is performed using a comparison-based sorting algorithm, which has a complexity of $O(N \times logN)$.

During the main iterative process, the algorithm runs for T iterations. In each iteration, the population is divided into calm, herding, and panic groups, and the positions of individuals in each group are updated according to different rules. The complexity for updating positions is $O(N \times D)$, and fitness reevaluation adds another $O(N \times D)$, and fitness reevaluation adds another $O(N \times logN)$ time. Thus, the total complexity per iteration is $O(N \times D + NlogN)$. Consequently, the overall computational complexity of the ESC algorithm is $O(T \times N \times (D + logN))$.

Next, we will compare the complexities of the ESC with the Slime Mould Algorithm (SMA)[62] and HHO [61] based on the calculation methods from their original papers. To ensure consistency in our analysis, we merged some computational items when evaluating the complexities of SMA and HHO, in line with their original descriptions. For the SMA algorithm, the overall complexity is $O(T \times N \times (D + logN))$. This reflects the detailed handling of fitness evaluations and position updates in SMA, as well as the sorting and weight adjustments involved in each iteration. The complexity of the HHO algorithm is $O(T \times N \times D)$, mainly covering initialization, fitness evaluation, and position updates, without significant logarithmic terms. This indicates that the HHO algorithm focuses on direct position updates during each iteration, involving fewer sorting or other complex operations.

Overall, the complexity of the ESC algorithm is $O(T \times N \times (D + logN))$, indicating that it performs fitness evaluations and position updates and also includes comparison-based sorting operations in each iteration, potentially making it more effective in handling structured optimization problems. ESC and SMA incorporate additional structured elements like sorting and weight updates, making them particularly suitable for complex optimization environments requiring these operations. Meanwhile, HHO, with its more streamlined iterative update strategy, is better suited for fast response and adaptation in dynamic optimization scenarios. **Fig 6** shows the flowchart of ESC.

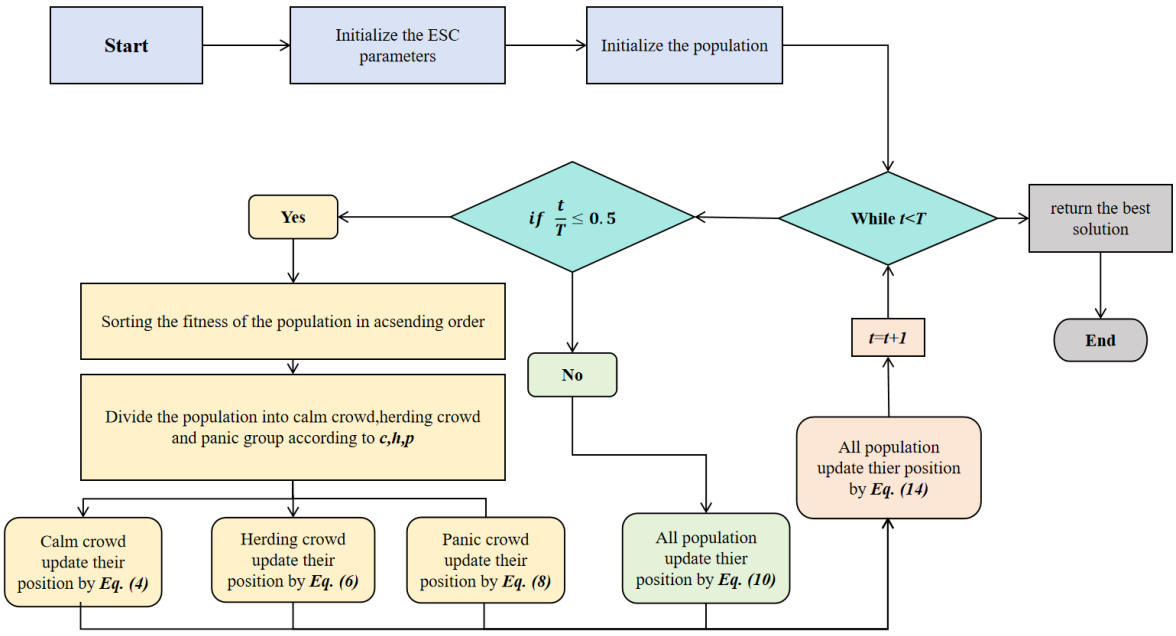

Fig. 6 Flowchart of the escape (ESC) algorithm

Algorithm 1. Pseudocode of escape optimization algorithm (ESC)

1: Initialize ESC parameters
2: **Initialize Population:**
3: **for** each individual x_i do
4: **for** each dimension j do
5: Set $x_{i,j} = lb_j + r_j \times (ub_j - lb_j)$ where $r_j \sim U(0, 1)$
6: **end for**
7: **end for**
8: Evaluate fitness of each individual $fi = f(x_i)$
9: Sort population by fitness in ascending order
10: Store the top eliteSize individuals in the Elite Pool:
$E = \{x_1, x_2, \ldots, x_{eliteSize}\}$
11: while $t \leq T$ do
12: **if** $t/T \leq 0.5$ then
13: Compute Panic Index $P(t) = \cos(\pi t/6T)$
14: Sort population by fitness
15: Divide population into: Calm group (proportion c), Conforming group (proportion h), and
Panic group (proportion p)
16: Update Calm Group using Eq. (4)
17: Update Conforming Group using Eq. (6)
18: Update Panic Group using Eq. (8)
19: **else**
20: ► Enter exploitation phase
21: Update population using Eq. (10)
22: **end if**
23: Evaluate the fitness of each individual
24: Apply greedy selection (Eq. 12)
25: Update Elite Pool with best solutions found

26: t = t + 1
27: **end while**
28: Return Best Solutions from Elite Pool

4. Experimental Results and Discussions

In this section, we assess the performance of the ESC across multiple benchmark test suites. We conducted convergence behavior analyses to confirm ESC's effectiveness and compared its numerical results with those of other leading algorithms. Furthermore, we showcased ESC's scalability by applying it to large-scale global optimization problems. Finally, we utilized two nonparametric tests—the Wilcoxon rank sum test and the Friedman mean rank test—to evaluate the differences and overall performance of the competing algorithms.

4.1 Benchmark Test Functions

As part of the study, CEC 2017 [63](Dim=10,30,50,100), and CEC 2022[64] (Dim=10,20) test suites were used to evaluate the performance of the proposed ESC algorithm. We chose F1-F30 of CEC 2017 and F1-F12 of CEC 2022 as a total of 42 test functions. Characteristics differentiate the function categories in these suites and uses: single-optimum unimodal functions gauge the speed and precision of an algorithm's optimization; multimodal types, with multiple optima, assess robustness; hybrid and composition functions test an algorithm's ability to solve complex problems by combining features of the first two. An Intel Core i5-12400,2.50 GHz CPU,16 GB RAM were used on the MATLAB 2023a platform for the analysis. The number of iterations is set to 500, and the population size to 30.

Table 2 Review the CEC 2017 test suite

Type	ID	Description	Dim	f_{min}
Unimodal	CEC 2017-F1	Shifted and Rotated Bent Cigar Function	30/50/100	100
	CEC 2017-F2	Shifted and Rotated Sum of Different Power Function	30/50/100	200
	CEC 2017-F3	Shifted and Rotated Zakharov Function	30/50/100	300
Multimodal	CEC 2017-F4	Shifted and Rotated Rosenbrock's Function	30/50/100	400
	CEC 2017-F5	Shifted and Rotated Rastrigin's Function	30/50/100	500
	CEC 2017-F6	Shifted and Rotated Expanded Scaffer's F6 Function	30/50/100	600
	CEC 2017-F7	Shifted and Rotated Lunacek Bi_Rastrigin Function	30/50/100	700
	CEC 2017-F8	Shifted and Rotated Non-Continuous Rastrigin's Function	30/50/100	800
	CEC 2017-F9	Shifted and Rotated Levy Function	30/50/100	900
	CEC 2017-F10	Shifted and Rotated Schwefel's Function	30/50/100	1000
Hybrid	CEC 2017-F11	Hybrid Function 1 (N=3)	30/50/100	1100
	CEC 2017-F12	Hybrid Function 2 (N=3)	30/50/100	1200
	CEC 2017-F13	Hybrid Function 3 (N=3)	30/50/100	1300
	CEC 2017-F14	Hybrid Function 4 (N=4)	30/50/100	1400
	CEC 2017-F15	Hybrid Function 5 (N=4)	30/50/100	1500
	CEC 2017-F16	Hybrid Function 6 (N=4)	30/50/100	1600
	CEC 2017-F17	Hybrid Function 6 (N=5)	30/50/100	1700
	CEC 2017-F18	Hybrid Function 6 (N=5)	30/50/100	1800
	CEC 2017-F19	Hybrid Function 6 (N=5)	30/50/100	1900
	CEC 2017-F20	Hybrid Function 6 (N=6)	30/50/100	2000
Composition	CEC 2017-F21	Composition Function 1 (N=5)	30/50/100	2100
	CEC 2017-F22	Composition Function 2 (N=5)	30/50/100	2200
	CEC 2017-F23	Composition Function 3 (N=5)	30/50/100	2300

CEC 2017-F24	Composition Function 4 (N=5)	30/50/100	2400
CEC 2017-F25	Composition Function 5 (N=3)	30/50/100	2500
CEC 2017-F26	Composition Function 6 (N=3)	30/50/100	2600
CEC 2017-F27	Composition Function 7 (N=5)	30/50/100	2700
CEC 2017-F28	Composition Function 8 (N=5)	30/50/100	2800
CEC 2017-F29	Composition Function 9 (N=5)	30/50/100	2900
CEC 2017-F30	Composition Function 10 (N=3)	30/50/100	3000
Search Range: [-100,100]			

Table 3 Review the CEC 2022 test suite

Type	ID	Description	Dim	f_{min}
Unimodal Function	CEC 2022-F1	Shifted and full Rotated Zakharov Function	10/20	300
Basic Functions	CEC 2022-F2	Shifted and full Rotated Zakharov Function	10/20	400
	CEC 2022-F3	Shifted and full Rotated Expanded Schaffer's f6 Function	10/20	600
	CEC 2022-F4	Shifted and full Rotated Non-Continuous Rastrigin's Function	10/20	800
	CEC 2022-F5	Shifted and full Rotated Levy Function	10/20	900
Hybrid Functions	CEC 2022-F6	Hybrid Function 1 (N = 3)	10/20	1800
	CEC 2022-F7	Hybrid Function 2 (N = 6)	10/20	2000
	CEC 2022-F8	Hybrid Function 3 (N = 5)	10/20	2200
Composition Functions	CEC 2022-F9	Composition Function 1 (N = 5)	10/20	2300
	CEC 2022-F10	Composition Function 2 (N = 4)	10/20	2400
	CEC 2022-F11	Composition Function 3 (N = 5)	10/20	2600
	CEC 2022-F12	Composition Function 4 (N = 6)	10/20	2700
Search Range: [-100,100]				

4.2 Competitor Algorithms and Parameters Setting

We compare the results of with 12 other algorithms, namely Memory, evolutionary operator, and local search based improved Grey Wolf Optimizer (MELGWO)[65], Gaussian quantum-behaved particle swarm optimization (GQPSO)[66], improved dung beetle optimizer (IDBO) [67], Dominant Swarm with Adaptive T-distribution Mutation-based Slime Mould Algorithm (DTSMA) [68], constriction coefficient-based particle swarm optimization and gravitational search algorithm (CPSOGSA) [69], Whale Optimization Algorithm (WOA) [70], Sine Cosine Algorithm (SCA) [71], HHO[61], Crayfish Optimization Algorithm (COA) [72], Chernobyl Disaster Optimizer (CDO) [53], Optical Microscope Algorithm (OMA) [73], Spider Wasp Optimizer (SWO) [74]. The parameter Settings for the algorithms used for comparison are shown in **Table 4.** In the experiment, the population size N for each algorithm is set to 30, and the maximum number of iterations T is set to 500. The algorithm terminates when the maximum number of iterations T is reached.

Table 4 Parameter settings of the chosen algorithms.

Algorithms	Name of the parameter	Value of the parameter	N	T
MELGWO	$\theta, Crossover,$ Stochastic Local Search	2 to 0,0.6,0.5	30	500
GQPSO	w_1, w_2, c_1, c_2	0.5,1,1.5,1.5	30	500
IDBO	k, λ, b, S	0.1,0.1,0.3,0.5	30	500
DTSMA	z, q	0.03,0.9	30	500
CPSOGSA	φ_1, φ_2	2.05,2.05	30	500
WOA	a	2	30	500
SCA	a	2	30	500
HHO	E_0	[-1,1]	30	500
COA	C_1, C_3, μ, σ	0.2,3,25,3	30	500

CDO	α, β, γ	16000,270000,300000	30	500
OMA	$None$	*None*	*30*	500
SWO	TR, CR	0.3,0.2	30	500
ESC	$\beta_{base}, c, h, p, exist$	0.15,0.15,0.35,0.5,3	30	500

4.3 Analysis of the Convergence Behavior

To illustrate the effectiveness of ESC, we exhibit their convergence properties in **Fig.7**. This figure includes a set of 6 visuals, each depicting outcomes for various benchmark tests. We selected three tests from the CEC 2017 suite and three from the CEC 2022 suite. In each image, the first column depicts the 2D landscape of the benchmark function, while the second column highlights the search agent's final location. A red dot marks the optimal solution. Observations from these images reveal that, although search agents are spread across the entire parameter space, they predominantly cluster near the optimal solution. This clustering underscores the impressive capability of the ESC in both exploring and exploiting the search space.

Furthermore, the third column of the figure showcases the evolution of the average fitness value across iterations. Initially, this average fitness value is quite elevated, but it steadily decreases and stabilizes after about 100 iterations, demonstrating the rapid convergence capabilities of the ESC. The fourth column visually presents the trajectory of the search agent within the first dimension. Here, notable variations are evident in the early stages of iterations, which diminish as the count approaches 100. This pattern indicates the ESC's robustness in sidestepping local optima and effectively achieving global optimization.

The final column displays the convergence curve. This curve is notably smooth for unimodal functions, signifying that optimal values are attainable via iterative procedures. In contrast, for multimodal functions characterized by numerous local optima, the search process necessitates ongoing avoidance of these local peaks to reach global optima. This is reflected in the distinctly stepped appearance of the convergence curve in these cases. In conclusion, ESC has obvious convergence.

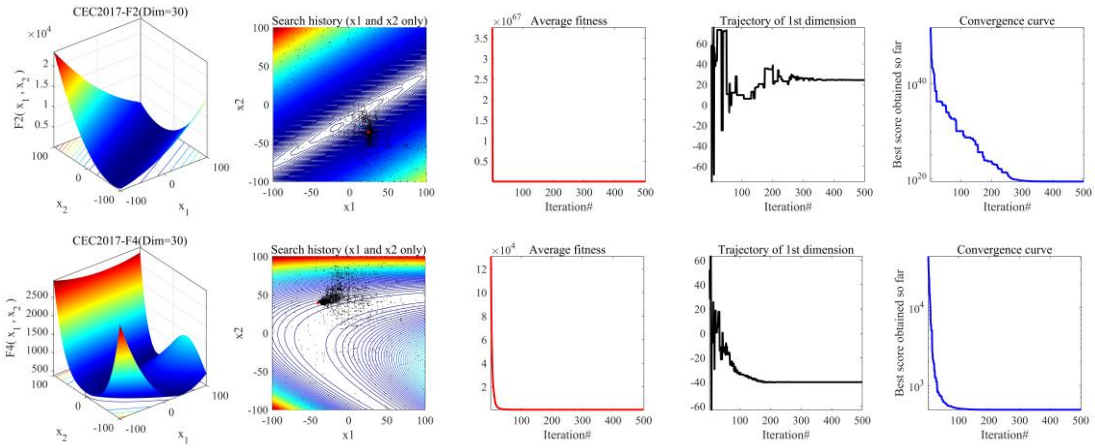

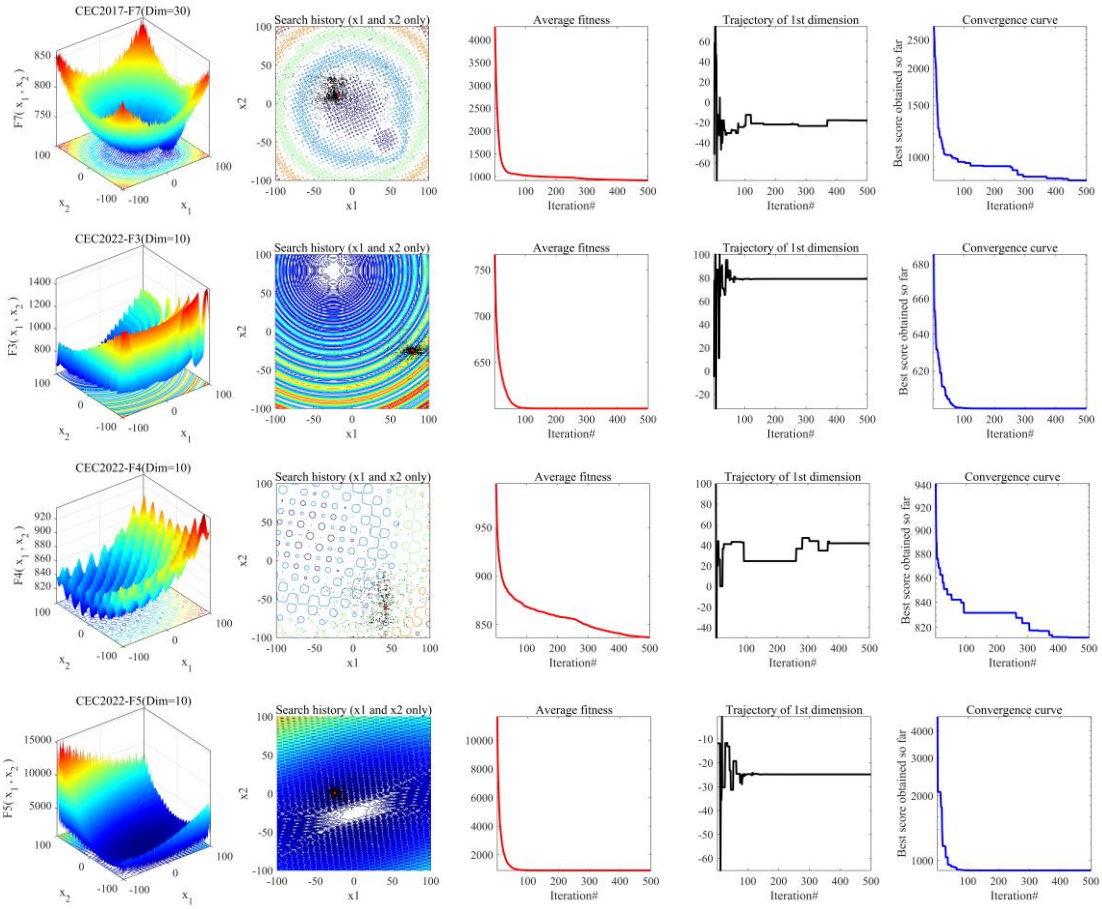

Fig.7 Convergence behaviors of ESC in the search process

4.4 Quantitative Evaluation

4.4.1 Comparison with other competitive algorithms on CEC 2017

In this section, we will detail the performance results of the ESC algorithm against 12 competing methods and evaluate them on 10, 30, 50, and 100 dimensions using the CEC 2017 benchmark suite. This check records the mean value (Ave) and standard deviation (Std) of each algorithm based on 30 independent experiments, as shown in **Table 5**, **6**, **7** and **8**. A key aspect of our analysis focuses on the algorithm's convergence rate, comparing the iteration progress of different algorithms. As shown in **Fig. 8**, the ESC algorithm converges significantly faster than most other algorithms.

In addition, to evaluate the stability of the algorithm, **Fig.9** provides a boxplot analysis of the ESC and its comparison algorithm. The ESC algorithm shows a small variance, indicating its stability. In addition, **Fig.10** aims to visually represent the efficiency of different algorithms in solving optimization problems for various functions using the Friedman average ranking as a comparative metric.

In the CEC 2017 benchmark tests, the ESC demonstrated strong performance across various dimensions. It achieved top rankings in the Friedman mean ranking, securing first place in the 10 and 30 dimensions, second in the 50 dimensions, and maintaining second in the 100 dimensions. This highlights ESC's capability to handle multi-dimensional optimization problems. A detailed comparison between ESC and other algorithms shows that ESC outperformed major competitors such as MELGWO, GQPSO,

and IDBO in the 10-dimensional test. In the 30-dimensional tests, ESC outperformed MELGWO on 26 functions, only slightly trailing on 2 functions. In the 50 and 100-dimensional scenarios, although MELGWO showed marginally better performance on some functions as the dimensionality increased, ESC maintained a significant advantage overall. Compared to IDBO, ESC demonstrated stable performance in the 30 and 50 dimensions, consistently maintaining its lead. However, in the 100-dimensional test, while IDBO showed strength in certain functions, ESC still held an overall advantage. Notably, the DTSMA algorithm closely competed with ESC, particularly in the 100-dimensional scenario where their performances were very close. DTSMA managed to outperform ESC on several functions, but ESC excelled on an equal number, indicating its robustness in handling high-dimensional problems. In contrast, algorithms like GQPSO and SCA posed no significant threat to ESC across all dimensions, with ESC consistently outperforming these algorithms on most functions. GQPSO consistently ranked lower, showing poor performance on most functions, while SCA, despite some success in lower-dimensional problems, lagged behind ESC overall. CPSOGSA, WOA, and HHO exhibited moderate performance in the medium and high-dimensional tests. CPSOGSA struggled to significantly outperform ESC in the 50 and 100 dimensions, particularly facing challenges with higher-dimensional problems. WOA and HHO showed average performance in lower-dimensional problems, with HHO's performance improving slightly as the dimensionality increased, yet they still did not pose a challenge to ESC.COA performed comparably to ESC in the 30 and 50-dimensional tests, especially in medium dimensions where it showed good performance. However, in the high-dimensional 100-dimensional problems, COA's limitations became apparent, with its performance clearly inferior to ESC. OMA performed well in the 30 and 50-dimensional tests, approaching ESC's level, but in the high-dimensional 100-dimensional problems, ESC maintained a significant lead. CDO and SWO consistently performed poorly across all dimensions, particularly in high-dimensional tests where both algorithms ranked low in the Friedman mean ranking, highlighting their inadequacies in handling complex multi-dimensional optimization problems. In comparison, ESC significantly outperformed these algorithms on almost all functions.

The analysis of the iteration curves in **Fig. 8** shows that the ESC algorithm's convergence speed was superior to other algorithms in most cases, particularly during the early stages of iteration, where ESC's convergence speed was notably faster than its competitors. The boxplot in **Fig. 9** illustrates that the ESC algorithm exhibited low variance, indicating more stable results across different experiments. Despite some slight disadvantages in specific high-dimensional functions, the overall ranking and convergence efficiency still highlight ESC as the most outstanding algorithm.

However, the ESC algorithm does have some limitations. As the problem dimensionality increases, ESC's performance on certain functions becomes less prominent, especially in the 100-dimensional scenarios where its competition with DTSMA becomes more intense. While ESC performs well on most functions, it sometimes shows a lack of adaptability to certain complex functions in high-dimensional problems, leading to slightly inferior performance compared to DTSMA on these specific functions. Additionally, ESC's performance advantage is most apparent in lower and medium-dimensional problems, but this advantage diminishes as the dimensionality

increases. This is a crucial area for future improvements to the ESC algorithm.

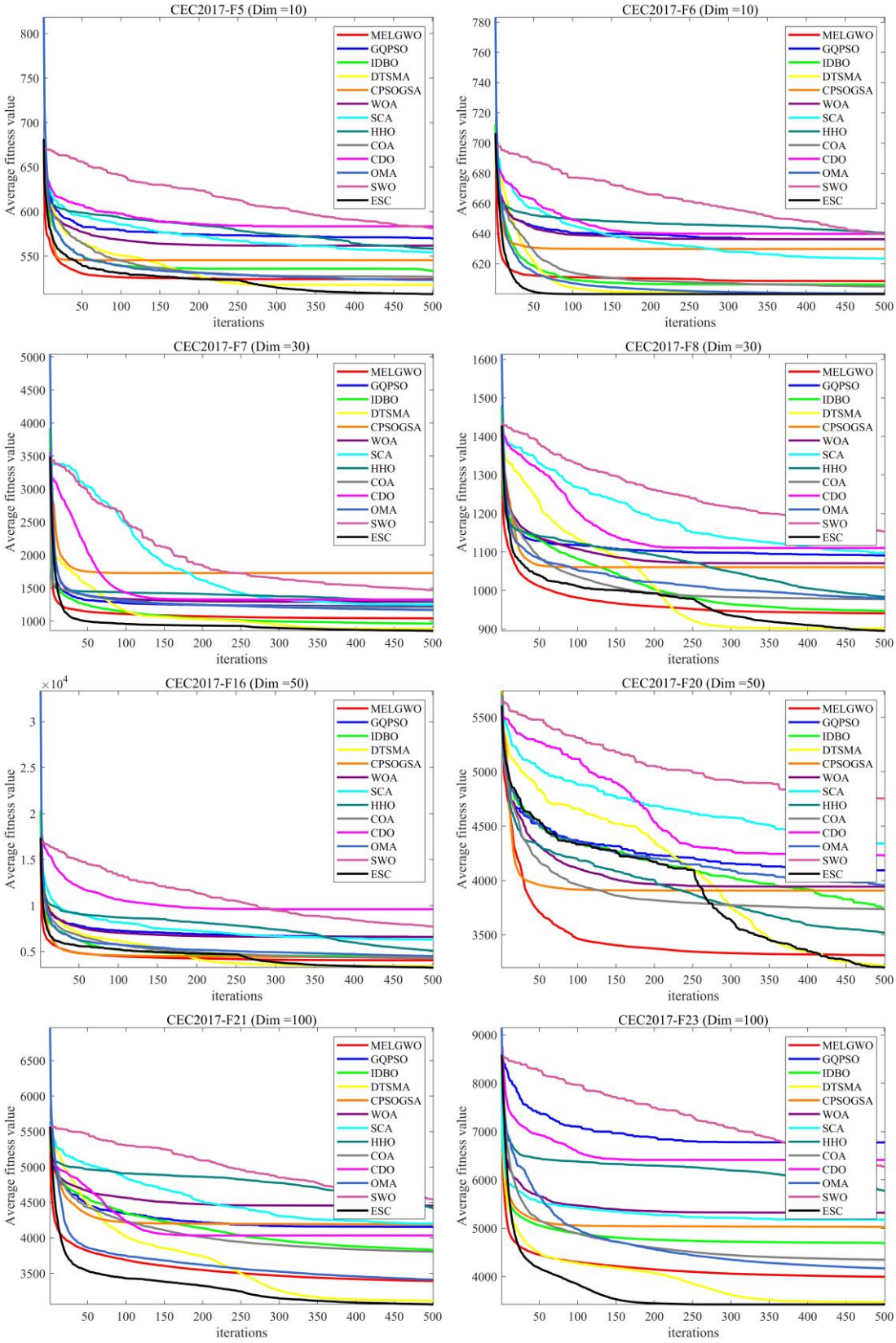

Fig.8 Comparison of iteration curves of different algorithms on CEC 2017 test suite

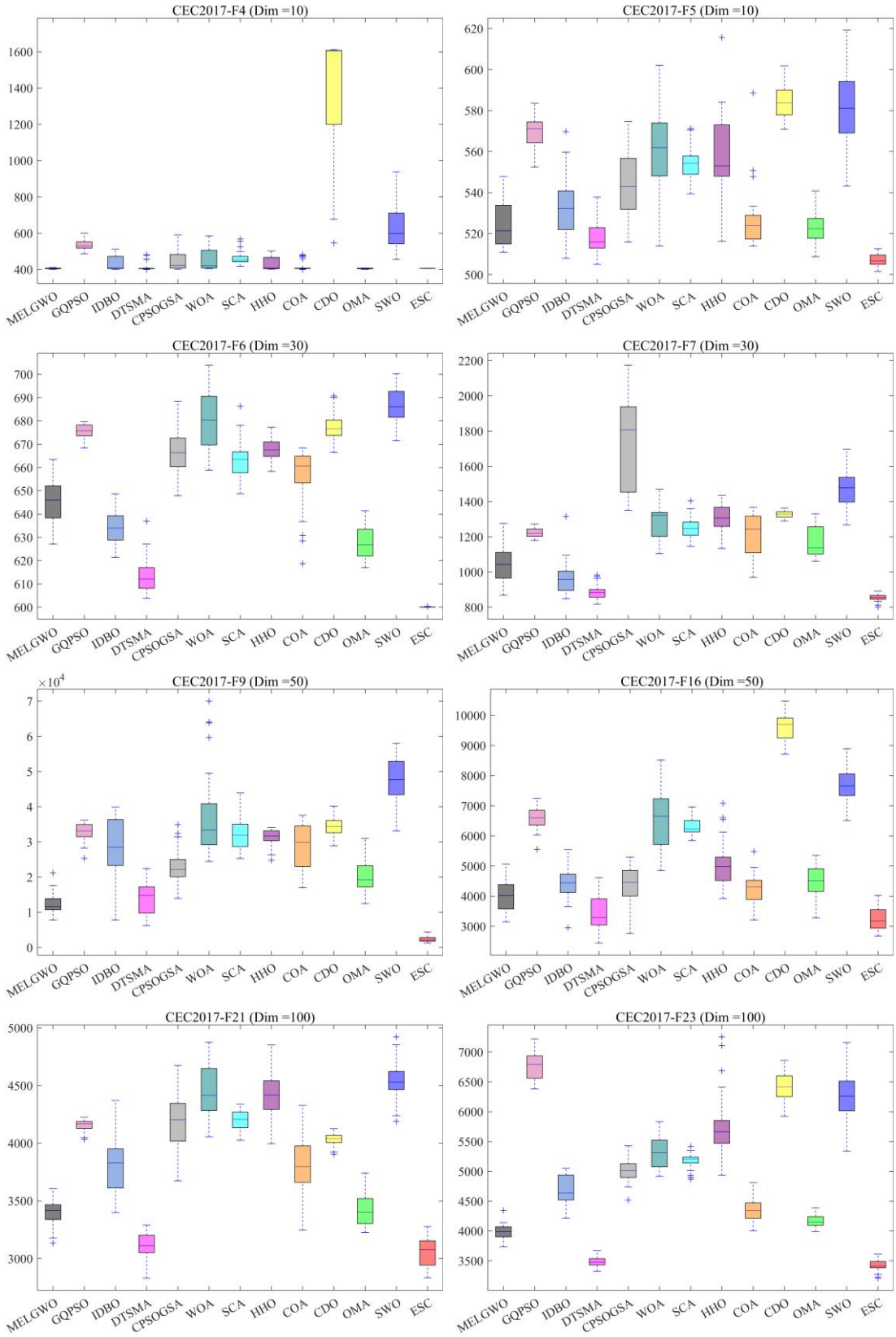

Fig. 9 Comparison of boxplot of different algorithms on CEC 2017 test suite

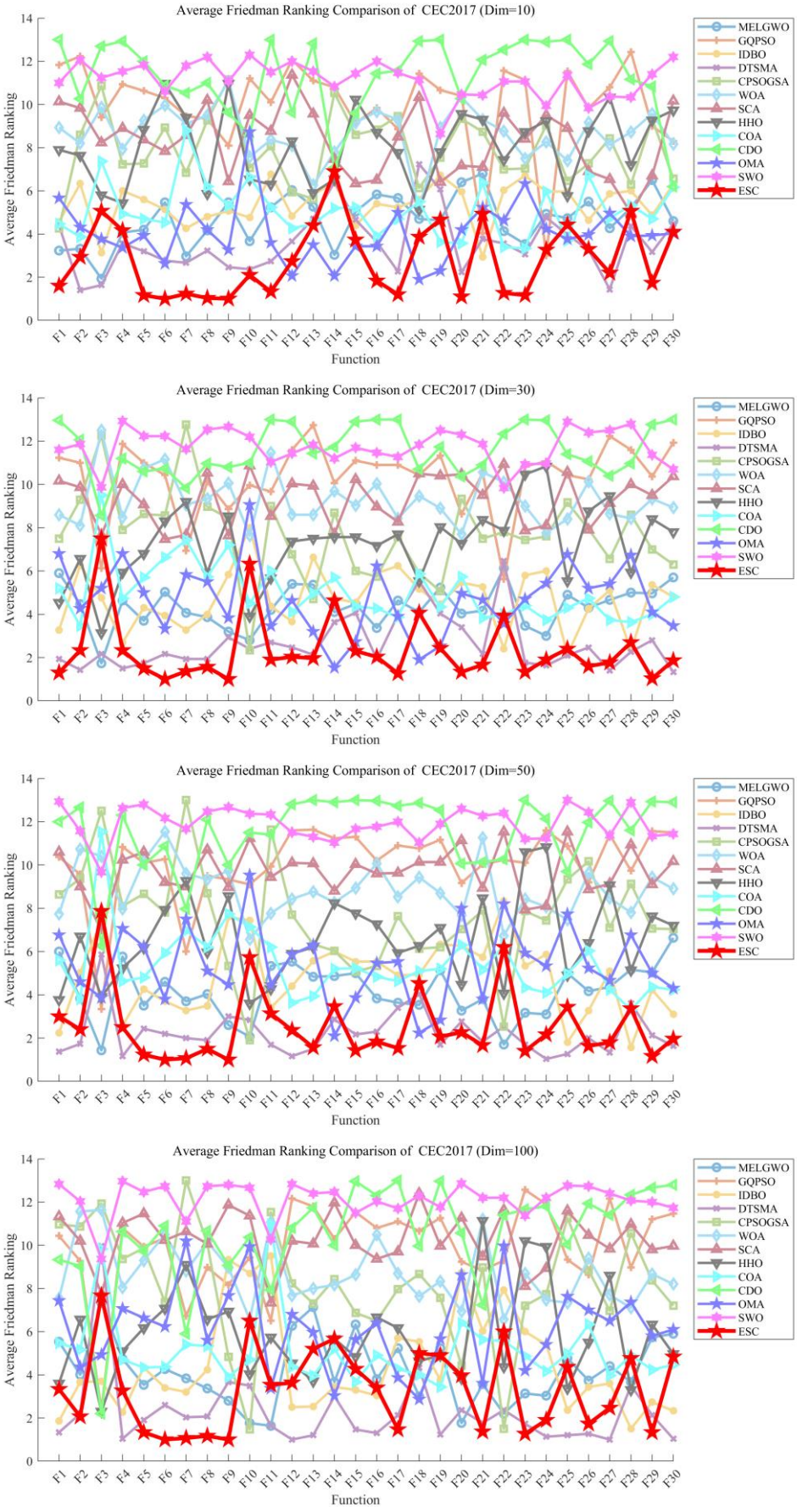

Fig.10 Average Friedman ranking of different algorithms on the CEC 2017 test suite

Table 5 Experimental results of 13 algorithms on the CEC 2017(Dim=10)

ID	index	MELGWO	GQPSO	IDBO	DTSMA	CPSOGSA	WOA	SCA	HHO	COA	CDO	OMA	SWO	ESC
F1	**Ave**	4.655E+03	4.409E+09	2.899E+06	6.147E+03	4.501E+07	6.106E+07	1.106E+09	2.594E+06	7.068E+03	1.396E+10	5.732E+04	2.898E+09	**1.248E+03**
	Std	4.066E+05	9.645E+05	8.485E+05	3.515E+05	9.381E+05	1.778E+06	2.064E+06	2.806E+06	5.331E+05	4.549E+05	**1.888E+05**	1.080E+07	2.441E+05
F2	**Ave**	3.270E+03	1.603E+09	9.567E+06	**2.073E+02**	2.912E+09	2.305E+07	1.998E+08	5.739E+06	2.175E+03	5.961E+07	3.306E+05	3.914E+09	1.559E+03
	Std	5.973E+03	1.592E+09	5.002E+07	**3.344E+01**	1.454E+10	3.930E+07	4.528E+08	1.259E+07	5.533E+03	1.125E+07	1.781E+06	7.184E+09	2.898E+03
F3	**Ave**	3.031E+02	5.337E+03	3.407E+02	**3.028E+02**	1.727E+04	7.789E+03	3.415E+03	7.973E+02	2.472E+03	1.798E+04	3.445E+02	1.199E+04	5.752E+02
	Std	5.708E+00	9.851E+02	1.036E+02	**6.797E+00**	2.052E+04	5.489E+03	1.615E+03	5.009E+02	1.724E+03	2.314E+02	5.484E+01	4.387E+03	3.900E+02
F4	**Ave**	4.057E+02	5.346E+02	4.309E+02	4.132E+02	4.422E+02	4.530E+02	4.619E+02	4.286E+02	4.170E+02	1.414E+03	**4.049E+02**	6.257E+02	4.064E+02
	Std	2.775E+00	2.563E+01	3.994E+01	2.217E+01	4.544E+01	5.763E+01	3.487E+01	3.575E+01	2.531E+01	3.062E+02	2.406E+00	1.204E+02	**5.799E-01**
F5	**Ave**	4.057E+02	5.346E+02	4.309E+02	4.132E+02	4.422E+02	4.530E+02	4.619E+02	4.286E+02	4.170E+02	1.414E+03	**4.049E+02**	6.257E+02	4.064E+02
	Std	1.094E+01	6.921E+00	1.371E+01	8.130E+00	1.558E+01	2.292E+01	7.342E+00	1.984E+01	1.461E+01	7.755E+00	8.219E+00	1.849E+01	**2.963E+00**
F6	**Ave**	6.086E+02	6.363E+02	6.063E+02	6.002E+02	6.299E+02	6.364E+02	6.235E+02	6.405E+02	6.051E+02	6.399E+02	6.004E+02	6.397E+02	**6.000E+02**
	Std	7.247E+00	4.101E+00	4.109E+00	2.197E-01	1.983E+01	1.190E+01	5.220E+00	1.140E+01	8.395E+00	4.048E+00	5.122E-01	1.316E+01	**5.275E-05**
F7	**Ave**	7.328E+02	7.898E+02	7.431E+02	7.304E+02	7.712E+02	7.879E+02	7.839E+02	7.920E+02	7.813E+02	7.972E+02	7.541E+02	8.211E+02	**7.191E+02**
	Std	1.246E+01	6.265E+00	1.331E+01	8.403E+00	4.118E+01	2.493E+01	1.453E+01	2.465E+01	2.272E+01	7.443E+00	1.284E+01	3.005E+01	**2.719E+00**
F8	**Ave**	8.208E+02	8.447E+02	8.242E+02	8.178E+02	8.457E+02	8.484E+02	8.496E+02	8.293E+02	8.307E+02	8.540E+02	8.217E+02	8.671E+02	**8.064E+02**
	Std	8.713E+00	5.069E+00	9.297E+00	5.742E+00	1.786E+01	1.916E+01	7.867E+00	1.045E+01	5.376E+00	7.419E+00	6.777E+00	1.250E+01	**2.080E+00**
F9	**Ave**	1.004E+03	1.172E+03	9.665E+02	9.008E+02	1.738E+03	1.600E+03	1.062E+03	1.574E+03	1.030E+03	1.334E+03	9.079E+02	1.627E+03	**9.000E+02**
	Std	1.609E+02	4.672E+01	6.460E+01	1.952E+00	5.036E+02	4.002E+02	6.865E+01	2.647E+02	1.918E+02	6.144E+01	2.105E+01	3.962E+02	**3.174E-07**
F10	**Ave**	1.004E+03	1.172E+03	9.665E+02	9.008E+02	1.738E+03	1.600E+03	1.062E+03	1.574E+03	1.030E+03	1.334E+03	9.079E+02	1.627E+03	**9.000E+02**
	Std	3.187E+02	2.035E+02	4.104E+02	2.107E+02	4.247E+02	2.648E+02	2.445E+02	2.672E+02	3.280E+02	2.073E+02	**1.943E+02**	2.153E+02	2.408E+02
F11	**Ave**	1.004E+03	1.172E+03	9.665E+02	9.008E+02	1.738E+03	1.600E+03	1.062E+03	1.574E+03	1.030E+03	1.334E+03	9.079E+02	1.627E+03	**9.000E+02**
	Std	3.734E+01	7.473E+01	1.192E+02	4.397E+01	1.056E+02	8.234E+01	9.200E+01	6.316E+01	4.631E+01	5.497E+02	1.292E+01	6.009E+02	**5.677E+00**
F12	**Ave**	5.773E+05	2.807E+07	2.314E+06	6.156E+04	1.292E+06	4.961E+06	2.173E+07	5.781E+06	5.760E+04	8.392E+06	**1.230E+04**	4.858E+07	2.167E+04
	Std	3.734E+01	7.473E+01	1.192E+02	4.397E+01	1.056E+02	8.234E+01	9.200E+01	6.316E+01	4.631E+01	5.497E+02	1.292E+01	6.009E+02	**5.677E+00**
F13	**Ave**	9.066E+03	5.684E+05	1.380E+04	1.334E+04	1.290E+04	1.627E+04	6.223E+04	1.198E+04	7.173E+03	8.130E+07	**4.853E+03**	9.577E+05	8.326E+03
	Std	7.123E+03	5.219E+05	1.280E+04	1.349E+04	1.082E+04	1.232E+04	4.212E+04	8.317E+03	5.956E+03	4.872E+07	**3.152E+03**	1.635E+06	6.721E+03
F14	**Ave**	1.554E+03	4.510E+03	2.068E+03	3.112E+03	6.623E+03	2.904E+03	2.346E+03	2.121E+03	1.751E+03	2.163E+03	**1.483E+03**	1.482E+04	3.804E+03
	Std	1.348E+02	1.730E+03	6.593E+02	2.406E+03	5.108E+03	1.733E+03	1.158E+03	9.297E+02	3.491E+02	6.984E+02	**2.936E+01**	2.729E+04	3.984E+03
F15	**Ave**	4.198E+03	6.537E+03	2.477E+03	3.002E+03	8.493E+03	9.078E+03	3.528E+03	8.269E+03	2.711E+03	6.571E+03	**2.196E+03**	2.374E+04	2.529E+03
	Std	1.348E+02	1.730E+03	6.593E+02	2.406E+03	5.108E+03	1.733E+03	1.158E+03	9.297E+02	3.491E+02	6.984E+02	**2.936E+01**	2.729E+04	3.984E+03
F16	**Ave**	1.759E+03	2.002E+03	1.747E+03	1.670E+03	1.952E+03	1.994E+03	1.793E+03	1.942E+03	1.690E+03	2.080E+03	1.650E+03	2.152E+03	**1.630E+03**
	Std	1.044E+02	5.368E+01	1.114E+02	7.809E+01	1.921E+02	1.683E+02	8.312E+01	1.183E+02	7.736E+01	**4.467E+01**	5.609E+01	1.281E+02	4.586E+01

F17	**Ave**	1.764E+03	1.800E+03	1.757E+03	1.728E+03	1.852E+03	1.820E+03	1.796E+03	1.794E+03	1.755E+03	1.861E+03	1.755E+03	1.898E+03	**1.710E+03**
	Std	3.714E+01	1.365E+01	2.023E+01	1.299E+01	1.025E+02	5.741E+01	1.835E+01	5.169E+01	3.267E+01	4.317E+01	1.233E+01	8.994E+01	**9.552E+00**
F18	**Ave**	1.764E+03	1.800E+03	1.757E+03	1.728E+03	1.852E+03	1.820E+03	1.796E+03	1.794E+03	1.755E+03	1.861E+03	1.755E+03	1.898E+03	**1.710E+03**
	Std	1.182E+04	1.056E+06	1.082E+04	1.313E+04	1.475E+04	1.082E+04	2.681E+05	1.103E+04	9.889E+03	1.015E+09	2.167E+03	6.837E+06	**1.000E+04**
F19	**Ave**	7.222E+03	1.137E+05	1.168E+04	9.390E+03	1.643E+04	1.699E+05	1.008E+04	2.061E+04	4.180E+03	1.332E+06	**2.586E+03**	4.160E+04	6.647E+03
	Std	6.986E+03	1.130E+05	9.645E+03	7.582E+03	1.633E+04	3.153E+05	8.276E+03	2.635E+04	3.675E+03	4.046E+05	**1.161E+03**	5.169E+04	7.082E+03
F20	**Ave**	2.111E+03	2.212E+03	2.088E+03	2.017E+03	2.193E+03	2.222E+03	2.124E+03	2.202E+03	2.050E+03	2.220E+03	2.048E+03	2.222E+03	**2.004E+03**
	Std	6.594E+01	4.708E+01	5.409E+01	1.129E+01	8.888E+01	8.517E+01	4.231E+01	8.565E+01	5.257E+01	5.680E+01	1.246E+01	7.571E+01	**7.710E+00**
F21	**Ave**	2.319E+03	2.253E+03	**2.229E+03**	2.258E+03	2.328E+03	2.338E+03	2.294E+03	2.328E+03	2.310E+03	2.370E+03	2.284E+03	2.354E+03	2.304E+03
	Std	2.374E+01	2.473E+01	4.809E+01	6.185E+01	5.596E+01	4.265E+01	6.665E+01	6.043E+01	3.759E+01	**6.668E+00**	4.825E+01	4.356E+01	2.508E+01
F22	**Ave**	2.301E+03	2.557E+03	2.310E+03	**2.298E+03**	2.433E+03	2.444E+03	2.389E+03	2.316E+03	2.301E+03	3.206E+03	2.304E+03	2.582E+03	2.300E+03
	Std	1.613E+01	4.346E+01	**1.471E+01**	1.793E+01	3.862E+02	3.756E+02	3.766E+01	5.690E+00	1.475E+01	4.754E+02	2.659E+00	2.166E+02	3.179E-01
F23	**Ave**	2.623E+03	2.699E+03	2.648E+03	2.619E+03	2.655E+03	2.656E+03	2.663E+03	2.674E+03	2.623E+03	2.884E+03	2.648E+03	2.701E+03	**2.609E+03**
	Std	1.360E+01	6.600E+00	1.540E+01	6.047E+00	1.945E+01	2.004E+01	8.523E+00	3.415E+01	8.584E+00	7.622E+01	3.014E+01	1.878E+01	**2.556E+00**
F24	**Ave**	2.743E+03	**2.696E+03**	2.727E+03	2.740E+03	2.781E+03	2.764E+03	2.783E+03	2.792E+03	2.754E+03	2.916E+03	2.716E+03	2.800E+03	2.741E+03
	Std	4.781E+01	6.284E+01	8.453E+01	4.606E+01	2.970E+01	6.347E+01	3.974E+01	1.045E+02	7.767E+00	2.430E+01	6.355E+01	6.396E+01	**3.298E+00**
F25	**Ave**	2.937E+03	3.134E+03	2.944E+03	2.929E+03	2.947E+03	2.949E+03	2.973E+03	2.944E+03	2.922E+03	3.593E+03	**2.915E+03**	3.138E+03	2.934E+03
	Std	2.665E+01	2.626E+01	3.198E+01	2.377E+01	7.845E+01	6.724E+01	2.318E+01	3.163E+01	6.399E+01	7.167E+01	6.278E+01	1.446E+02	**2.192E+01**
F26	**Ave**	3.143E+03	3.590E+03	3.014E+03	**2.951E+03**	3.376E+03	3.629E+03	3.123E+03	3.585E+03	3.316E+03	4.089E+03	2.975E+03	3.575E+03	3.013E+03
	Std	3.583E+02	1.266E+02	9.247E+01	5.401E+01	5.647E+02	6.126E+02	**3.727E+01**	5.319E+02	4.889E+02	2.462E+02	1.421E+02	3.510E+02	2.845E+02
F27	**Ave**	3.106E+03	3.194E+03	3.111E+03	**3.091E+03**	3.146E+03	3.141E+03	3.107E+03	3.188E+03	3.108E+03	3.291E+03	3.102E+03	3.187E+03	3.093E+03
	Std	2.550E+01	1.470E+01	2.574E+01	**2.486E+00**	3.696E+01	3.806E+01	3.187E+00	4.903E+01	2.522E+01	2.353E+01	6.729E+00	3.563E+01	3.313E+00
F28	**Ave**	3.332E+03	3.661E+03	3.353E+03	3.279E+03	3.359E+03	3.480E+03	3.306E+03	3.403E+03	3.332E+03	3.602E+03	**3.257E+03**	3.553E+03	3.353E+03
	Std	1.380E+02	3.842E+01	1.308E+02	1.368E+02	1.337E+02	1.832E+02	7.335E+01	1.480E+02	1.387E+02	**2.252E+00**	1.314E+02	1.084E+02	1.021E+02
F29	**Ave**	3.259E+03	3.325E+03	3.241E+03	3.194E+03	3.348E+03	3.368E+03	3.274E+03	3.361E+03	3.225E+03	3.391E+03	3.208E+03	3.434E+03	**3.167E+03**
	Std	7.697E+01	4.193E+01	5.912E+01	4.950E+01	8.633E+01	9.064E+01	6.730E+01	1.004E+02	4.937E+01	7.640E+01	2.638E+01	9.926E+01	**1.465E+01**
F30	**Ave**	4.066E+05	9.645E+05	8.485E+05	3.515E+05	9.381E+05	1.778E+06	2.064E+06	2.806E+06	5.331E+05	4.549E+05	**1.888E+05**	1.080E+07	2.441E+05
	Std	5.946E+05	4.053E+05	1.281E+06	4.564E+05	1.664E+06	2.026E+06	1.224E+06	3.208E+06	5.762E+05	**2.162E+05**	3.667E+05	8.906E+06	3.443E+05

Table 6 Experimental results of 13 algorithms on the CEC 2017(Dim=30)

ID	index	MELGWO	GQPSO	IDBO	DTSMA	CPSOGSA	WOA	SCA	HHO	COA	CDO	OMA	SWO	ESC
F1	**Ave**	1.725E+09	3.014E+10	1.127E+08	6.701E+06	4.752E+09	5.484E+09	2.327E+10	3.938E+08	1.133E+09	5.275E+10	1.893E+09	3.671E+10	**3.511E+05**
	Std	1.475E+09	2.272E+09	1.726E+08	1.444E+07	5.762E+09	2.270E+09	4.443E+09	2.463E+08	1.912E+09	3.210E+08	9.962E+08	9.464E+09	**1.783E+06**
F2	**Ave**	4.206E+31	6.259E+38	7.319E+33	2.992E+21	7.110E+41	5.277E+37	1.903E+38	5.576E+33	1.605E+27	5.376E+39	7.319E+28	4.427E+44	**9.259E+25**
	Std	1.469E+32	1.184E+39	3.414E+34	1.120E+22	3.869E+42	2.881E+38	6.476E+38	2.932E+34	8.471E+27	7.560E+39	3.671E+29	2.413E+45	**4.664E+26**
F3	**Ave**	**4.453E+04**	7.596E+04	6.742E+04	4.730E+04	2.487E+05	2.742E+05	8.983E+04	5.655E+04	1.249E+05	9.075E+04	6.928E+04	1.352E+05	9.055E+04
	Std	**1.062E+04**	5.575E+03	8.276E+03	1.438E+04	7.046E+04	7.152E+04	1.876E+04	7.179E+03	4.325E+04	4.307E+03	1.709E+04	4.557E+04	2.881E+04
F4	**Ave**	6.556E+02	5.937E+03	5.514E+02	**5.159E+02**	1.171E+03	1.275E+03	2.927E+03	7.114E+02	6.268E+02	5.500E+03	8.265E+02	1.017E+04	5.251E+02
	Std	1.380E+02	3.280E+02	3.954E+01	**2.470E+01**	4.571E+02	2.991E+02	8.088E+02	8.375E+01	6.927E+01	1.249E+02	1.528E+02	3.195E+03	3.207E+01
F5	**Ave**	6.757E+02	8.634E+02	6.870E+02	6.174E+02	8.080E+02	8.679E+02	8.280E+02	7.662E+02	7.328E+02	8.597E+02	7.161E+02	9.080E+02	**6.016E+02**
	Std	3.584E+01	**1.200E+01**	4.014E+01	2.933E+01	5.800E+01	6.597E+01	2.262E+01	4.041E+01	5.594E+01	1.855E+01	3.344E+01	4.138E+01	2.631E+01
F6	**Ave**	6.451E+02	6.753E+02	6.343E+02	6.136E+02	6.674E+02	6.816E+02	6.631E+02	6.675E+02	6.563E+02	6.777E+02	6.278E+02	6.869E+02	**6.001E+02**
	Std	8.268E+00	3.390E+00	7.152E+00	7.516E+00	1.031E+01	1.233E+01	8.019E+00	4.299E+00	1.293E+01	6.005E+00	6.720E+00	7.422E+00	**8.891E-02**
F7	**Ave**	1.043E+03	1.223E+03	9.642E+02	8.847E+02	1.729E+03	1.294E+03	1.251E+03	1.306E+03	1.210E+03	1.327E+03	1.168E+03	1.469E+03	**8.531E+02**
	Std	9.878E+01	2.645E+01	9.297E+01	4.494E+01	2.490E+02	9.342E+01	5.964E+01	7.232E+01	1.194E+02	1.948E+01	8.007E+01	1.016E+02	**1.895E+01**
F8	**Ave**	9.407E+02	1.090E+03	9.464E+02	9.012E+02	1.061E+03	1.071E+03	1.098E+03	9.833E+02	9.773E+02	1.110E+03	9.789E+02	1.153E+03	**8.951E+02**
	Std	2.803E+01	**1.210E+01**	4.014E+01	2.248E+01	5.197E+01	5.145E+01	2.447E+01	2.589E+01	2.501E+01	2.088E+01	3.034E+01	3.169E+01	2.332E+01
F9	**Ave**	3.919E+03	8.573E+03	6.189E+03	3.423E+03	8.360E+03	1.113E+04	7.949E+03	8.554E+03	7.490E+03	1.026E+04	4.342E+03	1.410E+04	**9.211E+02**
	Std	1.007E+03	8.422E+02	2.223E+03	1.405E+03	2.308E+03	3.930E+03	1.327E+03	1.110E+03	1.737E+03	1.030E+03	1.301E+03	2.651E+03	**2.921E+01**
F10	**Ave**	5.354E+03	8.705E+03	7.953E+03	**5.140E+03**	5.319E+03	7.718E+03	8.924E+03	6.052E+03	6.268E+03	8.966E+03	8.397E+03	9.404E+03	7.203E+03
	Std	6.945E+02	**2.517E+02**	1.100E+03	1.010E+03	6.587E+02	8.739E+02	3.168E+02	7.822E+02	9.231E+02	3.417E+02	6.507E+02	5.044E+02	4.521E+02
F11	**Ave**	1.576E+03	5.126E+03	1.477E+03	**1.340E+03**	4.821E+03	8.772E+03	3.738E+03	1.569E+03	1.773E+03	4.641E+04	1.386E+03	7.900E+03	1.349E+03
	Std	5.585E+02	5.839E+02	1.522E+02	**5.250E+01**	3.128E+03	2.718E+03	8.073E+02	1.546E+02	5.108E+02	7.877E+04	9.086E+01	2.662E+03	4.304E+02
F12	**Ave**	5.583E+07	7.088E+09	1.607E+07	3.997E+06	3.358E+08	5.667E+08	2.684E+09	1.198E+08	1.260E+07	9.907E+09	1.677E+07	6.530E+09	**2.974E+06**
	Std	1.098E+08	7.953E+08	2.556E+07	**2.858E+06**	7.631E+08	4.259E+08	6.308E+08	1.245E+08	8.493E+06	1.379E+08	1.409E+07	2.532E+09	3.659E+06
F13	**Ave**	1.223E+05	4.289E+09	7.161E+06	2.763E+04	8.588E+07	1.366E+07	8.959E+08	1.170E+06	1.568E+05	2.509E+09	2.709E+05	3.057E+09	**2.322E+04**
	Std	5.657E+04	9.769E+08	1.824E+07	2.686E+04	3.316E+08	2.809E+07	3.641E+08	1.106E+06	2.206E+05	1.317E+08	9.731E+05	1.598E+09	**1.507E+04**
F14	**Ave**	2.023E+05	1.936E+06	2.778E+05	1.145E+05	1.970E+06	2.647E+06	8.814E+05	1.255E+06	4.517E+05	2.892E+06	**2.267E+04**	3.780E+06	3.139E+05
	Std	2.051E+05	6.022E+05	3.444E+05	7.499E+04	1.954E+06	2.875E+06	8.864E+05	1.353E+06	5.497E+05	1.827E+05	**2.256E+04**	2.890E+06	3.818E+05
F15	**Ave**	2.324E+04	1.277E+08	4.186E+04	2.147E+04	5.605E+04	5.421E+06	6.574E+07	1.345E+05	2.325E+04	6.520E+08	1.005E+04	3.059E+08	**9.352E+03**
	Std	1.408E+04	5.376E+07	7.206E+04	1.505E+04	5.015E+04	4.477E+06	5.658E+07	9.205E+04	1.369E+04	3.834E+05	7.430E+03	2.769E+08	**6.759E+03**
F16	**Ave**	2.760E+03	4.640E+03	3.345E+03	**2.509E+03**	3.311E+03	4.423E+03	4.087E+03	3.678E+03	2.993E+03	9.851E+03	3.401E+03	4.972E+03	2.533E+03
	Std	3.456E+02	2.564E+02	3.919E+02	2.542E+02	4.241E+02	7.634E+02	2.433E+02	5.682E+02	4.010E+02	2.292E+03	**1.993E+02**	3.912E+02	2.386E+02

F17	**Ave**	2.326E+03	3.126E+03	2.521E+03	2.296E+03	2.727E+03	2.809E+03	2.754E+03	2.727E+03	2.285E+03	2.093E+04	2.285E+03	3.289E+03	**1.913E+03**
	Std	2.063E+02	1.710E+02	3.003E+02	2.568E+02	3.431E+02	2.888E+02	2.022E+02	3.610E+02	1.764E+02	1.540E+04	1.636E+02	3.966E+02	**1.523E+02**
F18	**Ave**	1.575E+06	1.153E+07	2.825E+06	2.215E+06	3.256E+06	1.250E+07	1.415E+07	2.039E+06	2.423E+06	1.128E+07	**3.043E+05**	3.231E+07	1.244E+06
	Std	2.441E+06	4.239E+06	4.509E+06	1.817E+06	3.324E+06	1.358E+07	8.974E+06	1.833E+06	2.478E+06	1.896E+06	**4.122E+05**	2.500E+07	1.924E+06
F19	**Ave**	5.697E+04	1.329E+08	1.427E+05	2.537E+04	6.706E+04	1.623E+07	9.324E+07	1.797E+06	2.812E+04	1.461E+08	1.052E+04	3.403E+08	**9.181E+03**
	Std	7.648E+04	4.357E+07	3.883E+05	1.941E+04	1.004E+05	1.889E+07	4.167E+07	1.753E+06	2.922E+04	9.637E+06	1.062E+04	3.138E+08	**7.845E+03**
F20	**Ave**	2.543E+03	2.898E+03	2.669E+03	2.492E+03	2.953E+03	2.854E+03	3.018E+03	2.792E+03	2.641E+03	3.022E+03	2.639E+03	3.235E+03	**2.239E+03**
	Std	1.679E+02	**9.725E+01**	1.812E+02	1.774E+02	2.721E+02	2.014E+02	1.494E+02	2.041E+02	2.583E+02	1.463E+02	1.400E+02	1.766E+02	1.283E+02
F21	**Ave**	2.457E+03	2.634E+03	2.481E+03	2.413E+03	2.563E+03	2.651E+03	2.616E+03	2.588E+03	2.457E+03	2.644E+03	2.474E+03	2.684E+03	**2.406E+03**
	Std	3.507E+01	**1.386E+01**	6.690E+01	2.438E+01	5.613E+01	7.377E+01	2.670E+01	5.108E+01	5.367E+01	2.275E+01	3.341E+01	4.378E+01	1.634E+01
F22	**Ave**	5.754E+03	6.039E+03	**2.769E+03**	6.158E+03	6.987E+03	8.474E+03	9.414E+03	6.920E+03	3.661E+03	1.035E+04	2.873E+03	8.523E+03	4.283E+03
	Std	1.714E+03	2.500E+02	1.460E+03	1.554E+03	**1.078E+03**	1.310E+03	2.103E+03	1.787E+03	2.286E+03	4.181E+02	4.426E+02	1.859E+03	2.855E+03
F23	**Ave**	2.828E+03	3.284E+03	2.957E+03	2.758E+03	3.071E+03	3.173E+03	3.100E+03	3.308E+03	2.887E+03	3.751E+03	2.893E+03	3.325E+03	**2.731E+03**
	Std	5.203E+01	5.225E+01	7.522E+01	**2.700E+01**	9.851E+01	1.160E+02	3.944E+01	1.462E+02	7.119E+01	7.752E+01	4.331E+01	8.630E+01	3.090E+01
F24	**Ave**	2.983E+03	3.551E+03	3.119E+03	**2.925E+03**	3.220E+03	3.243E+03	3.259E+03	3.546E+03	3.020E+03	3.852E+03	3.095E+03	3.549E+03	2.940E+03
	Std	4.802E+01	4.205E+01	6.696E+01	3.818E+01	1.011E+02	9.775E+01	3.962E+01	1.689E+02	6.245E+01	4.556E+01	5.228E+01	1.243E+02	**2.168E+01**
F25	**Ave**	2.988E+03	3.543E+03	2.922E+03	**2.921E+03**	3.387E+03	3.241E+03	3.565E+03	3.014E+03	2.976E+03	3.623E+03	3.074E+03	4.873E+03	2.927E+03
	Std	3.969E+01	1.007E+02	3.228E+01	2.683E+01	2.790E+02	7.879E+01	2.020E+02	3.656E+01	4.531E+01	3.051E+01	5.136E+01	8.662E+02	**2.618E+01**
F26	**Ave**	5.919E+03	8.862E+03	5.854E+03	4.782E+03	7.867E+03	8.898E+03	7.862E+03	7.967E+03	6.072E+03	9.010E+03	6.489E+03	9.928E+03	**4.348E+03**
	Std	8.665E+02	4.375E+02	1.141E+03	**2.323E+02**	1.070E+03	1.263E+03	4.701E+02	1.692E+03	1.475E+03	3.501E+02	6.640E+02	8.315E+02	3.044E+02
F27	**Ave**	3.305E+03	3.930E+03	3.323E+03	**3.226E+03**	3.390E+03	3.521E+03	3.560E+03	3.614E+03	3.281E+03	3.670E+03	3.323E+03	4.006E+03	3.231E+03
	Std	5.030E+01	1.167E+02	6.095E+01	1.328E+01	6.618E+01	1.462E+02	7.455E+01	2.106E+02	4.315E+01	4.891E+01	3.572E+01	2.667E+02	**1.116E+01**
F28	**Ave**	3.473E+03	5.136E+03	3.319E+03	**3.317E+03**	4.141E+03	3.977E+03	4.540E+03	3.506E+03	3.371E+03	5.063E+03	3.614E+03	6.242E+03	3.336E+03
	Std	1.666E+02	1.234E+02	5.912E+01	1.111E+02	6.348E+02	3.695E+02	4.770E+02	1.173E+02	4.626E+01	**3.706E+01**	1.443E+02	6.687E+02	4.501E+01
F29	**Ave**	4.386E+03	5.559E+03	4.481E+03	3.949E+03	4.769E+03	5.305E+03	5.272E+03	5.117E+03	4.183E+03	6.545E+03	4.203E+03	6.033E+03	**3.591E+03**
	Std	2.597E+02	2.346E+02	4.166E+02	1.711E+02	3.954E+02	4.677E+02	3.617E+02	5.636E+02	2.802E+02	3.138E+02	1.818E+02	6.735E+02	**1.182E+02**
F30	**Ave**	2.398E+06	7.017E+08	3.276E+06	**2.504E+04**	4.499E+06	5.389E+07	2.162E+08	1.263E+07	9.953E+05	3.002E+09	2.859E+05	3.603E+08	4.698E+04
	Std	1.993E+06	1.566E+08	5.948E+06	**2.047E+04**	5.531E+06	3.941E+07	7.210E+07	8.218E+06	7.362E+05	8.355E+08	2.674E+05	2.111E+08	4.582E+04

Table 7 Experimental results of 13 algorithms on the CEC 2017(Dim=50)

ID	index	MELGWO	GQPSO	IDBO	DTSMA	CPSOGSA	WOA	SCA	HHO	COA	CDO	OMA	SWO	ESC
F1	**Ave**	1.392E+10	6.599E+10	1.725E+09	**1.056E+09**	3.110E+10	2.170E+10	6.880E+10	5.349E+09	1.205E+10	8.091E+10	1.696E+10	9.987E+10	3.192E+09
	Std	5.538E+09	2.098E+09	1.557E+09	1.437E+09	1.537E+10	5.476E+09	8.029E+09	1.752E+09	5.606E+09	**9.562E+08**	4.520E+09	1.337E+10	2.729E+09
F2	**Ave**	1.392E+10	6.599E+10	1.725E+09	**1.056E+09**	3.110E+10	2.170E+10	6.880E+10	5.349E+09	1.205E+10	8.091E+10	1.696E+10	9.987E+10	3.192E+09
	Std	2.981E+58	1.310E+75	2.363E+60	**1.401E+49**	8.083E+77	1.404E+85	3.578E+73	1.769E+66	1.596E+58	3.383E+77	2.773E+57	1.207E+82	4.149E+56
F3	**Ave**	**1.284E+05**	1.660E+05	2.194E+05	1.938E+05	4.237E+05	2.983E+05	2.155E+05	1.711E+05	3.367E+05	1.974E+05	1.670E+05	3.204E+05	2.288E+05
	Std	1.987E+04	**9.630E+03**	3.520E+04	4.076E+04	9.948E+04	8.035E+04	4.461E+04	2.069E+04	6.946E+04	1.544E+04	3.081E+04	2.520E+05	3.798E+04
F4	**Ave**	2.344E+03	1.635E+04	9.275E+02	**6.647E+02**	5.698E+03	4.821E+03	1.414E+04	1.898E+03	1.792E+03	2.232E+04	3.175E+03	2.639E+04	9.471E+02
	Std	1.105E+03	1.384E+03	2.018E+02	**6.038E+01**	2.857E+03	1.518E+03	2.908E+03	4.797E+02	8.996E+02	4.828E+02	1.035E+03	5.975E+03	2.441E+02
F5	**Ave**	8.414E+02	1.116E+03	8.665E+02	7.961E+02	1.062E+03	1.128E+03	1.135E+03	9.298E+02	8.951E+02	1.118E+03	9.490E+02	1.233E+03	**7.251E+02**
	Std	5.571E+01	**1.915E+01**	8.312E+01	5.982E+01	9.225E+01	8.037E+01	4.089E+01	3.224E+01	2.866E+01	2.955E+01	6.955E+01	4.956E+01	5.534E+01
F6	**Ave**	6.566E+02	6.905E+02	6.488E+02	6.327E+02	6.785E+02	6.987E+02	6.848E+02	6.797E+02	6.675E+02	6.930E+02	6.503E+02	7.026E+02	**6.032E+02**
	Std	6.999E+00	2.956E+00	8.026E+00	9.740E+00	9.762E+00	1.186E+01	7.637E+00	4.958E+00	5.160E+00	4.870E+00	9.231E+00	9.206E+00	**1.503E+00**
F7	**Ave**	1.438E+03	1.755E+03	1.344E+03	1.162E+03	3.240E+03	1.912E+03	1.866E+03	1.882E+03	1.752E+03	1.822E+03	1.788E+03	2.106E+03	**1.056E+03**
	Std	1.319E+02	2.997E+01	1.385E+02	8.068E+01	4.264E+02	1.135E+02	8.768E+01	9.954E+01	9.924E+01	3.738E+01	1.415E+02	1.289E+02	**4.313E+01**
F8	**Ave**	1.167E+03	1.395E+03	1.134E+03	1.063E+03	1.355E+03	1.391E+03	1.444E+03	1.235E+03	1.240E+03	1.508E+03	1.211E+03	1.549E+03	**1.053E+03**
	Std	5.024E+01	**1.846E+01**	4.289E+01	4.439E+01	7.084E+01	7.910E+01	2.783E+01	3.418E+01	2.831E+01	2.611E+01	7.191E+01	6.105E+01	4.211E+01
F9	**Ave**	1.222E+04	3.282E+04	2.828E+04	1.400E+04	2.323E+04	3.795E+04	3.243E+04	3.130E+04	2.869E+04	3.447E+04	2.019E+04	4.738E+04	**2.316E+03**
	Std	2.924E+03	2.453E+03	8.758E+03	4.464E+03	4.577E+03	1.268E+04	5.027E+03	2.271E+03	6.129E+03	2.792E+03	4.522E+03	6.282E+03	**7.461E+02**
F10	**Ave**	9.167E+03	1.482E+04	1.365E+04	9.773E+03	**9.030E+03**	1.328E+04	1.540E+04	1.061E+04	1.371E+04	1.564E+04	1.492E+04	1.625E+04	1.298E+04
	Std	9.932E+02	4.145E+02	2.003E+03	1.184E+03	1.103E+03	1.195E+03	5.040E+02	8.414E+02	8.132E+02	4.045E+02	**3.773E+02**	6.636E+02	5.896E+02
F11	**Ave**	4.471E+03	1.468E+04	2.998E+03	**2.017E+03**	2.773E+04	8.526E+03	1.297E+04	3.272E+03	5.553E+03	1.996E+04	3.564E+03	2.657E+04	2.974E+03
	Std	1.897E+03	9.533E+02	1.178E+03	**8.392E+02**	1.495E+04	2.299E+03	3.047E+03	7.617E+02	2.598E+03	9.743E+02	1.322E+03	6.519E+03	1.558E+03
F12	**Ave**	1.704E+09	4.222E+10	6.203E+08	**3.137E+07**	3.301E+09	4.077E+09	2.241E+10	1.181E+09	3.321E+08	5.630E+10	9.749E+08	4.139E+10	1.549E+08
	Std	2.719E+09	3.606E+09	5.649E+08	**2.051E+07**	2.522E+09	1.334E+09	5.241E+09	8.483E+08	2.083E+08	4.613E+08	6.337E+08	1.139E+10	1.999E+08
F13	**Ave**	3.860E+07	1.962E+10	8.132E+07	5.599E+04	4.359E+08	5.305E+08	7.154E+09	4.183E+07	1.881E+06	4.686E+10	5.847E+07	1.784E+10	**5.388E+04**
	Std	7.783E+07	3.177E+09	1.214E+08	3.065E+04	7.547E+08	2.650E+08	2.923E+09	5.957E+07	1.973E+06	3.064E+09	7.421E+07	6.473E+09	**2.754E+04**
F14	**Ave**	1.539E+06	2.163E+07	3.267E+06	6.331E+05	3.173E+06	6.293E+06	8.707E+06	6.930E+06	1.954E+06	7.251E+07	**3.322E+05**	3.576E+07	1.114E+06
	Std	1.201E+06	5.419E+06	3.438E+06	5.828E+05	3.640E+06	4.692E+06	9.257E+06	5.059E+06	1.720E+06	6.512E+06	**2.806E+05**	2.515E+07	1.465E+06
F15	**Ave**	2.467E+06	2.910E+09	1.417E+05	2.097E+04	1.411E+07	8.235E+07	1.058E+09	3.488E+06	1.089E+05	1.511E+10	1.285E+05	3.988E+09	**1.232E+04**
	Std	1.032E+07	3.234E+08	1.584E+05	1.072E+04	7.635E+07	8.392E+07	2.368E+08	7.888E+06	7.978E+04	2.378E+09	2.249E+05	1.791E+09	**6.209E+03**
F16	**Ave**	4.045E+03	6.594E+03	4.440E+03	3.422E+03	4.385E+03	6.594E+03	6.301E+03	5.064E+03	4.252E+03	9.601E+03	4.514E+03	7.717E+03	**3.251E+03**

	Std	5.728E+02	3.401E+02	4.968E+02	5.625E+02	5.923E+02	9.341E+02	**2.912E+02**	7.498E+02	4.893E+02	4.280E+02	5.179E+02	6.481E+02	3.735E+02
F17	**Ave**	3.415E+03	5.685E+03	3.620E+03	3.310E+03	4.379E+03	4.694E+03	5.091E+03	3.814E+03	3.595E+03	8.873E+03	3.757E+03	8.202E+03	**2.954E+03**
	Std	4.230E+02	4.109E+02	4.732E+02	3.954E+02	6.140E+02	6.517E+02	4.104E+02	4.028E+02	4.638E+02	3.821E+02	3.652E+02	3.565E+03	**2.573E+02**
F18	**Ave**	4.839E+06	7.117E+07	7.915E+06	5.257E+06	1.395E+07	5.251E+07	5.819E+07	1.178E+07	7.219E+06	2.080E+08	**2.203E+06**	9.986E+07	7.502E+06
	Std	4.914E+06	1.796E+07	7.535E+06	3.977E+06	1.819E+07	4.214E+07	3.161E+07	9.060E+06	4.655E+06	5.523E+06	1.901E+06	6.476E+07	7.945E+06
F19	**Ave**	5.176E+05	1.350E+09	3.348E+06	**2.004E+04**	2.235E+08	1.567E+07	6.999E+08	2.507E+06	3.895E+05	1.911E+09	7.242E+04	1.789E+09	3.040E+04
	Std	5.844E+05	3.714E+08	4.079E+06	**1.641E+04**	7.223E+08	1.303E+07	2.715E+08	2.349E+06	3.936E+05	3.202E+07	1.018E+05	1.075E+09	3.183E+04
F20	**Ave**	3.312E+03	4.093E+03	3.734E+03	3.213E+03	3.907E+03	3.943E+03	4.339E+03	3.518E+03	3.737E+03	4.231E+03	3.959E+03	4.753E+03	**3.198E+03**
	Std	3.307E+02	**1.265E+02**	4.322E+02	3.428E+02	3.379E+02	3.764E+02	2.080E+02	3.452E+02	2.846E+02	2.413E+02	1.732E+02	2.843E+02	2.848E+02
F21	**Ave**	2.658E+03	2.987E+03	2.765E+03	2.561E+03	2.900E+03	3.050E+03	2.955E+03	2.923E+03	2.732E+03	2.992E+03	2.662E+03	3.092E+03	**2.552E+03**
	Std	7.746E+01	**2.177E+01**	1.084E+02	4.974E+01	1.209E+02	9.201E+01	5.223E+01	1.144E+02	7.248E+01	2.883E+01	5.611E+01	7.529E+01	4.170E+01
F22	**Ave**	1.023E+04	1.680E+04	1.535E+04	**1.075E+04**	1.082E+04	1.489E+04	1.720E+04	1.239E+04	1.456E+04	1.678E+04	1.548E+04	1.779E+04	1.456E+04
	Std	9.272E+02	5.567E+02	2.886E+03	1.369E+03	7.610E+02	8.877E+02	3.998E+02	8.652E+02	1.647E+03	**5.366E+02**	2.632E+03	6.842E+02	5.649E+02
F23	**Ave**	3.158E+03	3.948E+03	3.437E+03	**2.997E+03**	3.743E+03	3.785E+03	3.739E+03	4.068E+03	3.310E+03	4.827E+03	3.509E+03	4.168E+03	2.974E+03
	Std	1.158E+02	5.838E+01	1.190E+02	**5.128E+01**	1.970E+02	1.656E+02	8.192E+01	2.068E+02	1.211E+02	2.249E+02	2.331E+02	2.077E+02	6.915E+01
F24	**Ave**	3.286E+03	4.526E+03	3.606E+03	**3.121E+03**	3.827E+03	3.890E+03	3.887E+03	4.437E+03	3.405E+03	4.600E+03	3.548E+03	4.466E+03	3.198E+03
	Std	7.681E+01	9.155E+01	1.655E+02	4.112E+01	1.658E+02	1.415E+02	7.904E+01	2.792E+02	1.257E+02	8.718E+01	9.776E+01	1.816E+02	**3.328E+01**
F25	**Ave**	4.003E+03	8.327E+03	3.282E+03	**3.203E+03**	7.071E+03	5.207E+03	9.089E+03	3.825E+03	3.905E+03	7.437E+03	5.167E+03	1.456E+04	3.513E+03
	Std	4.594E+02	1.912E+02	7.689E+01	**9.497E+01**	2.404E+03	6.007E+02	9.659E+02	1.954E+02	3.565E+02	1.235E+02	8.095E+02	2.050E+03	1.691E+02
F26	**Ave**	9.755E+03	1.403E+04	8.438E+03	6.532E+03	1.483E+04	1.448E+04	1.374E+04	1.194E+04	1.179E+04	1.650E+04	1.098E+04	1.693E+04	**6.029E+03**
	Std	1.502E+03	2.716E+02	2.596E+03	8.937E+02	1.850E+03	1.551E+03	7.964E+02	1.398E+03	1.547E+03	**2.219E+02**	8.629E+02	1.142E+03	6.626E+02
F27	**Ave**	3.886E+03	6.344E+03	3.984E+03	**3.491E+03**	4.315E+03	4.962E+03	4.990E+03	5.193E+03	3.858E+03	8.534E+03	3.945E+03	6.394E+03	3.574E+03
	Std	1.717E+02	1.760E+02	2.086E+02	9.089E+01	3.176E+02	6.770E+02	2.583E+02	6.416E+02	1.480E+02	1.035E+03	1.733E+02	4.828E+02	**5.767E+01**
F28	**Ave**	4.938E+03	8.164E+03	**3.875E+03**	4.441E+03	7.715E+03	6.118E+03	9.047E+03	4.906E+03	4.419E+03	9.356E+03	5.544E+03	1.152E+04	4.418E+03
	Std	4.113E+02	2.683E+02	3.062E+02	7.031E+02	1.871E+03	7.124E+02	9.038E+02	3.607E+02	4.735E+02	**1.124E+02**	5.738E+02	1.213E+03	4.346E+02
F29	**Ave**	5.927E+03	1.549E+04	5.661E+03	4.658E+03	7.044E+03	9.887E+03	9.337E+03	7.448E+03	5.700E+03	2.443E+04	5.965E+03	1.572E+04	**4.106E+03**
	Std	6.346E+02	2.579E+03	6.688E+02	4.619E+02	8.027E+02	2.151E+03	1.473E+03	1.093E+03	6.552E+02	1.397E+03	4.404E+02	4.990E+03	**2.764E+02**
F30	**Ave**	1.014E+08	2.734E+09	2.788E+07	**7.240E+06**	1.607E+08	3.350E+08	1.343E+09	1.475E+08	3.409E+07	5.517E+09	4.284E+07	2.996E+09	1.010E+07
	Std	3.262E+07	4.934E+08	2.619E+07	**3.624E+06**	1.831E+08	1.301E+08	3.994E+08	7.783E+07	1.375E+07	6.064E+07	1.947E+07	1.782E+09	4.337E+06

Table 8 Experimental results of 13 algorithms on the CEC 2017(Dim=100)

ID	index	MELGWO	GQPSO	IDBO	DTSMA	CPSOGSA	WOA	SCA	HHO	COA	CDO	OMA	SWO	ESC
F1	**Ave**	7.541E+10	1.903E+11	3.341E+10	2.710E+10	2.062E+11	1.132E+11	2.131E+11	4.987E+10	7.464E+10	1.738E+11	1.144E+11	2.594E+11	**5.121E+10**
	Std	1.473E+09	2.649E+10	**1.405E+08**	1.559E+07	3.142E+09	3.006E+09	1.362E+10	7.889E+08	1.067E+09	3.105E+10	1.521E+09	2.714E+10	7.969E+08
F2	**Ave**							3.106E+16			4.388E+15			
		6.179E+144	6.674E+158	5.395E+145	7.821E+138	1.610E+171	1.229E+175	3	2.857E+155	2.482E+153	7	1.032E+141	2.828E+174	**6.678E+136**
	Std	2.138E+145	-	2.953E+146	3.447E+139	-	-	-	-	-	-	4.346E+141	-	**3.657E+137**
F3	**Ave**	5.857E+05	**3.483E+05**	3.778E+05	7.678E+05	9.945E+05	9.089E+05	6.132E+05	3.523E+05	7.499E+05	3.488E+05	4.264E+05	9.086E+05	5.974E+05
	Std	1.731E+05	1.365E+04	2.782E+04	1.275E+05	2.340E+05	1.545E+05	8.742E+04	3.098E+04	1.224E+05	**1.072E+04**	5.006E+04	7.881E+05	7.007E+04
F4	**Ave**	8.921E+03	4.986E+04	4.674E+03	**1.891E+03**	3.991E+04	2.320E+04	5.178E+04	9.577E+03	9.324E+03	5.028E+04	1.613E+04	8.168E+04	6.265E+03
	Std	2.308E+03	3.641E+03	1.314E+03	**7.271E+02**	1.288E+04	4.482E+03	7.434E+03	1.900E+03	2.883E+03	1.164E+03	3.051E+03	1.658E+04	1.553E+03
F5	**Ave**	1.481E+03	1.981E+03	1.540E+03	1.313E+03	1.972E+03	1.966E+03	2.071E+03	1.678E+03	1.523E+03	1.976E+03	1.730E+03	2.183E+03	**1.242E+03**
	Std	9.002E+01	2.892E+01	1.385E+02	9.752E+01	1.144E+02	1.470E+02	6.550E+01	5.425E+01	3.838E+01	**3.030E+01**	9.355E+01	9.121E+01	8.882E+01
F6	**Ave**	1.481E+03	1.981E+03	1.540E+03	1.313E+03	1.972E+03	1.966E+03	2.071E+03	1.678E+03	1.523E+03	1.976E+03	1.730E+03	2.183E+03	**1.242E+03**
	Std	5.107E+00	**2.130E+00**	1.047E+01	6.462E+00	8.646E+00	9.933E+00	5.493E+00	3.346E+00	2.994E+00	4.221E+00	9.925E+00	5.239E+00	2.609E+00
F7	**Ave**	3.047E+03	3.529E+03	2.813E+03	2.410E+03	7.623E+03	3.810E+03	4.082E+03	3.840E+03	3.366E+03	3.452E+03	4.078E+03	4.164E+03	**2.043E+03**
	Std	1.768E+02	**6.627E+01**	2.342E+02	1.592E+02	4.475E+02	1.693E+02	2.035E+02	1.008E+02	1.354E+02	9.419E+01	4.210E+02	1.993E+02	1.793E+02
F8	**Ave**	1.831E+03	2.345E+03	1.913E+03	1.643E+03	2.407E+03	2.422E+03	2.409E+03	2.132E+03	2.042E+03	2.432E+03	2.051E+03	2.635E+03	**1.535E+03**
	Std	9.939E+01	**4.483E+01**	1.798E+02	1.183E+02	1.415E+02	1.288E+02	6.521E+01	6.369E+01	5.871E+01	4.583E+01	1.304E+02	9.050E+01	1.079E+02
F9	**Ave**	3.670E+04	7.161E+04	7.530E+04	4.351E+04	5.352E+04	7.916E+04	9.195E+04	6.720E+04	4.468E+04	7.426E+04	6.833E+04	1.034E+05	**1.785E+04**
	Std	1.009E+04	**3.244E+03**	6.754E+03	1.247E+04	9.263E+03	1.767E+04	8.715E+03	5.205E+03	1.108E+04	4.704E+03	9.511E+03	6.849E+03	3.304E+03
F10	**Ave**	**1.937E+04**	3.222E+04	3.113E+04	2.292E+04	1.890E+04	2.911E+04	3.305E+04	2.391E+04	2.529E+04	3.253E+04	3.235E+04	3.413E+04	2.936E+04
	Std	1.184E+03	5.866E+02	2.119E+03	2.315E+03	1.319E+03	1.402E+03	6.402E+02	1.674E+03	3.363E+03	7.422E+02	**4.427E+02**	7.743E+02	8.710E+02
F11	**Ave**	6.716E+04	1.677E+05	2.537E+05	**6.150E+04**	3.232E+05	3.325E+05	1.841E+05	1.484E+05	3.072E+05	1.960E+05	9.623E+04	2.723E+05	1.037E+05
	Std	**1.178E+04**	1.369E+04	6.585E+04	1.836E+04	7.472E+04	1.234E+05	3.296E+04	3.421E+04	8.471E+04	2.496E+04	1.783E+04	7.326E+04	2.238E+04
F12	**Ave**	2.291E+10	1.248E+11	5.020E+09	**1.236E+09**	4.124E+10	2.923E+10	9.895E+10	1.215E+10	1.233E+10	1.086E+11	2.496E+10	1.481E+11	9.023E+09
	Std	1.212E+10	4.478E+09	3.215E+09	**5.746E+08**	1.539E+10	5.460E+09	9.817E+09	4.486E+09	7.118E+09	1.989E+09	9.442E+09	2.113E+10	3.659E+09
F13	**Ave**	2.923E+09	2.786E+10	1.378E+08	**1.327E+07**	2.493E+09	3.169E+09	1.773E+10	3.106E+08	8.156E+08	2.814E+10	1.304E+09	3.304E+10	8.836E+08
	Std	2.454E+09	1.312E+09	1.546E+08	**3.521E+07**	1.518E+09	1.033E+09	3.309E+09	2.070E+08	1.261E+09	3.788E+08	1.212E+09	7.663E+09	7.047E+08
F14	**Ave**	6.250E+06	3.058E+07	6.239E+06	5.720E+06	2.905E+07	1.996E+07	6.751E+07	1.064E+07	9.929E+06	3.045E+07	**5.470E+06**	9.315E+07	1.102E+07
	Std	2.938E+06	4.709E+06	5.852E+06	3.540E+06	2.432E+07	8.330E+06	2.585E+07	3.609E+06	5.028E+06	3.454E+06	**2.396E+06**	5.308E+07	6.047E+06
F15	**Ave**	2.352E+08	1.289E+10	1.924E+07	**3.296E+05**	3.853E+08	4.563E+08	6.310E+09	2.131E+07	1.384E+07	2.625E+10	3.456E+07	1.335E+10	9.791E+07
	Std	3.785E+08	1.649E+09	5.117E+07	**7.131E+05**	7.563E+08	2.689E+08	1.953E+09	3.548E+07	3.964E+07	9.858E+07	4.123E+07	4.404E+09	2.341E+08
F16	**Ave**	8.072E+03	1.694E+04	7.571E+03	**6.472E+03**	9.753E+03	1.661E+04	1.477E+04	9.977E+03	8.681E+03	1.895E+04	9.924E+03	1.887E+04	7.712E+03

	Std	9.890E+02	**5.172E+02**	8.664E+02	7.066E+02	1.316E+03	2.724E+03	9.014E+02	1.382E+03	1.012E+03	8.069E+02	1.181E+03	1.964E+03	9.236E+02
F17	**Ave**	9.540E+03	2.520E+05	8.029E+03	5.740E+03	6.332E+04	2.772E+04	7.317E+04	8.742E+03	6.959E+03	1.123E+07	6.810E+03	1.097E+06	**5.442E+03**
	Std	6.836E+03	1.011E+05	1.545E+03	5.345E+02	1.815E+05	2.925E+04	5.662E+04	2.043E+03	1.055E+03	2.542E+05	1.405E+03	1.356E+06	**5.257E+02**
F18	**Ave**	**5.384E+06**	5.048E+07	1.162E+07	8.195E+06	3.311E+07	1.996E+07	1.311E+08	9.490E+06	8.287E+06	4.096E+07	5.616E+06	1.669E+08	1.061E+07
	Std	3.098E+06	1.202E+07	6.461E+06	3.603E+06	2.005E+07	1.012E+07	6.334E+07	5.197E+06	5.521E+06	6.112E+06	**2.445E+06**	1.072E+08	6.984E+06
F19	**Ave**	3.792E+08	1.125E+10	4.365E+07	**1.562E+06**	8.526E+08	4.835E+08	5.579E+09	3.831E+07	2.045E+07	2.281E+10	8.414E+07	1.389E+10	1.841E+08
	Std	9.387E+08	1.421E+09	6.159E+07	**6.783E+06**	1.796E+09	2.282E+08	1.373E+09	1.792E+07	2.962E+07	7.503E+07	7.477E+07	3.587E+09	2.738E+08
F20	**Ave**	**5.430E+03**	7.620E+03	7.449E+03	5.743E+03	6.368E+03	7.077E+03	8.075E+03	6.247E+03	6.925E+03	7.886E+03	7.478E+03	8.656E+03	6.307E+03
	Std	4.846E+02	3.001E+02	4.677E+02	6.441E+02	5.468E+02	6.748E+02	3.324E+02	4.756E+02	5.181E+02	3.066E+02	**2.514E+02**	2.816E+02	3.722E+02
F21	**Ave**	3.393E+03	4.155E+03	3.829E+03	3.113E+03	4.189E+03	4.455E+03	4.202E+03	4.419E+03	3.805E+03	4.034E+03	3.411E+03	4.540E+03	**3.062E+03**
	Std	1.034E+02	**4.643E+01**	2.415E+02	1.088E+02	2.199E+02	2.346E+02	9.074E+01	2.050E+02	2.310E+02	5.805E+01	1.276E+02	1.720E+02	1.179E+02
F22	**Ave**	2.340E+04	3.450E+04	3.318E+04	2.399E+04	**2.187E+04**	3.192E+04	3.557E+04	2.781E+04	3.007E+04	3.538E+04	3.467E+04	3.629E+04	3.123E+04
	Std	1.785E+03	6.179E+02	1.731E+03	1.946E+03	1.662E+03	1.084E+03	**4.741E+02**	1.401E+03	2.738E+03	5.731E+02	6.926E+02	1.063E+03	1.116E+03
F23	**Ave**	3.996E+03	6.775E+03	4.690E+03	3.472E+03	5.028E+03	5.321E+03	5.177E+03	5.771E+03	4.349E+03	6.413E+03	4.171E+03	6.273E+03	**3.424E+03**
	Std	1.184E+02	2.318E+02	2.429E+02	**8.188E+01**	2.186E+02	2.729E+02	1.231E+02	5.177E+02	1.921E+02	2.113E+02	1.018E+02	4.145E+02	9.954E+01
F24	**Ave**	4.720E+03	9.658E+03	5.794E+03	**4.026E+03**	6.772E+03	6.658E+03	7.412E+03	8.425E+03	5.296E+03	9.774E+03	5.836E+03	9.871E+03	4.207E+03
	Std	2.443E+02	1.845E+02	4.067E+02	**1.082E+02**	4.340E+02	3.642E+02	2.793E+02	5.943E+02	3.389E+02	5.130E+02	2.945E+02	8.896E+02	1.413E+02
F25	**Ave**	7.826E+03	1.743E+04	6.056E+03	**5.174E+03**	2.356E+04	1.091E+04	2.344E+04	6.724E+03	8.384E+03	1.785E+04	1.196E+04	2.813E+04	7.534E+03
	Std	1.235E+03	**4.076E+02**	1.054E+03	5.314E+02	5.272E+03	1.108E+03	2.140E+03	7.408E+02	1.186E+03	4.317E+02	1.645E+03	3.126E+03	1.026E+03
F26	**Ave**	2.518E+04	3.733E+04	2.338E+04	**1.396E+04**	3.791E+04	3.966E+04	4.141E+04	3.185E+04	3.284E+04	4.511E+04	3.451E+04	5.005E+04	1.569E+04
	Std	3.783E+03	**6.960E+02**	3.101E+03	1.207E+03	3.528E+03	3.258E+03	2.309E+03	1.449E+03	2.403E+03	8.656E+02	4.061E+03	4.492E+03	1.588E+03
F27	**Ave**	4.687E+03	1.082E+04	4.328E+03	**3.724E+03**	5.739E+03	6.020E+03	8.787E+03	7.087E+03	4.518E+03	1.028E+04	5.434E+03	1.134E+04	4.133E+03
	Std	3.460E+02	6.721E+02	2.923E+02	**7.362E+01**	7.123E+02	8.980E+02	7.392E+02	1.076E+03	4.345E+02	4.441E+02	3.180E+02	1.130E+03	1.350E+02
F28	**Ave**	9.904E+03	1.924E+04	**7.347E+03**	1.012E+04	2.765E+04	1.491E+04	2.835E+04	9.341E+03	1.096E+04	3.346E+04	1.535E+04	3.299E+04	1.129E+04
	Std	1.190E+03	5.557E+02	1.048E+03	3.997E+03	4.862E+03	1.463E+03	3.429E+03	8.426E+02	1.547E+03	**4.749E+02**	2.053E+03	3.798E+03	1.429E+03
F29	**Ave**	1.265E+04	7.954E+04	9.222E+03	8.596E+03	2.405E+04	2.240E+04	3.858E+04	1.343E+04	1.105E+04	1.869E+05	1.281E+04	1.529E+05	**7.782E+03**
	Std	1.687E+03	1.863E+04	9.850E+02	9.128E+02	1.231E+04	4.485E+03	1.709E+04	1.255E+03	1.030E+03	1.483E+04	1.126E+03	1.035E+05	**7.371E+02**
F30	**Ave**	1.473E+09	2.649E+10	1.405E+08	**1.559E+07**	3.142E+09	3.006E+09	1.362E+10	7.889E+08	1.067E+09	3.105E+10	1.521E+09	2.714E+10	7.969E+08
	Std	1.636E+09	1.720E+09	1.093E+08	**1.182E+07**	4.175E+09	1.294E+09	2.689E+09	4.201E+08	1.273E+09	5.485E+08	1.238E+09	4.645E+09	6.534E+08

4.4.2 Comparison with Other Competitive Algorithms on CEC 2022

In this section, we present a comprehensive evaluation of the ESC algorithm's performance in comparison with 12 other methodologies, specifically focusing on dimensions of 10 and 20 within the framework of the CEC 2022 benchmark suite. This analysis meticulously documents the mean value (Ave) and standard deviation (Std) derived from thirty independent trials for each algorithm, as depicted in **Table 9** and **10**. A pivotal element of our study centers on the convergence velocity of the algorithm through a comparative assessment of the iteration advancements among different algorithms. As shown in Fig.11, the ESC algorithm exhibits a markedly more rapid convergence rate than its counterparts.

In addition, to evaluate the stability of the algorithm, **Fig.12** provides a boxplot analysis of the ESC algorithm compared with similar algorithms. The ESC algorithm is characterized by small variance, which emphasizes its consistency and reliability across operations. In addition, **Fig.13** aims to visually convey the effectiveness of various algorithms in solving optimization challenges across different functions, using the Friedman average ranking as a benchmark for comparison.

In the CEC 2022 benchmark tests, the ESC algorithm exhibited impressive performance across the 10 and 20-dimensional tests, ranking first in the Friedman mean ranking for both dimensions. Overall, the ESC algorithm outperformed all other competing algorithms, particularly displaying stable performance across most functions. A detailed comparison between ESC and other algorithms reveals that, in the 10 and 20-dimensional tests, ESC outperformed MELGWO and IDBO on most functions. In the 10-dimensional scenario, ESC performed superior on 7 functions, with only slight inferiority on one function. In the 20-dimensional scenario, ESC outperformed MELGWO on 9 functions, demonstrating greater adaptability and superiority. IDBO's performance on some specific functions was close to ESC's, but overall, it could not surpass ESC's stability and convergence speed. The DTSMA algorithm exhibited very close competition with ESC in the CEC 2022 benchmark tests, particularly in the 10 and 20-dimensional Friedman mean rankings, where DTSMA closely followed ESC. While DTSMA outperformed ESC on certain functions, ESC maintained an overall performance and convergence speed advantage. GQPSO and SCA continued to perform poorly in the CEC 2022 benchmark tests, with these algorithms lagging behind ESC on most functions, particularly in terms of convergence speed and stability. HHO and WOA performed moderately in the 10 and 20-dimensional tests but fell short of ESC on most functions. CPSOGSA's performance in the 20-dimensional test was relatively average, with some success on specific functions, but overall, it did not surpass ESC. COA performed slightly better than WOA and HHO in the 10 and 20-dimensional tests, but still failed to overtake ESC in overall ranking. CDO and SWO continued to perform poorly across all dimensions, ranking low in the Friedman mean rankings, indicating their inadequacies in handling complex multi-dimensional optimization problems. OMA's performance in the 10 and 20-dimensional tests was also unable to surpass ESC, although it performed well on a few specific functions. However, in the overall ranking, it still fell behind. The analysis of the iteration curves in **Fig.11** shows that the ESC algorithm's convergence speed in the 10 and 20 dimensions was significantly superior to other algorithms. The boxplot in **Fig.12** further confirmed the stability of the ESC algorithm, with low variance indicating high consistency across different

experiments.

While the ESC algorithm performed excellently on most test functions, its advantage was less pronounced on some specific complex functions, and in a few cases, it even showed performance close to or slightly inferior to DTSMA. This suggests that, although the ESC algorithm excels in handling a wide range of optimization problems, there is room for improvement in dealing with certain extreme or specialized optimization problems.

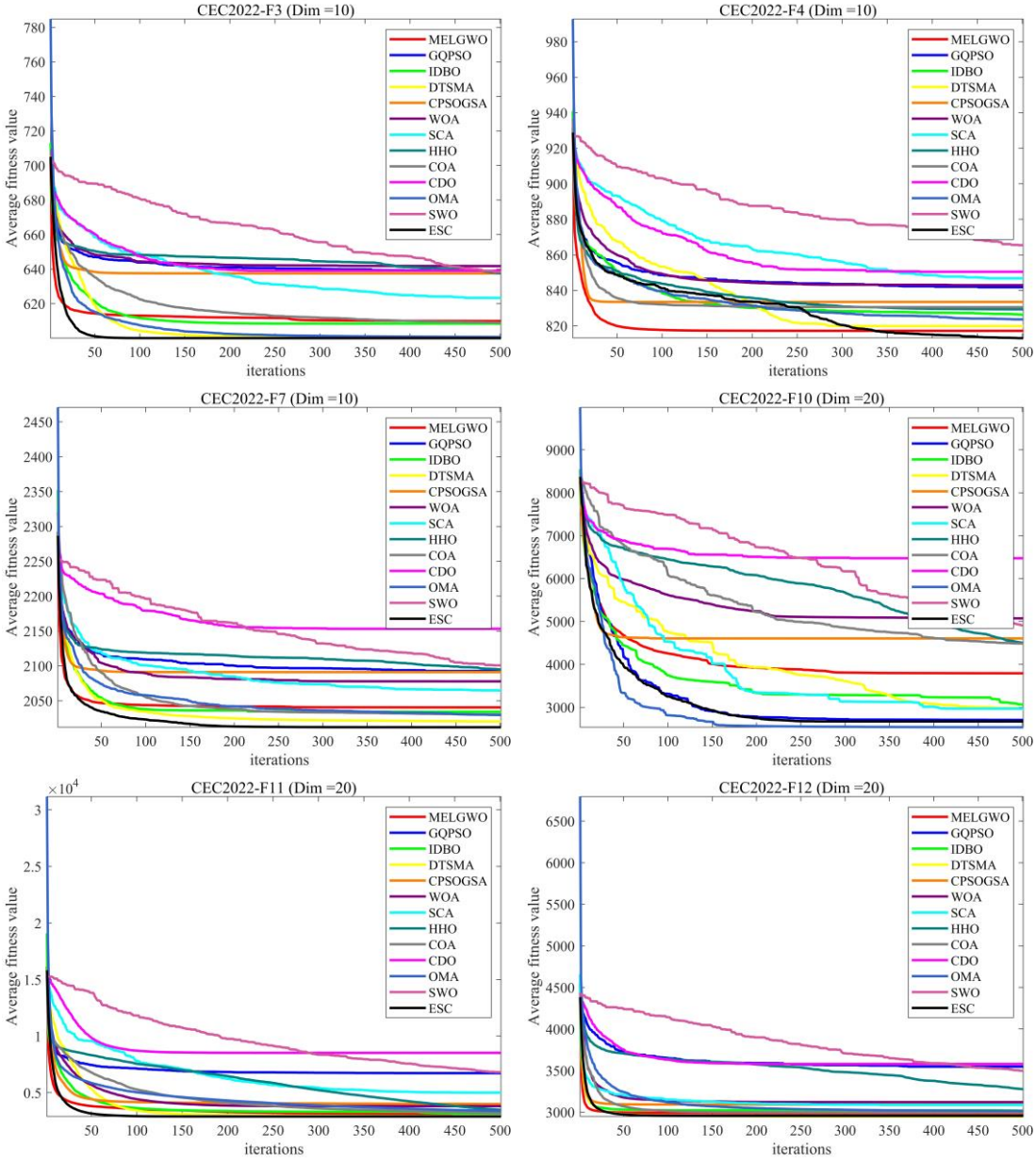

Fig.11 Comparison of iteration curves of different algorithms on CEC 2022 test suite

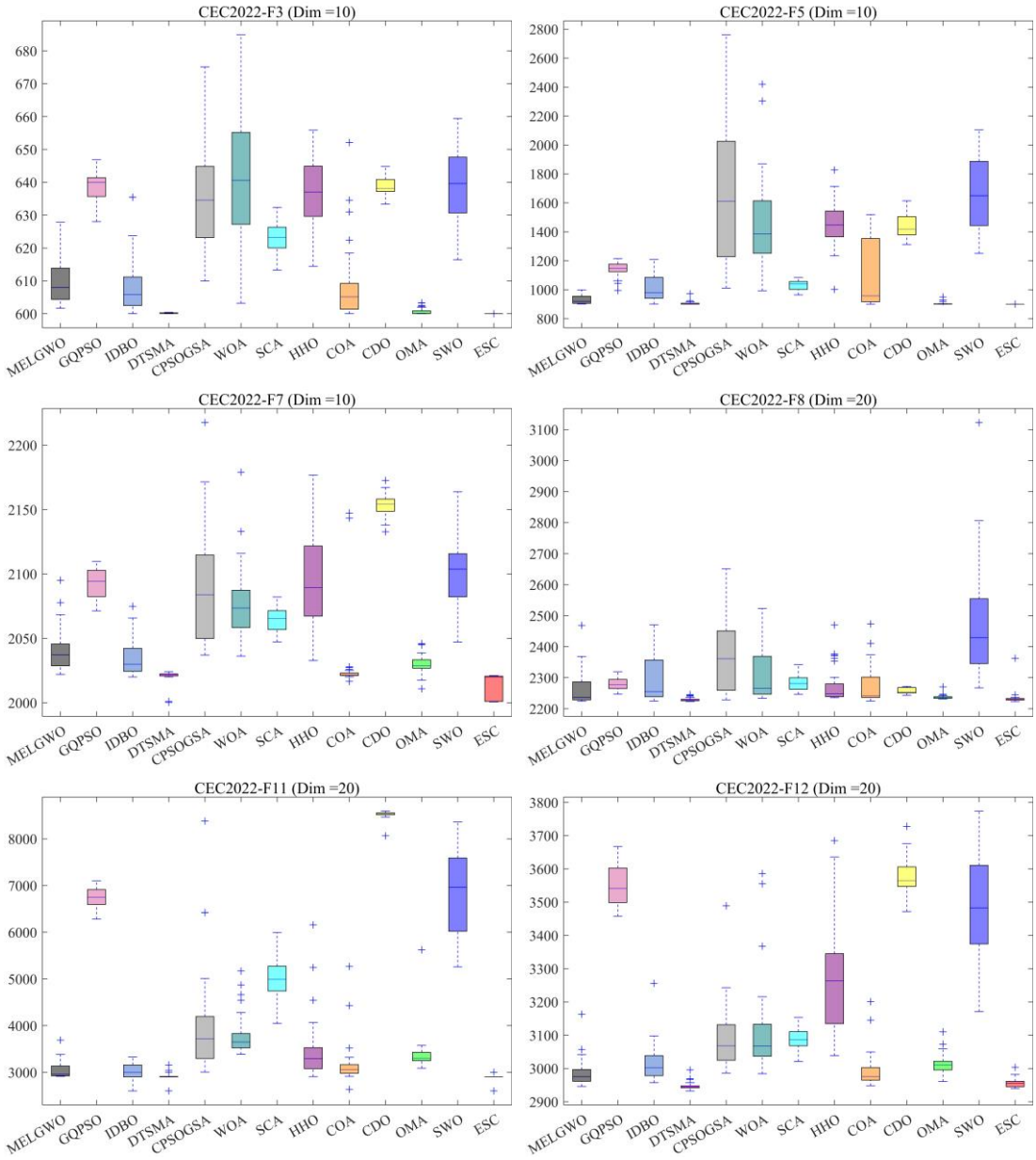

Fig. 12 Comparison of boxplot of different algorithms on CEC 2022 test suite

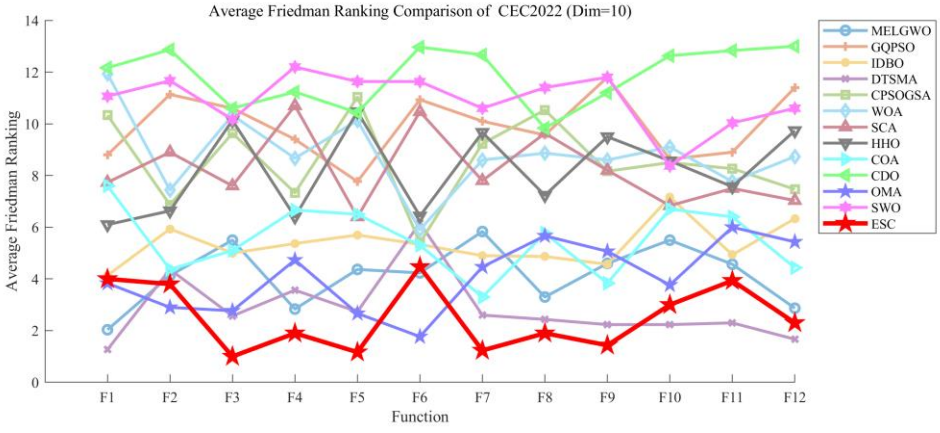

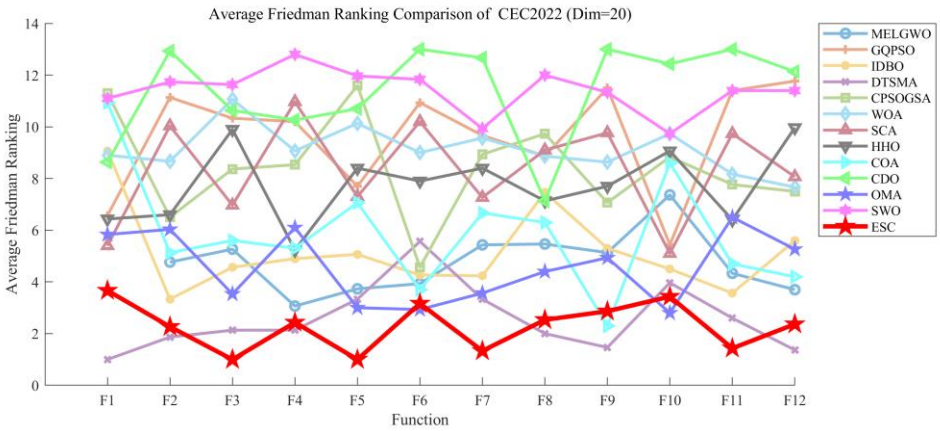

Fig.13 Friedman average ranking of different algorithms on the CEC 2022 test suite

Table 9 Experimental results of 13 algorithms on the CEC 2022(Dim=10)

ID	index	MELGWO	GQPSO	IDBO	DTSMA	CPSOGSA	WOA	SCA	HHO	COA	CDO	OMA	SWO	ESC
F1	**Ave**	3.029E+02	4.264E+03	5.706E+02	**3.005E+02**	1.377E+04	2.383E+04	2.433E+03	9.441E+02	2.998E+03	1.410E+06	3.623E+02	1.283E+04	4.193E+02
	Std	6.285E+00	8.248E+02	4.003E+02	**1.431E+00**	1.059E+04	1.168E+04	1.251E+03	3.729E+02	1.870E+03	7.568E+06	6.570E+01	6.379E+03	1.172E+02
F2	**Ave**	4.166E+02	5.995E+02	4.229E+02	4.114E+02	4.451E+02	4.618E+02	4.771E+02	4.526E+02	4.166E+02	8.711E+02	4.125E+02	6.841E+02	**4.059E+02**
	Std	2.620E+01	3.893E+01	2.683E+01	1.654E+01	4.993E+01	6.728E+01	2.250E+01	6.186E+01	2.543E+01	1.895E+01	2.413E+01	1.343E+02	**3.379E+00**
F3	**Ave**	6.099E+02	6.389E+02	6.083E+02	6.002E+02	6.375E+02	6.418E+02	6.233E+02	6.375E+02	6.089E+02	6.391E+02	6.007E+02	6.383E+02	**6.000E+02**
	Std	7.622E+00	4.206E+00	8.031E+00	1.148E-01	1.851E+01	1.882E+01	4.772E+00	1.173E+01	1.196E+01	3.151E+00	9.863E-01	1.214E+01	**1.511E-04**
F4	**Ave**	8.172E+02	8.418E+02	8.261E+02	8.199E+02	8.335E+02	8.429E+02	8.468E+02	8.293E+02	8.305E+02	8.505E+02	8.237E+02	8.654E+02	**8.131E+02**
	Std	7.213E+00	**3.845E+00**	9.933E+00	5.826E+00	1.317E+01	1.772E+01	7.245E+00	9.281E+00	4.239E+00	7.818E+00	5.864E+00	1.434E+01	4.894E+00
F5	**Ave**	9.305E+02	1.142E+03	1.007E+03	9.060E+02	1.653E+03	1.467E+03	1.032E+03	1.456E+03	1.095E+03	1.442E+03	9.041E+02	1.647E+03	**9.000E+02**
	Std	2.933E+01	5.025E+01	8.636E+01	1.377E+01	4.694E+02	3.263E+02	3.320E+01	1.670E+02	2.276E+02	8.546E+01	1.034E+01	2.540E+02	**3.887E-02**
F6	**Ave**	3.671E+03	5.792E+06	4.635E+03	5.582E+03	4.607E+03	5.375E+03	3.740E+06	6.830E+03	4.666E+03	8.184E+08	**2.189E+03**	2.160E+07	3.836E+03
	Std	1.884E+03	4.310E+06	2.175E+03	2.060E+03	2.257E+03	4.523E+03	2.977E+06	4.486E+03	2.050E+03	6.755E+08	**4.118E+02**	2.401E+07	1.655E+03
F7	**Ave**	2.041E+03	2.093E+03	2.034E+03	2.020E+03	2.091E+03	2.078E+03	2.065E+03	2.095E+03	2.031E+03	2.153E+03	2.030E+03	2.101E+03	**2.012E+03**
	Std	1.779E+01	1.170E+01	1.408E+01	**5.449E+00**	4.613E+01	2.889E+01	9.133E+00	3.679E+01	3.131E+01	8.288E+00	7.852E+00	2.409E+01	9.830E+00
F8	**Ave**	2.222E+03	2.237E+03	2.226E+03	2.221E+03	2.287E+03	2.235E+03	2.236E+03	2.232E+03	2.238E+03	2.239E+03	2.228E+03	2.248E+03	**2.217E+03**
	Std	5.337E+00	4.110E+00	5.380E+00	4.997E+00	5.595E+01	5.743E+00	3.147E+00	7.686E+00	3.755E+01	8.605E+00	**2.343E+00**	1.534E+01	8.314E+00
F9	**Ave**	2.536E+03	2.673E+03	2.537E+03	2.529E+03	2.585E+03	2.603E+03	2.581E+03	2.619E+03	2.534E+03	2.664E+03	2.529E+03	2.680E+03	**2.529E+03**
	Std	2.693E+01	1.249E+01	2.568E+01	4.425E-05	4.358E+01	4.885E+01	1.904E+01	5.048E+01	2.683E+01	3.215E+00	7.403E-01	4.286E+01	**1.112E-07**
F10	**Ave**	2.569E+03	2.553E+03	2.566E+03	**2.504E+03**	2.614E+03	2.688E+03	2.523E+03	2.613E+03	2.577E+03	2.825E+03	2.504E+03	2.561E+03	2.526E+03
	Std	1.046E+02	6.173E+01	6.648E+01	2.075E+01	1.252E+02	2.883E+02	5.105E+01	1.559E+02	9.949E+01	2.509E+02	**2.058E+01**	7.827E+01	4.775E+01
F11	**Ave**	2.698E+03	2.877E+03	2.745E+03	**2.633E+03**	2.911E+03	2.908E+03	2.795E+03	2.833E+03	2.787E+03	3.339E+03	2.741E+03	3.012E+03	2.717E+03
	Std	1.380E+02	**3.958E+01**	1.523E+02	8.649E+01	1.904E+02	3.100E+02	7.785E+01	1.771E+02	1.659E+02	5.670E+01	1.227E+02	2.504E+02	1.249E+02
F12	**Ave**	2.865E+03	2.955E+03	2.874E+03	**2.863E+03**	2.889E+03	2.907E+03	2.872E+03	2.917E+03	2.868E+03	3.071E+03	2.869E+03	2.937E+03	2.864E+03
	Std	4.235E+00	1.152E+01	9.101E+00	1.666E+00	2.974E+01	4.392E+01	3.259E+00	3.616E+01	7.611E+00	2.982E+01	3.997E+00	3.253E+01	**1.145E+00**

Table 10 Experimental results of 13 algorithms on the CEC 2022(Dim=20)

ID	index	MELGWO	GQPSO	IDBO	DTSMA	CPSOGSA	WOA	SCA	HHO	COA	CDO	OMA	SWO	ESC
F1	**Ave**	7.212E+03	2.373E+04	3.382E+04	**2.386E+03**	5.313E+04	3.265E+04	2.030E+04	2.331E+04	4.534E+04	3.050E+04	2.103E+04	4.680E+04	1.285E+04
	Std	2.810E+03	4.429E+03	1.011E+04	**1.648E+03**	1.812E+04	1.107E+04	5.839E+03	1.056E+04	1.458E+04	3.987E+03	6.668E+03	1.566E+04	5.189E+03
F2	**Ave**	4.985E+02	1.090E+03	4.719E+02	**4.500E+02**	5.552E+02	6.379E+02	8.610E+02	5.355E+02	5.092E+02	2.106E+03	5.231E+02	1.408E+03	4.543E+02

	Std	4.611E+01	7.134E+01	2.747E+01	1.320E+01	1.295E+02	8.911E+01	1.526E+02	4.210E+01	7.223E+01	4.719E+01	5.402E+01	3.839E+02	**9.147E+00**
F3	**Ave**	6.323E+02	6.660E+02	6.257E+02	6.039E+02	6.570E+02	6.730E+02	6.489E+02	6.635E+02	6.346E+02	6.676E+02	6.147E+02	6.742E+02	**6.000E+02**
	Std	1.225E+01	3.818E+00	1.044E+01	5.522E+00	9.728E+00	1.439E+01	6.890E+00	7.679E+00	1.933E+01	7.847E+00	8.259E+00	9.730E+00	**8.590E-03**
F4	**Ave**	8.645E+02	9.531E+02	8.887E+02	**8.548E+02**	9.283E+02	9.373E+02	9.610E+02	8.876E+02	8.890E+02	9.520E+02	8.965E+02	9.965E+02	8.573E+02
	Std	1.737E+01	**8.453E+00**	3.575E+01	1.577E+01	3.283E+01	2.951E+01	1.899E+01	1.592E+01	1.123E+01	1.060E+01	1.531E+01	1.810E+01	1.723E+01
F5	**Ave**	1.672E+03	2.819E+03	2.046E+03	1.523E+03	4.419E+03	4.055E+03	2.761E+03	2.970E+03	2.645E+03	3.633E+03	1.469E+03	4.666E+03	**9.029E+02**
	Std	3.617E+02	1.954E+02	5.914E+02	5.407E+02	1.125E+03	1.674E+03	5.488E+02	3.102E+02	5.191E+02	2.375E+02	3.919E+02	1.103E+03	**3.593E+00**
F6	**Ave**	6.859E+03	2.143E+08	2.711E+05	1.493E+04	9.291E+05	6.981E+06	1.295E+08	2.120E+05	5.772E+03	5.286E+09	**4.325E+03**	6.063E+08	5.934E+03
	Std	5.786E+03	9.305E+07	1.194E+06	8.462E+03	5.024E+06	1.024E+07	9.712E+07	1.001E+05	5.551E+03	1.249E+09	**2.730E+03**	3.640E+08	5.064E+03
F7	**Ave**	2.131E+03	2.202E+03	2.105E+03	2.088E+03	2.217E+03	2.223E+03	2.160E+03	2.190E+03	2.176E+03	2.348E+03	2.093E+03	2.232E+03	**2.042E+03**
	Std	5.422E+01	**1.766E+01**	3.453E+01	4.558E+01	8.677E+01	6.436E+01	2.534E+01	5.948E+01	1.239E+02	3.449E+01	1.911E+01	6.016E+01	1.992E+01
F8	**Ave**	2.270E+03	2.281E+03	2.291E+03	**2.230E+03**	2.369E+03	2.317E+03	2.286E+03	2.277E+03	2.275E+03	2.257E+03	2.238E+03	2.485E+03	2.235E+03
	Std	6.282E+01	1.964E+01	6.574E+01	**5.978E+00**	1.137E+02	9.190E+01	2.699E+01	5.903E+01	6.548E+01	9.290E+00	7.312E+00	1.866E+02	2.442E+01
F9	**Ave**	2.500E+03	2.810E+03	2.506E+03	**2.481E+03**	2.540E+03	2.591E+03	2.633E+03	2.554E+03	2.482E+03	3.477E+03	2.492E+03	2.814E+03	2.483E+03
	Std	1.838E+01	5.053E+01	2.779E+01	**2.448E-01**	5.314E+01	5.446E+01	4.415E+01	4.137E+01	3.081E+00	1.084E+02	5.505E+00	1.429E+02	2.083E+00
F10	**Ave**	3.793E+03	2.706E+03	3.055E+03	2.963E+03	4.605E+03	5.074E+03	2.970E+03	4.495E+03	4.485E+03	6.474E+03	**2.536E+03**	4.909E+03	2.671E+03
	Std	7.000E+02	1.447E+02	9.777E+02	6.115E+02	1.086E+03	1.161E+03	1.238E+03	8.179E+02	1.303E+03	3.167E+02	**7.741E+01**	1.899E+03	2.005E+02
F11	**Ave**	3.065E+03	6.727E+03	3.036E+03	2.928E+03	3.997E+03	3.809E+03	5.006E+03	3.491E+03	3.193E+03	8.519E+03	3.392E+03	6.818E+03	**2.897E+03**
	Std	2.017E+02	2.015E+02	1.761E+02	9.422E+01	1.109E+03	4.444E+02	5.103E+02	7.064E+02	4.892E+02	9.093E+01	4.407E+02	9.215E+02	**6.146E+01**
F12	**Ave**	2.987E+03	3.548E+03	3.019E+03	**2.948E+03**	3.091E+03	3.121E+03	3.087E+03	3.276E+03	2.996E+03	3.579E+03	3.015E+03	3.496E+03	2.956E+03
	Std	4.415E+01	5.860E+01	5.989E+01	**1.231E+01**	9.676E+01	1.454E+02	3.124E+01	1.748E+02	5.466E+01	5.460E+01	3.029E+01	1.584E+02	1.376E+01

4.5 Statistical Analysis

4.5.1 Wilcoxon rank sum test

The Wilcoxon rank sum test [75], a nonparametric method, is utilized to assess the disparities between ESC and its rival algorithms, with findings depicted in **Table 11**. A p-value below 0.05 signifies a significant variance between ESC and the competing algorithm, while a lack of significant difference is accordingly noted. The symbols '+/=/−' denote whether ESC outperforms, matches, or underperforms compared to its competitors.

The Wilcoxon rank sum test results from **Table 11** robustly demonstrate the ESC algorithm's exceptional performance across various dimensions of the CEC 2017 and CEC 2022 benchmarks. ESC shows consistent strength, starting from the 10-dimension tests in CEC 2017, where it outperforms or closely matches its counterparts all the way up to the 100 dimensions. In the 30-dimensional tests, ESC excels with a dominant performance against algorithms such as GQPSO, SCA, and WOA, achieving impressive results like a 29/0/1 score against GQPSO. Despite not always being the top performer in the 50 and 100 dimensions of CEC 2017, ESC's results remain competitive. For instance, it closely challenges DTSMA, which exhibits a marginal lead in these dimensions. In the CEC 2022 benchmarks, ESC extends its exemplary performance, particularly in the 10 and 20 dimensions, by securing perfect or near-perfect scores against most competitors, as seen with algorithms like WOA and CPSOGSA. These results underscore its capability to rapidly converge to optimal solutions, even in scenarios that are considered less complex. Across all tested dimensions, the comprehensive results affirm ESC's versatility and robust design, establishing it as an effective tool for managing and excelling in complex optimization environments.

Table 11 Wilcoxon rank sum test statistical results

ESC VS.	CEC 2017 (Dim=10)	CEC 2017 (Dim=30)	CEC 2017 (Dim=50)	CEC 2017 (Dim=100)	CEC 2022 (Dim=10)	CEC 2022 (Dim=20)
MELGWO	26/2/2	26/2/2	25/2/3	18/5/7	7/4/1	9/3/0
GQPSO	29/0/1	29/0/1	29/0/1	29/0/1	12/0/0	11/1/0
IDBO	24/3/3	24/3/3	23/4/3	17/4/9	9/3/0	10/2/0
DTSMA	15/7/8	15/7/8	8/10/12	7/5/18	6/4/2	5/3/4
CPSOGSA	29/0/1	29/0/1	27/1/2	27/1/2	11/1/0	12/0/0
WOA	30/0/0	30/0/0	28/2/0	29/1/0	11/1/0	12/0/0
SCA	29/1/0	29/1/0	29/1/0	29/1/0	12/0/0	11/1/0
HHO	28/0/2	28/0/2	27/0/3	17/7/6	12/0/0	12/0/0
COA	28/1/1	28/1/1	27/3/0	20/8/2	10/2/0	10/1/1
CDO	29/1/0	29/1/0	29/0/1	29/0/1	12/0/0	12/0/0
OMA	24/2/4	24/2/4	27/0/3	23/4/3	9/1/2	10/2/0
SWO	30/0/0	30/0/0	30/0/0	29/1/0	12/0/0	12/0/0
Overall (+/=/-)	301/17/22	321/17/22	309/23/28	273/37/49	123/16/5	126/13/5

4.5.2 Friedman mean rank test

In this part, we utilize the nonparametric Friedman mean rank test[76] to evaluate and position the performance of ESC relative to competing algorithms on the CEC 2017 and CEC 2022 global optimization suites. The findings from this evaluation are detailed in **Table 12**. The experimental data clearly shows that ESC maintains a high rank throughout. This result underscores the exceptional efficacy of the ESC algorithm we proposed, as demonstrated in the test suites, against the performance of other competing algorithms.

The Friedman mean rank test results from **Table 12** clearly illustrate the impressive performance of the ESC across various dimensions of the CEC 2017 and CEC 2022 benchmarks. ESC ranks first in both the 10 and 30 dimensions of CEC 2017, showcasing its efficacy in lower and mid-range dimensional challenges. In the 50 dimensions of CEC 2017, ESC is highly competitive, securing the second rank, just behind DTSMA, which takes the first place. This slight drop highlights DTSMA’s specific strength in this dimensional setting but still underscores ESC's robust performance across a spectrum of complexities. In the 100 dimensions of CEC 2017, ESC continues to demonstrate strong adaptability and robustness

by ranking second, indicating its capability to maintain high performance even as the complexity of the dimensionality increases. In the CEC 2022 benchmarks, ESC resumes its top position, ranking first in both the 10 and 20 dimensions, further validating its effectiveness and strategic advantages in navigating through dynamic and complex optimization scenarios. Comparatively, while ESC consistently outperforms or ranks near the top, other algorithms such as MELGWO, GQPSO, and IDBO show variable performance across the different dimensions. DTSMA emerges as a strong competitor, particularly excelling in the 50 and 100 dimensions of CEC 2017. Algorithms like CPSOGSA, WOA, and SCA tend to rank in the middle, reflecting their moderate adaptability across the tested dimensions. Overall, the rankings from the Friedman mean rank test underscores the consistent effectiveness of the ESC across multiple dimensions of the CEC 2017 and CEC 2022 benchmarks. ESC's strong performance across different test scenarios illustrates its efficient design and capability to manage complex optimization problems. This performance highlights ESC as a reliable and competent algorithm suitable for a variety of optimization tasks in evolutionary computing.

Table 12 Friedman mean rank test for all test suites.

Suites	CEC 2017								CEC 2022			
Dimensions	10		30		50		100		10		20	
Algorithms	Ave. Rank	Overall Rank	Ave. Rank	Overall Rank	Ave. Rank	Overall Rank	Ave. Rank	Overall Rank	Ave. Rank	Overall Rank	Ave. Rank	Overall Rank
MELGWO	4.684	4	4.353	3	4.154	3	4.179	3	4.147	4	4.745	4
GQPSO	9.982	11	10.327	11	10.084	11	9.872	10	9.919	13	9.625	11
IDBO	5.402	6	4.699	5	4.807	4	4.469	4	5.353	5	5.156	5
DTSMA	3.571	2	2.613	2	2.239	**1**	**2.237**	**1**	2.844	2	2.564	2
CPSOGSA	7.924	7	7.711	8	7.622	8	8.194	8	8.564	9	8.392	9
WOA	8.647	10	9.297	9	8.886	9	8.701	9	8.839	10	9.122	10
SCA	8.306	9	9.328	10	9.727	10	10.300	11	8.233	8	8.325	8
HHO	8.044	8	7.254	7	6.627	7	5.860	6	8.203	7	7.761	7
COA	5.097	5	5.016	6	5.387	5	5.116	5	5.497	6	5.875	6
CDO	11.311	13	11.610	12	11.584	12	10.444	12	11.869	12	11.378	12
OMA	4.058	3	4.692	4	5.419	6	6.196	7	4.089	3	4.575	3
SWO	11.154	12	11.753	13	11.921	13	12.117	13	10.931	11	11.406	13
ESC	**2.818**	**1**	**2.347**	**1**	2.543	2	3.316	2	**2.511**	**1**	**2.292**	**1**

5. Real World Problems

5.1 Engineering Problems

In this section, we use ESC to solve four engineering problems, namely the speed reducer design [77], pressure vessel design [78], tension/compression spring design[79], rolling element bearing design [80]. In this section, the maximum number of iterations T of each algorithm is set to 500. The population N was 30 and ran independently 30 times for comparison. **Figs. 14-17** show the schematics of these four engineering problems respectively.

5.1.1 Speed Reducer Design

The task entails creating a speed reducer for a small aircraft engine. This leads to an optimization problem that is characterized as follows:

Minimize:

$$f(\vec{x}) = 0.7854x_2^2x_1(14.9334x_3 - 43.0934 + 3.3333x_3^2) + 0.7854(x_5x_7^2 + x_4x_6^2) - 1.508x_1(x_7^2 + x_6^2) + 7.477(x_7^3 + x_6^3)$$

subject to:

$$g_1(\vec{x}) = -x_1x_2^2x_3 + 27 \le 0$$
$$g_2(\vec{x}) = -x_1x_2^2x_3^2 + 397.5 \le 0$$
$$g_3(\vec{x}) = -x_2x_6^4x_3x_4^{-3} + 1.93 \le 0$$
$$g_4(\vec{x}) = -x_2x_7^4x_3x_5^{-3} + 1.93 \le 0$$

$$g_5(\vec{x}) = 10x_6^{-3}\sqrt{16.91 \times 10^6 + (745x_4x_2^{-1}x_3^{-1})^2} - 1100 \le 0$$

$$g_6(\vec{x}) = 10x_7^{-3}\sqrt{157.5 \times 10^6 + (745x_5x_2^{-1}x_3^{-1})^2} - 850 \le 0 \quad (15)$$

$$g_7(\vec{x}) = x_2x_3 - 40 \le 0$$

$$g_8(\vec{x}) = -x_1x_2^{-1} + 5 \le 0$$

$$g_9(\vec{x}) = x_1x_2^{-1} - 12 \le 0$$

$$g_{10}(\vec{x}) = 1.5x_6 - x_4 + 1.9 \le 0$$

$$g_{11}(\vec{x}) = 1.1x_7 - x_5 + 1.9 \le 0$$

with bounds:

$$0.7 \le x_2 \le 0.8, 17 \le x_3 \le 28, 2.6 \le x_1 \le 3.6,$$
$$5 \le x_7 \le 5.5, 7.3 \le x_5, x_4 \le 8.3, 2.9 \le x_6 \le 3.9$$

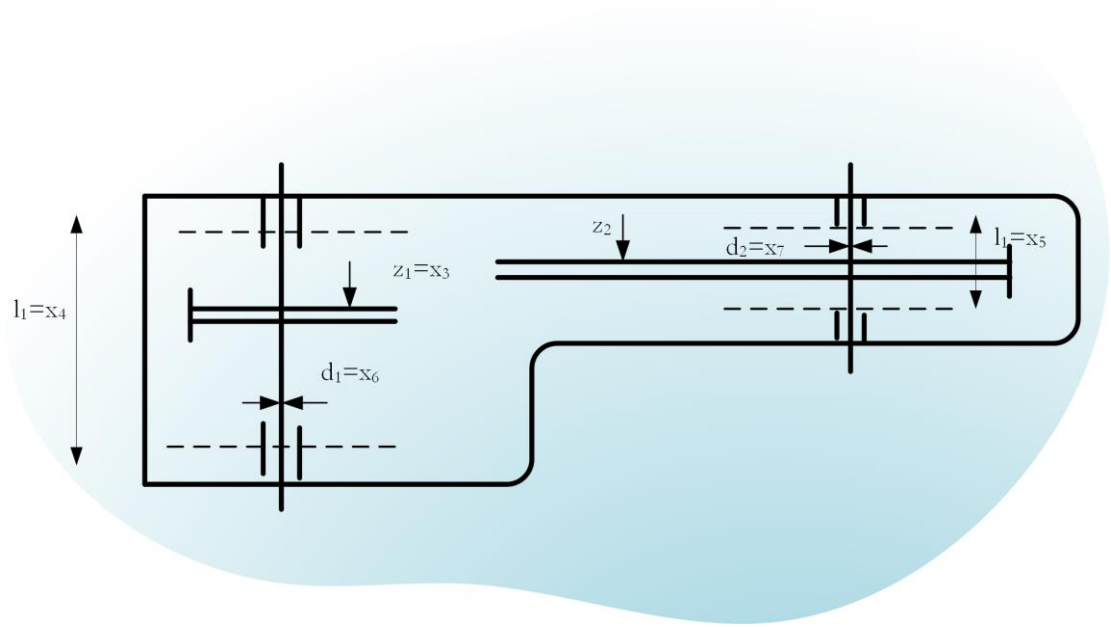

Fig.14 Speed reducer design

Table 13 Comparative results for speed reducer design

Algorithms	Worst	Best	Mean	Median	Std	Friedman Ranking	Wilcoxon
MELGWO	3.004E+03	2.995E+03	2.997E+03	2.996E+03	2.500E+00	3	(+)
GQPSO	6.487E+14	4.184E+03	2.007E+14	1.355E+14	1.861E+14	13	(+)
IDBO	3.311E+03	2.994E+03	3.073E+03	3.047E+03	8.046E+01	6	(+)
DTSMA	2.995E+03	2.994E+03	**2.994E+03**	**2.994E+03**	9.728E-02	**1**	(+)
CPSOGSA	3.016E+03	2.996E+03	3.007E+03	3.007E+03	5.223E+00	5	(+)
WOA	5.673E+03	3.018E+03	3.496E+03	3.177E+03	7.319E+02	10	(+)
SCA	3.221E+03	3.053E+03	3.156E+03	3.171E+03	4.233E+01	9	(+)
HHO	5.117E+03	3.018E+03	3.872E+03	3.824E+03	6.773E+02	11	(+)
COA	3.005E+03	2.995E+03	2.997E+03	2.996E+03	2.693E+00	4	(+)
CDO	3.200E+03	3.065E+03	3.145E+03	3.145E+03	4.234E+01	8	(+)
OMA	4.752E+03	3.013E+03	3.251E+03	3.133E+03	4.161E+02	7	(+)
SWO	2.361E+12	3.102E+03	8.693E+10	3.396E+03	4.319E+11	12	(+)
ESC	**2.995E+03**	**2.994E+03**	2.995E+03	2.994E+03	**8.428E-02**	2	/

In **Table 13**, the ESC algorithm demonstrated exceptional performance, consistently ranking among the top algorithms across all key metrics. ESC achieved one of the best worst-case

performances at 2.995E+03 and matched DTSMA with the most optimal best-case result at 2.994E+03. Its mean value of 2.995E+03 and median of 2.994E+03 were among the lowest, indicating high accuracy and reliability. Moreover, ESC's standard deviation was remarkably small at 8.428E-02, reflecting minimal variability in its results and underscoring its robustness. While DTSMA ranked first in the Friedman test with the lowest standard deviation and nearly identical performance metrics, ESC still demonstrated superior consistency overall, securing second place in the Friedman ranking. MELGWO, COA, and CPSOGSA also performed well, securing third, fourth, and fifth places in the Friedman ranking, respectively, but each showed slightly higher variability than ESC. IDBO, although displaying some strength in finding near-optimal solutions, exhibited greater variability and lower overall consistency. The remaining algorithms, including GQPSO, WOA, SCA, HHO, CDO, OMA, and SWO, all lagged behind ESC, with significantly higher standard deviations and less stable performances. Overall, ESC's impressive results in both accuracy and stability, combined with its high ranking, highlight its effectiveness and reliability in complex optimization landscapes, despite its second-place finish in the Friedman test.

5.1.2 Pressure Vessel Design

The problem of Pressure vessel design aims at minimizing the welding cost, material, and form by optimizing the dimensions such as head thickness (Th), the length of the container excluding the head (L), the thickness of the container (TS), and the inner radius (R). The structural representation is depicted in **Fig. 15**, while the mathematical formulation is provided in Eq. (15).

Minimize:

$$f(\vec{x}) = 0.6224x_1x_3x_4 + 1.7781x_2x_3^2 + 3.1661x_1^2x_4 + 19.84x_1^2x_3$$

subject to:

$$\begin{gathered} g_1(\vec{x}) = -x_1 + 0.0193x_3 \le 0 \\ g_2(\vec{x}) = -x_2 + 0.00954x_3 \le 0 \\ g_3(\vec{x}) = x_4 - 240 \le 0 \\ g_4(\vec{x}) = -\pi x_3^2 x_4 - \frac{4}{3}\pi x_3^3 + 1296000 \le 0 \end{gathered} \tag{16}$$

with bounds:

$$\begin{gathered} 1 \le x_1, x_2 \le 99(integer\ variables) \\ 10 \le x_3, x_4 \le 200 \end{gathered}$$

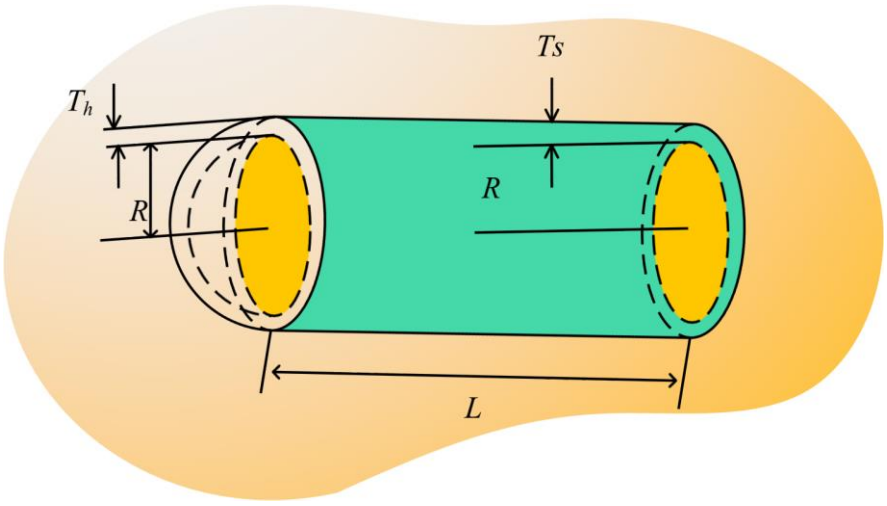

Fig.15 Pressure vessel design

Table 14 Comparative results for pressure vessel design

Algorithms	Worst	Best	Mean	Median	Std	Friedman	Wilcoxon

						Ranking	
MELGWO	1.431E-02	1.267E-02	1.298E-02	1.279E-02	4.048E-04	3	(+)
GQPSO	7.404E+13	1.288E-02	5.085E+12	1.322E-02	1.674E+13	12	(+)
IDBO	1.790E-02	1.271E-02	1.399E-02	1.319E-02	1.828E-03	9	(+)
DTSMA	1.656E-02	1.269E-02	1.356E-02	1.285E-02	1.052E-03	6	(+)
CPSOGSA	1.515E-02	1.267E-02	1.310E-02	1.284E-02	6.403E-04	5	(+)
WOA	1.663E-02	1.267E-02	1.370E-02	1.338E-02	9.771E-04	11	(+)
SCA	1.328E-02	1.279E-02	1.309E-02	1.315E-02	1.575E-04	8	(+)
HHO	1.778E-02	1.267E-02	1.377E-02	1.325E-02	1.276E-03	10	(+)
COA	1.508E-02	1.268E-02	1.309E-02	1.281E-02	6.132E-04	4	(+)
CDO	1.383E-02	1.276E-02	1.309E-02	1.306E-02	2.402E-04	7	(+)
OMA	1.289E-02	1.268E-02	1.276E-02	1.275E-02	5.558E-05	2	(+)
SWO	4.440E-02	1.435E-02	2.312E-02	2.093E-02	7.272E-03	13	(+)
ESC	**1.275E-02**	**1.268E-02**	**1.272E-02**	**1.273E-02**	**1.982E-05**	1	/

In **Table 14**, the ESC algorithm exhibited outstanding performance, securing the top position across all key metrics. ESC achieved the best worst-case result of 1.275E-02 and the most optimal best-case value of 1.268E-02. It also maintained the lowest mean and median values of 1.272E-02 and 1.273E-02, respectively. Furthermore, ESC demonstrated remarkable stability with the smallest standard deviation of 1.982E-05, indicating high consistency and reliability in its results. These factors contributed to ESC's first-place ranking in the Friedman test, outperforming all other algorithms. MELGWO followed closely, ranking third in the Friedman test. While MELGWO showed a solid performance with a mean of 1.298E-02 and a median of 1.279E-02, its higher standard deviation of 4.048E-04 suggested more variability compared to ESC. DTSMA, although ranking higher in the Wilcoxon test, only managed sixth place in the Friedman ranking due to its higher standard deviation of 1.052E-03, reflecting less consistency. Other algorithms like COA and CPSOGSA showed competitive results but could not match the stability and overall performance of ESC.

5.1.3 Tension/compression Spring Design

The primary aim of this problem is to enhance the optimization of tension or compression spring weight. This issue involves four constraints, and the weight calculation relies on three variables: wire diameter (x_1), the mean of coil diameter (x_2), and the count of active coils (x_3). The problem is articulated in the following manner:

Minimize:

$$f(\vec{x}) = x_1^2 x_2 (x_3 + 2)$$

subject to:

$$\begin{aligned} g_1(\vec{x}) &= 1 - \frac{x_2^3 x_3}{71785 x_1^4} \leq 0 \\ g_2(\vec{x}) &= \frac{1}{5108 x_1^2} + \frac{4x_2^2 - x_1 x_2}{12566(x_2 x_1^3 - x_1^4)} - 1 \leq 0 \\ g_3(\vec{x}) &= 1 - \frac{140.45 x_1}{x_2^2 x_3} \leq 0 \\ g_4(\vec{x}) &= \frac{x_1 + x_2}{1.5} - 1 \leq 0 \end{aligned} \tag{17}$$

with bounds:

$$\begin{aligned} 0.05 \leq x_1 \leq 2.00 \\ 0.25 \leq x_2 \leq 1.30 \\ 2.00 \leq x_3 \leq 15.0 \end{aligned}$$

consider:

$$\vec{x} = [x_1, x_2, x_3] = [D, d, P]$$

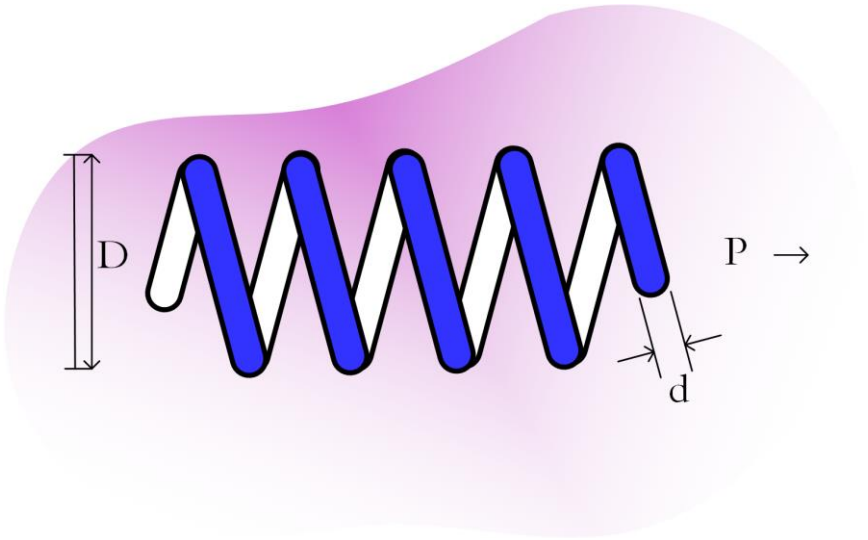

Fig.16 Tension/compression spring design

Table 15 Comparative results for Tension/compression spring design

Algorithms	Worst	Best	Mean	Median	Std	Friedman Ranking	Wilcoxon
MELGWO	7.544E+03	6.060E+03	6.599E+03	6.604E+03	5.140E+02	6	(−)
GGPSO	8.560E+03	6.603E+03	7.455E+03	7.484E+03	5.065E+02	11	(+)
IDBO	7.544E+03	6.060E+03	6.642E+03	6.410E+03	5.455E+02	8	(+)
DTSMA	7.544E+03	6.060E+03	6.452E+03	**6.091E+03**	5.354E+02	2	(−)
CPSOGSA	7.544E+03	**6.060E+03**	6.521E+03	6.390E+03	4.375E+02	7	(+)
WOA	2.606E+04	6.074E+03	9.960E+03	8.175E+03	4.251E+03	12	(+)
SCA	8.998E+03	6.421E+03	7.531E+03	7.331E+03	8.606E+02	10	(+)
HHO	1.186E+04	6.290E+03	7.049E+03	6.891E+03	9.774E+02	9	(+)
COA	7.800E+03	6.060E+03	6.510E+03	6.373E+03	5.077E+02	4	(+)
CDO	6.930E+03	6.182E+03	6.461E+03	6.444E+03	1.876E+02	5	(+)
OMA	7.333E+03	6.060E+03	6.347E+03	6.207E+03	3.754E+02	3	(+)
SWO	2.203E+04	7.604E+03	1.124E+04	1.006E+04	3.676E+03	13	(+)
ESC	**6.187E+03**	6.061E+03	**6.103E+03**	6.097E+03	**3.163E+01**	**1**	/

In **Table 15**, the ESC algorithm once again outperformed all other algorithms. ESC achieved the best worst-case performance of 6.187E+03 and the most optimal best-case result of 6.061E+03. It also demonstrated the lowest mean and median values of 6.103E+03 and 6.097E+03, respectively, coupled with an exceptionally low standard deviation of 3.163E+01, highlighting its minimal variability and consistent performance. This exceptional performance earned ESC the top spot in the Friedman ranking. DTSMA followed in second place, showcasing strong results but with a higher standard deviation of 5.354E+02, indicating less consistency compared to ESC. MELGWO, COA, and CPSOGSA also performed well but exhibited greater variability, as evidenced by their higher standard deviations, which prevented them from surpassing ESC's superior performance.

5.1.4 Rolling Element Bearing Design

This problem aims to enhance the load-bearing ability of a rolling element bearing by utilizing five design variables and parameters. The design variables specified are the pitch diameter (D_m), ball diameter (D_b), coefficients of outer and inner raceway curvature (f_0 andf_1), and the total ball count (Z). The design parameters include e,ε,ζ, K_{Dmax}, and K_{Dmin}, which only appear in the

constraints. These are all treated as variables, combining both the five design variables and five design parameters. The problem is characterized by nine non-linear constraints that reflect manufacturing and kinematic considerations.

Maximize:

$$f(\vec{x}) = \begin{cases} D_b^{1.8} f_c Z^{\frac{2}{3}} \ , if\ D_b \leq 25.4mm \\ 3.647 D_b^{1.4} f_c Z^{\frac{2}{3}} \ , \text{otherwise} \end{cases}$$

subject to:

$$\begin{aligned} g_1(\vec{x}) &= Z - \frac{\phi_0}{2\sin^{-1}(\frac{D_b}{D_m})} - 1 \leq 0 \\ g_2(\vec{x}) &= K_{D_{min}}(\mathrm{D} - \mathrm{d}) - 2D_b \leq 0 \\ g_3(\vec{x}) &= 2D_b - K_{D_{max}}(D - d) \leq 0 \\ g_4(\vec{x}) &= \zeta B_w - D_b \leq 0 \\ g_5(\vec{x}) &= D_m - 0.5(D + d) \geq 0 \\ g_6(\vec{x}) &= (0.5 + e)(D + d) - D_m \geq 0 \\ g_7(\vec{x}) &= \varepsilon D_b - 0.5(D - D_m - D_b) \leq 0 \\ g_8(\vec{x}) &= f_i - 0.515 \geq 0 \\ g_9(\vec{x}) &= f_0 - 0.515 \geq 0 \end{aligned} \tag{18}$$

where:

$$f_c = 37.91\{1 + \{1.04\left(\frac{1-\gamma}{1+\gamma}\right)^{1.72}\left(\frac{f_i(2f_0-1)}{f_0(2f_i-1)}\right)^{0.41}\}^{0.41}\}^{\frac{10}{3}}\}^{-0.3}$$

$$\gamma = \frac{D_b\cos(\alpha)}{D_m}, f_i = \frac{r_i}{D_b}, f_0 = \frac{r_0}{D_b}$$

$$\phi_0 = 2\pi - 2 \times \cos^{-1}\left(\frac{(\frac{D-d}{2} - \frac{3T}{4})^2 + (\frac{D}{2} - \frac{T}{4} - D_b)^2 - (\frac{d}{2} + \frac{T}{4})^2}{2(\frac{D-d}{2} - \frac{3T}{4})(\frac{D}{2} - \frac{T}{4} - D_b)}\right)$$

$$T = D - d - 2D_b, D = 160, d = 90, B_w = 30$$

with bounds:

$$\begin{aligned} &0.5(D + d) \leq D_m \leq 0.6(D + d) \\ &0.15(D - d) \leq D_b \leq 0.45(D - d) \\ &4 \leq Z \leq 50 \\ &0.515 \leq f_i \leq 0.6 \\ &0.515 \leq f_0 \leq 0.6 \\ &0.4 \leq K_{Dmin} \leq 0.5 \\ &0.6 \leq K_{Dmax} \leq 0.7 \\ &0.3 \leq \varepsilon \leq 0.4 \\ &0.02 \leq e \leq 0.1 \\ &0.6 \leq \zeta \leq 0.85 \end{aligned}$$

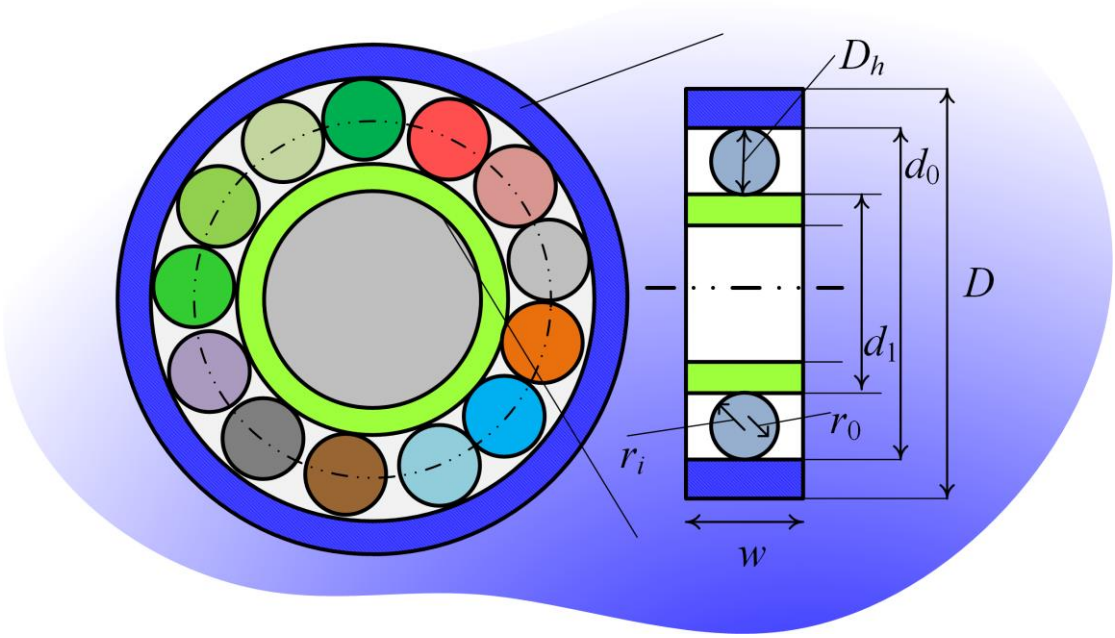

Fig.17 Rolling element bearing design

Table 16 Comparative results for rolling element bearing design

Algorithms	Worst	Best	Mean	Median	Std	Friedman Ranking	Wilcoxon
MELGWO	1.703E+04	1.696E+04	1.698E+04	1.698E+04	2.172E+01	5	(+)
GGPSO	1.086E+16	3.488E+04	3.619E+14	3.489E+04	1.982E+15	13	(+)
IDBO	3.488E+04	1.696E+04	1.843E+04	1.706E+04	3.797E+03	8	(+)
DTSMA	1.696E+04	1.696E+04	1.696E+04	1.696E+04	1.632E-01	2	(+)
CPSOGSA	1.706E+04	1.702E+04	1.705E+04	1.705E+04	1.022E+01	6	(+)
WOA	2.886E+04	1.698E+04	1.882E+04	1.778E+04	2.797E+03	11	(+)
SCA	1.842E+04	1.709E+04	1.743E+04	1.734E+04	3.130E+02	10	(+)
HHO	2.879E+04	1.697E+04	1.806E+04	1.706E+04	2.684E+03	7	(+)
COA	1.702E+04	1.696E+04	1.697E+04	1.696E+04	1.279E+01	4	(+)
CDO	1.759E+04	1.706E+04	1.721E+04	1.717E+04	1.330E+02	9	(+)
OMA	1.832E+04	1.696E+04	1.700E+04	1.696E+04	2.489E+02	3	(+)
SWO	1.277E+15	1.989E+04	4.852E+13	2.796E+04	2.328E+14	12	(+)
ESC	**1.696E+04**	**1.696E+04**	**1.696E+04**	**1.696E+04**	**7.898E-02**	**1**	/

In **Table 16**, the ESC algorithm demonstrated unparalleled performance, achieving the best results across all metrics. ESC achieved the lowest worst-case and best-case results of 1.696E+04, maintaining consistent performance with a mean and median of 1.696E+04. The standard deviation was also the lowest at 7.898E-02, indicating minimal variability and superior stability. These attributes allowed ESC to secure first place in the Friedman ranking, outperforming all other algorithms. DTSMA closely followed ESC, ranking second in the Friedman test. It showed almost identical results to ESC, but with a slightly higher standard deviation, reflecting minor performance variability. MELGWO, COA, and OMA also showed competitive results, but their higher standard deviations indicated less consistency, keeping them behind ESC in overall performance.

5.2 Three-dimensional UAV Path Planning

Path planning problem is one of the well-known cases in engineering domain [81]. This section addresses the path planning issue for UAVs by integrating the optimal criterion with the UAV's constraint cost function. To further demonstrate the ESC algorithm's capability in tackling complex problems, we

examine two distinct UAV 3D path planning scenarios, each defined by different optimization criteria and constraints. In this section, the maximum number of iterations T of each algorithm is set to 500. The population N was 30 and ran independently 30 times for comparison.

5.2.1 Three-dimensional UAV path planning (case 1)

To ensure UAVs operate effectively, the chosen path must meet an optimal standard tailored to the task at hand. Focusing on activities like aerial photography, mapping, and surface inspection, our strategy is to reduce the overall path distance. The UAV's navigation, directed from a ground control station (GCS), is defined by a sequence of n waypoints that it is required to traverse. Each waypoint corresponds to a coordinate-based path node $P_{ij} = (x_{ij}, y_{ij}, z_{ij})$ on the search map. By representing the Euclidean distance between two nodes as $\left\|\overrightarrow{P_{\iota J}P_{\iota,J+1}}\right\|$, the cost F_1 related to the path length can be computed using Eq. (23).[82]

$$F_1(X_i) = \sum_{j=1}^{n-1}\left\|\overrightarrow{P_{\iota J}P_{\iota,J+1}}\right\| \tag{19}$$

In addition to achieving optimality, the planned route must guarantee the UAV's safe operation by steering it clear of potential hazards, typically from obstacles present in the operational zone. Let K represents the set of all threats, each presumed to be depicted by a cylinder with a central coordinate coordinate C_k and radius R_k, as illustrated in **Fig.18**. For a specified path segment $\left\|P_{ij}P_{i,j+1}\right\|$, the corresponding threat cost is directly related to its distance, d_k, from C_k.Taking into account the UAV's diameter, D, and the safety margin, S, around the collision zone, the threat cost F_2 is calculated across waypoints P_{ij} for the obstacle set K as follows:

$$\begin{cases} F_2(X_i) = \sum_{j=1}^{n-1}\sum_{k=1}^{K} T_k(\overrightarrow{P_{\iota J}P_{\iota,J+1}}), \\ T_k(\overrightarrow{P_{\iota J}P_{\iota,J+1}}) = \begin{cases} 0, & if\ d_k > S + D + R_k \\ (S + D + R_k) - d_k, & if\ D + R_k < d_k \le S + D + R_k \\ \infty & if\ d_k \le S + D + R_k \end{cases} \end{cases} \tag{20}$$

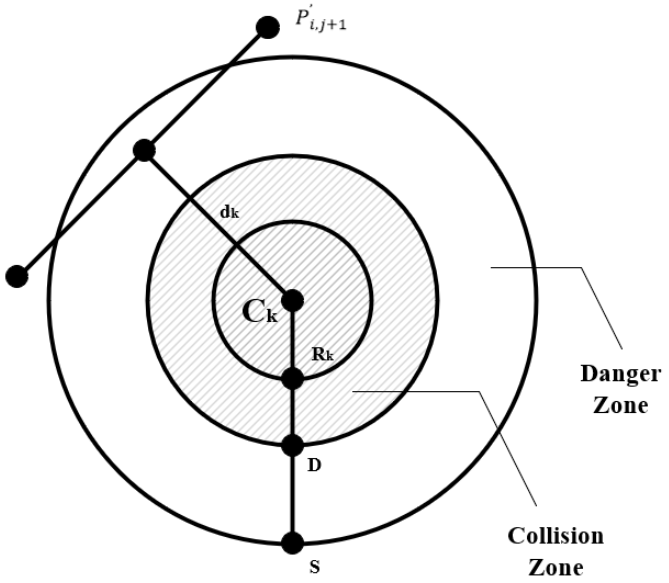

Fig.18 Determination of the threat cost.

It should be noted that the UAV's size determines the diameter D, whereas the distance S is affected by several factors such as the specific application, operational conditions, and accuracy of positioning. For example, in static environments with reliable GPS signals, S may be set at tens of meters, whereas in environments with dynamic obstacles and poor GPS signal strength, S could extend to hundreds of meters to ensure safe positioning.

The flying altitude is usually confined within two defined limits: the minimum and maximum

heights. For instance, in applications like surveying and search tasks, it is crucial to gather visual data using a camera with a designated resolution and field of view, requiring restrictions on the altitude at which the UAV flies. Let $h_{min}$and h_{max} indicate the minimum and maximum heights, respectively. The altitude cost associated with a waypoint $P_{ij}$is calculated as:

$$H_{ij} = \begin{cases} \left| h_{ij} - \dfrac{(h_{\max} + h_{\min})}{2} \right|, & if\ h_{\min} \le h_{ij} \le h_{\max} \\ \infty, & \text{otherwise,} \end{cases} \tag{21}$$

where h_{ij} represents the flight height relative to the ground, as depicted in **Fig.19**. This formulation ensures that H_{ij}maintains the average height while penalizing out-of-range values. Summing H_{ij} for all waypoints yields the altitude cost:

$$F_3(X_i) = \sum_{j=1}^{n} H_{ij} \tag{22}$$

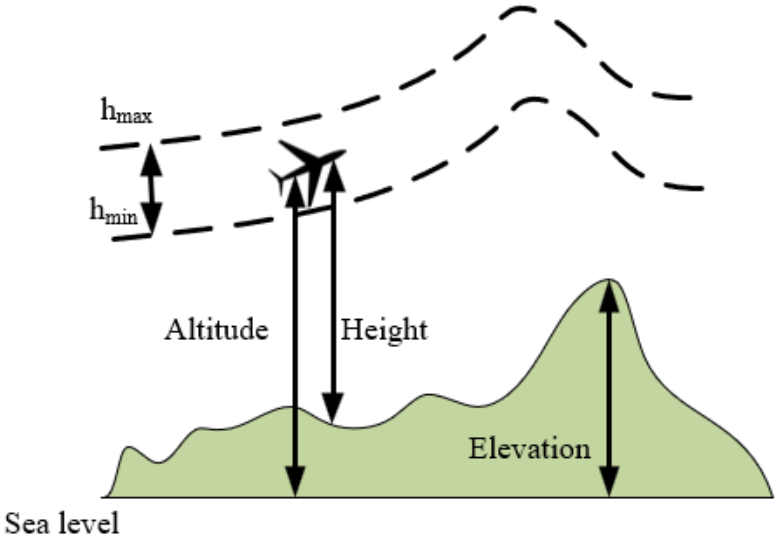

Fig.19 Altitude cost explanation.

The smooth cost evaluates the rates of turning and climbing, which are essential for creating feasible paths. As depicted in **Fig.20**, the turning angle,ϕ_{ij}, represents the angle between two consecutive path segments.$\overrightarrow{P'_{ij}P'_{i,j+1}}$ and $\overrightarrow{P'_{i,j+1}P'_{i,j+2}}$,projected onto the horizontal plane Oxy. Let $\vec{k}$ represent the unit vector along the z-axis, the projected vector can be computed as follows:

$$\overrightarrow{P'_{ij}P'_{i,j+1}} = \vec{k} \times (\overrightarrow{P_{ij}P_{i,j+1}} \times \vec{k}) \tag{23}$$

Therefore, the turning angle is calculated as follows:

$$\phi_{ij} = arctan\left(\frac{\left\|\overrightarrow{P'_{ij}P'_{i,j+1}} \times \overrightarrow{P'_{i,j+1}P'_{i,j+2}}\right\|}{\overrightarrow{P'_{ij}P'_{i,j+1}} \cdot \overrightarrow{P'_{i,j+1}P'_{i,j+2}}}\right) \tag{24}$$

The climbing angle, ψ_{ij}, represents the angle between the path section $\overrightarrow{P_{ij}P_{i,j+1}}$and its projected image $\overrightarrow{P'_{ij}P'_{i,j+1}}$ onto the horizontal plane. It is expressed as:

$$\psi_{ij} = arctan\left(\frac{z_{i,j+1} - z_{ij}}{\left\|\overrightarrow{P'_{ij}P'_{i,j+1}}\right\|}\right) \tag{25}$$

The smooth cost is subsequently calculated as:

$$F_4(X_i) = a_1 \sum_{j=1}^{n-2} \phi_{ij} + a_2 \sum_{j=1}^{n-1} \left|\psi_{ij} - \psi_{i,j-1}\right| \tag{26}$$

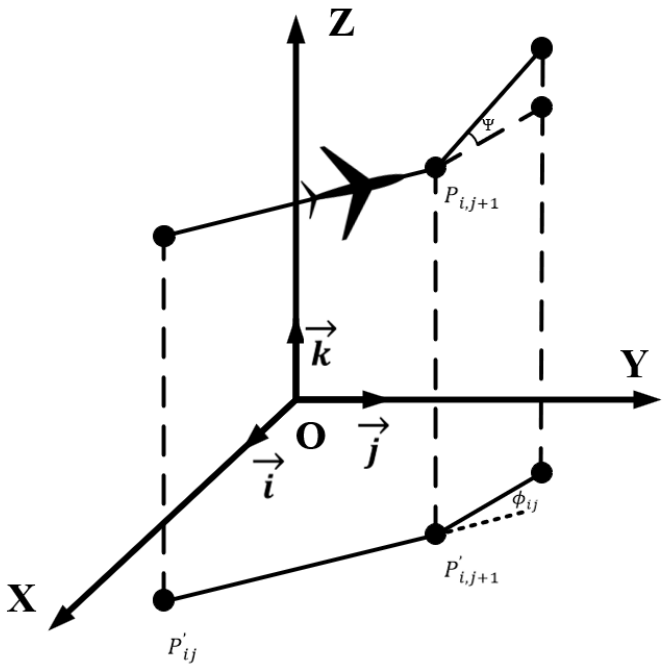

Fig.20 Turning and climbing angle calculation.

where $a_1$and a_2 denote the penalty factors for the turning and climbing angles, respectively. Taking into account the optimality, safety, and feasibility constraints linked to a path X_i, the overall cost function can be formulated as follows:

$$F(X_i) = \sum_{k=1}^{4} b_k F_k(X_i) \quad (27)$$

where b_k is the weight coefficient, and $F_1(X_i)$to $F_4(X_i)$correspondingly represent the costs associated with path length (19), threat (20), flight height (22), and smoothness (26). The decision variable is X_i, comprising the list of n waypoints $P_{ij} = (x_{ij}, y_{ij}, z_{ij})$such that $P_{ij} \epsilon O$, where O denotes the operating space of UAVs. With these definitions established, the cost function F is fully determined and can serve as the input for the path planning process.

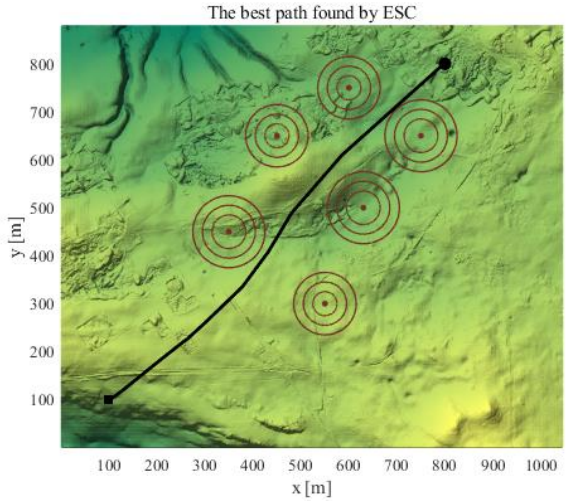

Fig.21 The best path found by ESC (case 1)

In this article, we set b_1,b_2 ,b_3 and b_4 to 5,1,10,1, respectively. The starting point coordinates Start= (100,100,150) and the end point coordinates are set to end= (800,800,150). **Fig.21** shows the results of the optimal path found by the ESC algorithm, and **Fig.22** shows the results of other competitors, which shows that the ESC algorithm can find a shorter and smoother path.

Table 17 Comparative results for Three-dimensional UAV path planning (case 1)

Algorithms	Worst	Best	Mean	Median	Std	Friedman	Wilcoxon

						Ranking	
MELGWO	6.176E+03	5.120E+03	5.456E+03	5.287E+03	3.630E+02	4	(+)
GQPSO	7.094E+03	5.503E+03	6.423E+03	6.414E+03	3.776E+02	9	(+)
IDBO	7.175E+03	5.023E+03	6.060E+03	6.060E+03	6.155E+02	6	(+)
DTSMA	5.886E+03	**5.005E+03**	5.141E+03	**5.066E+03**	2.020E+02	2	(−)
CPSOGSA	7.669E+03	6.654E+03	7.167E+03	7.187E+03	2.955E+02	11	(+)
WOA	9.596E+03	6.184E+03	7.653E+03	7.453E+03	8.637E+02	13	(+)
SCA	7.709E+03	5.426E+03	6.296E+03	6.100E+03	6.518E+02	8	(+)
HHO	9.101E+03	5.498E+03	6.704E+03	6.619E+03	8.633E+02	10	(+)
COA	7.416E+03	5.066E+03	5.896E+03	5.982E+03	5.964E+02	5	(+)
CDO	1.100E+04	5.218E+03	6.539E+03	5.662E+03	1.846E+03	7	(+)
OMA	**5.839E+03**	5.087E+03	5.262E+03	5.180E+03	2.012E+02	3	(+)
SWO	8.403E+03	6.379E+03	7.440E+03	7.531E+03	5.992E+02	12	(+)
ESC	5.901E+03	5.029E+03	**5.110E+03**	5.081E+03	**1.518E+02**	**1**	/

In **Table 17**, the ESC algorithm did not lead in terms of the worst and best performances but topped the Friedman rankings. While ESC's worst performance was not the lowest at 5.901E+03, and its best performance was not the highest at 5.029E+03, it exhibited the best consistency across all metrics. It achieved the lowest mean at 5.110E+03 and the lowest median at 5.081E+03. Significantly, it had the smallest standard deviation of 1.518E+02 among all algorithms, indicating the highest stability and the least variability. DTSMA followed closely but had a higher standard deviation of 2.020E+02, suggesting slightly less consistency. MELGWO, COA, and OMA also performed well, but their higher standard deviations meant they could not match ESC's superior stability and overall performance.

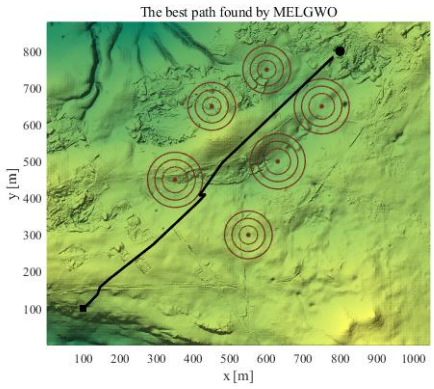
The best path found by MELGWO
y [m]
x [m]

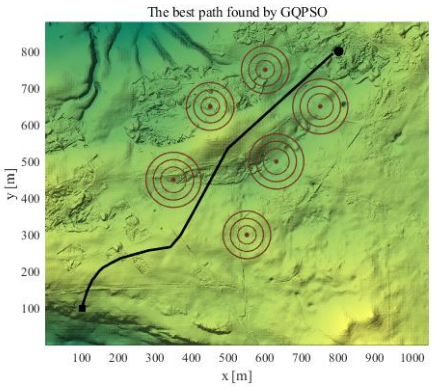
The best path found by GQPSO
y [m]
x [m]

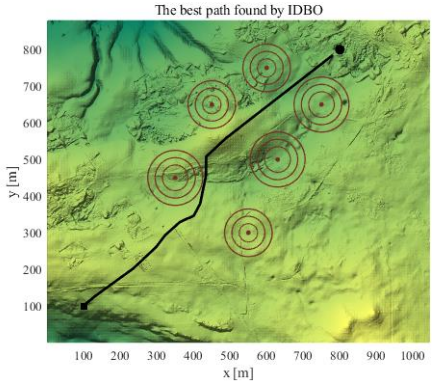
The best path found by IDBO
y [m]
x [m]

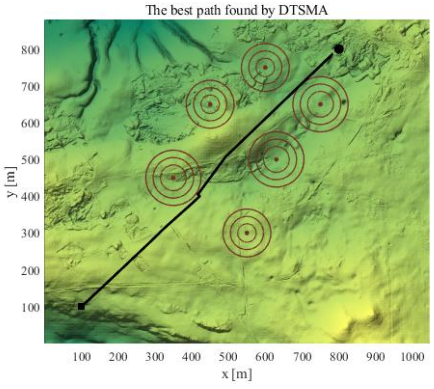
The best path found by DTSMA
y [m]
x [m]

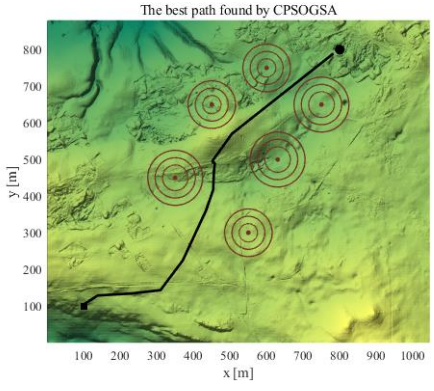
The best path found by CPSOGSA
y [m]
x [m]

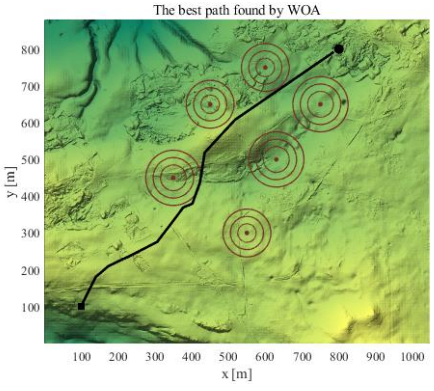
The best path found by WOA
y [m]
x [m]

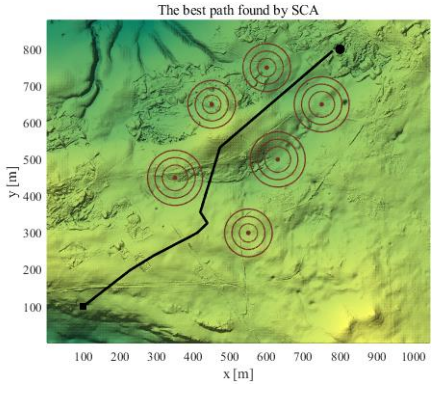
The best path found by SCA
y [m]
x [m]

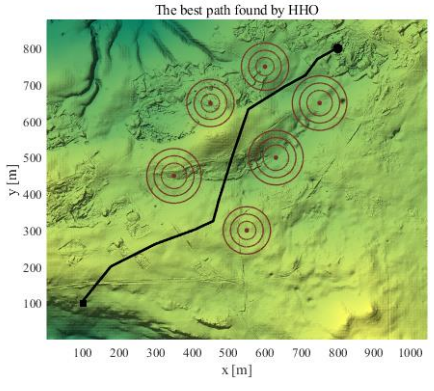
The best path found by HHO
y [m]
x [m]

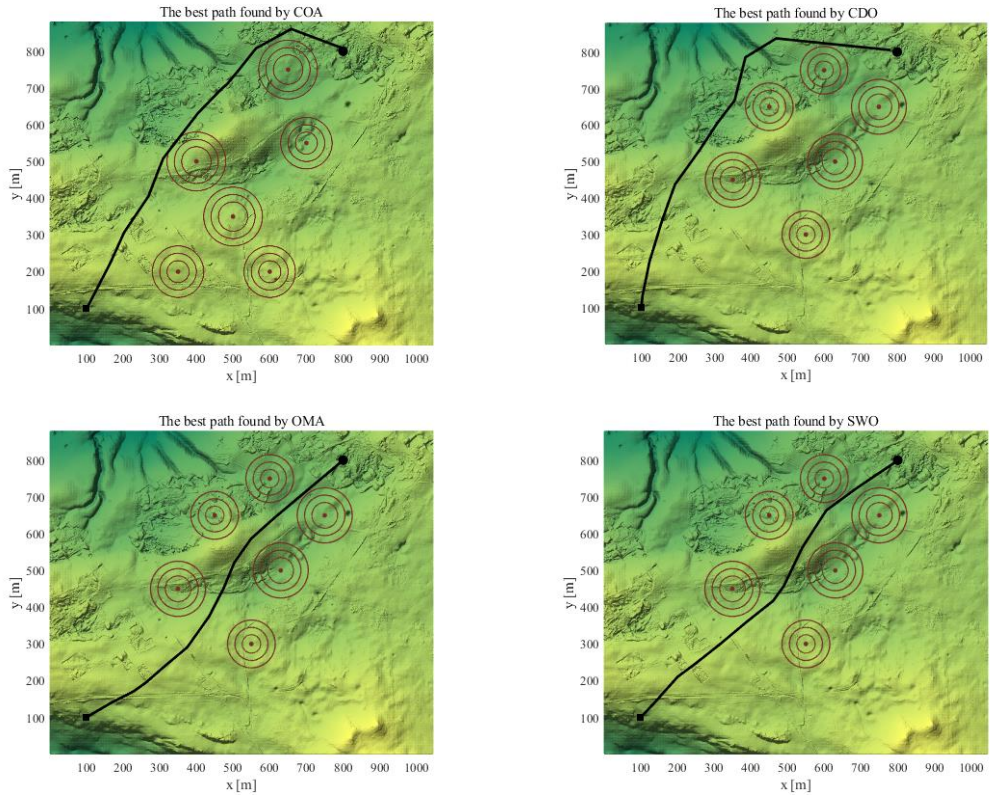

Fig.22 The best path found by other algorithms (case 1)

5.2.2 Three-dimensional UAV path planning (case 2)

Let the starting point of the UAV flight be represented as (x_s, y_s, z_s), and the ending point as (x_e, y_e, z_e). Utilizing cubic spline interpolation, a smooth curve is generated with g discrete points(x_s, y_s, z_s), (x_1, y_1, z_1), …, $(x_{g-1}, y_{g-1}, z_{g-1})$,$(x_e, y_e, z_e)$. This curve is then discretized into a series of points$(h_1, h_2 \ldots h_g)$, where the coordinates of hm are(x_m, y_m, z_m). Therefore, the objective function for this problem can be derived, as expressed in Equation (28).[83]

$$F_{tc} = w_1 \times F_{pc} + w_2 \times F_{hc} + w_3 \times F_{sc} \tag{28}$$

where F_{tc}represents the total cost, F_{pc} denotes the cost of path length, F_{hc} represents the cost associated with the height's standard deviation,F_{sc} indicates the cost of path planning smoothness, and w_i (i = 1,2,3) represents the weight coefficients. The constraints on the weight coefficients are specified in Equation (29).

$$\begin{cases} w_i \geq 0 \\ \sum_{i=1}^{3} w_i = 1 \end{cases} \tag{29}$$

Typically, in UAV flight operations, optimizing path length is critical to saving time and reducing costs while ensuring safety. The mathematical model of UAV is depicted in Equation (30).

$$F_{pc} = \sum_{m=1}^{g-1} \|(x_{m+1}, y_{m+1}, z_{m+1}) - (x_m, y_m, z_m)\|_2 \tag{30}$$

where (x_m, y_m, z_m) represents the mth waypoint in the UAV planning path.

Furthermore, the flight altitude of the UAV significantly affects the control system and safety, necessitating consideration of this factor. Equation (31) represents the mathematical model.

$$F_{hc} = \sqrt{\sum_{m=1}^{g} (z_m - \frac{1}{n} \sum_{k=1}^{g} z_m)^2} \tag{31}$$

Lastly, we must also account for the impact of UAV turning maneuvers, and the corresponding mathematical model is provided in Equation (32).

$$F_{sc} = \sum_{m=1}^{g-2}(arccos(\frac{\varphi_{m+1}\times\varphi_m}{|\varphi_{m+1}|\times|\varphi_m|})) \tag{32}$$

where φ_m represents $(x_{m+1} - x_m, y_{m+1} - y_m, z_{m+1} - z_m)$.

In conclusion, we can derive the model for the UAV path planning optimization problem, as presented in Equation (33).

$$\min_{L} F_{tc}(L)$$
$$s.t. path(L) \notin Ground \cup Obstacle \tag{33}$$

where L represents the feasible flight path, $Ground$ and $Obstacle$ denote the ground and obstacles, respectively. In this paper, we characterize the ground and obstacle sets using Equation (34).

$$z = sin(y+1) + sin(x) + cos(x^2 + y^2) + 2 \times cos(y) + sin(x^2 + y^2) \tag{34}$$

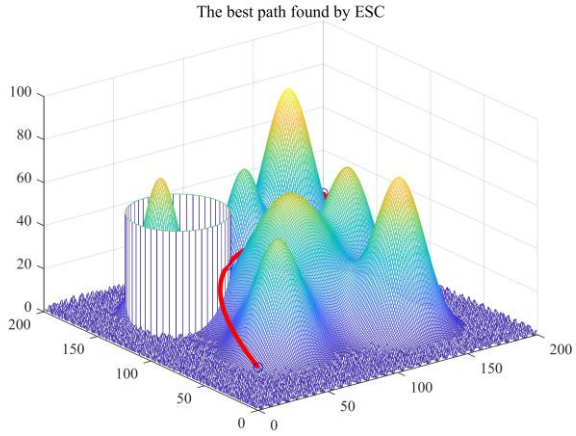

Fig.23 The best path found by ESC (case 2)

In this study, we set w_1,w_2, and w_3 to 0.4, 0.4, and 0.2, respectively, with corresponding Start= (0,0,20) and end= (200, 200, 20). **Fig.23** displays the outcomes of the optimal path found by the ESC algorithm, and **Fig.24** displays the outcomes of the optimal path found by other competitors, which shows that the ESC algorithm can find a shorter path than other algorithms.

Table 18 Comparative results for Three-dimensional UAV path planning (case 2)

Algorithms	Worst	Best	Ave	Median	Std	Friedman Ranking	Wilcoxon
MELGWO	6.755E+02	3.401E+02	4.950E+02	5.144E+02	9.598E+01	3	(+)
GQPSO	6.218E+02	5.388E+02	5.648E+02	5.632E+02	2.103E+01	12	(+)
IDBO	6.172E+02	**2.741E+02**	5.161E+02	5.451E+02	8.685E+01	8	(+)
DTSMA	5.693E+02	3.400E+02	5.062E+02	5.310E+02	7.808E+01	5	(+)
CPSOGSA	7.529E+02	3.400E+02	5.196E+02	5.141E+02	1.237E+02	7	(+)
WOA	7.501E+02	3.631E+02	5.489E+02	5.390E+02	1.109E+02	9	(+)
SCA	7.675E+02	5.220E+02	5.611E+02	5.544E+02	4.305E+01	11	(+)
HHO	6.952E+02	3.518E+02	5.518E+02	5.675E+02	5.980E+01	10	(+)
COA	6.036E+02	3.485E+02	5.064E+02	5.347E+02	7.944E+01	6	(+)
CDO	6.726E+02	4.065E+02	5.119E+02	5.239E+02	5.572E+01	4	(+)
OMA	4.951E+02	3.404E+02	4.166E+02	4.271E+02	6.096E+01	2	(+)
SWO	8.863E+02	5.581E+02	6.971E+02	6.855E+02	9.090E+01	13	(+)
ESC	**3.793E+02**	3.402E+02	**3.457E+02**	**3.419E+02**	**1.009E+01**	**1**	/

In **Table 18**, ESC continued to demonstrate its dominance by ranking first in the Friedman test. ESC achieved the lowest worst-case performance of 3.793E+02 and the most optimal best-case result of 3.402E+02. The algorithm maintained a consistent mean of 3.457E+02 and median of 3.419E+02, with the lowest standard deviation of 1.009E+01, indicating exceptional stability and minimal variability. MELGWO followed in third place, showing strong results but with a higher standard deviation of 9.598E+01, indicating less consistency compared to ESC. DTSMA and COA also showed competitive performance, but their higher standard deviations reflected greater variability, which kept them behind ESC in overall performance.

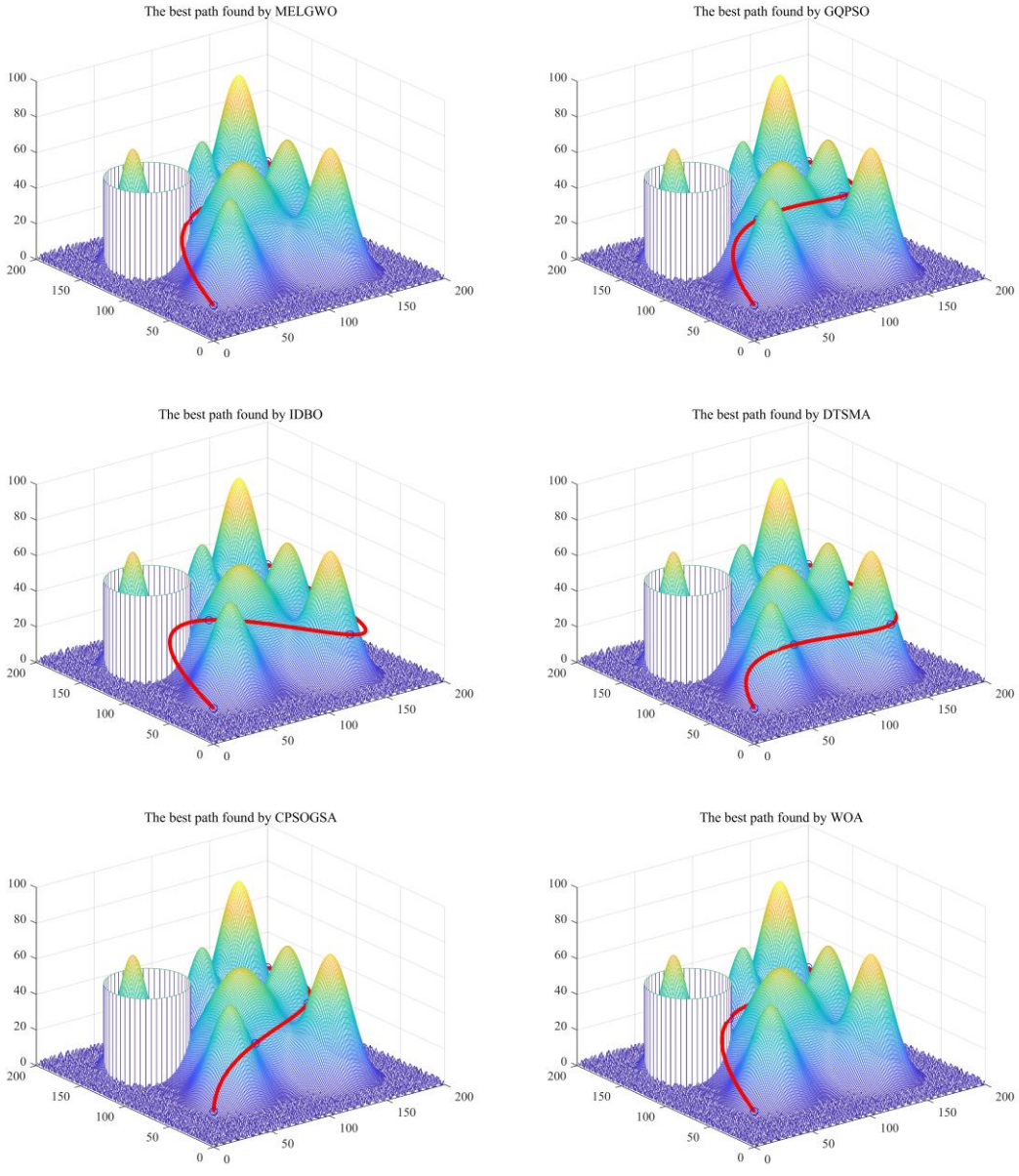

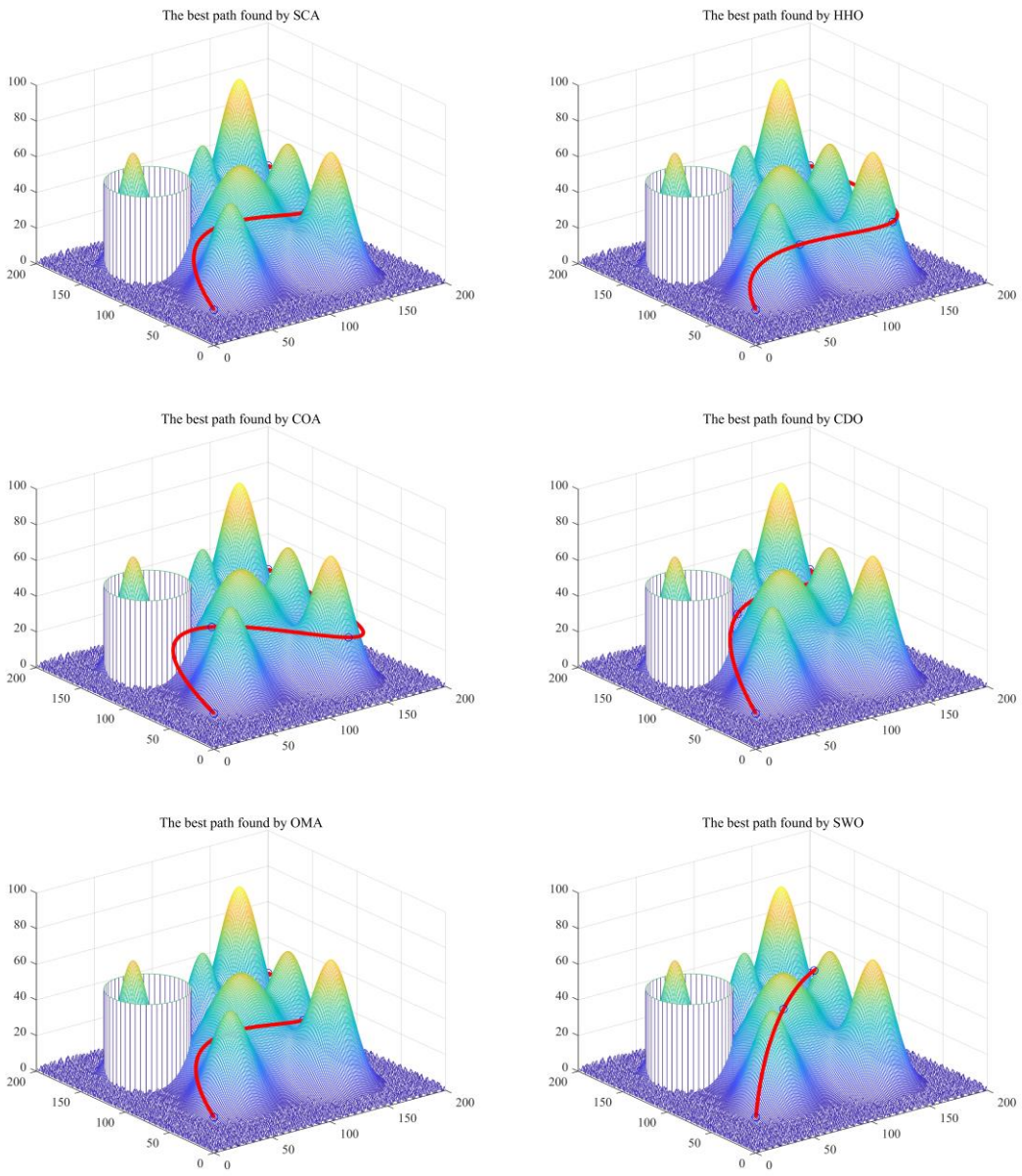

Fig. 24 The best path found by other algorithms (case 2)

6. Conclusion and Prospects

This study introduces a new meta-heuristic algorithm named the ESC as an alternative approach for solving optimization problems. ESC's main inspiration comes from the crowds' interactions during the evacuation process. The algorithm's performance was validated through a series of experiments using 30 benchmark functions from the CEC 2017 test suite with dimensions of 10,30, 50, and 100, and 12 benchmark functions from the CEC 2022 test suite with dimensions of 10 and 20. These tests assess the proposed algorithm's capability for exploration and exploitation and avoid local optima and convergence. Additionally, we conducted a comprehensive qualitative and statistical analysis to verify the effectiveness and robustness of the algorithm. Further, we evaluated the ability of the proposed algorithm to solve practical and Complex problems through four realistic engineering problems and two UAV path planning problems. Our experiments showed that the average performance of ESC is superior to that of MELGWO, GQPSO, IDBO, DTSMA,

CPSOGSA, WOA, SCA, HHO, COA, CDO, OMA, and SWO.

However, despite its strong performance, the ESC algorithm has some limitations. In higher-dimensional optimization problems, the difference in performance between ESC and other competitive algorithms, such as DTSMA, becomes less pronounced. DTSMA even slightly outperforms ESC in certain specific test cases, indicating that ESC may encounter challenges when dealing with more complex, high-dimensional spaces. Additionally, while ESC is effective across a range of benchmark functions and practical problems, its performance can vary depending on the nature of the optimization landscape, particularly in cases where the problem's complexity or constraints are highly specialized.

Future research could extend the capabilities of ESC by developing binary, multi-objective, and dynamic multi-objective variants, which would broaden its applicability to a wider range of optimization problems in engineering and beyond. Additionally, incorporating diverse strategies for managing constraints could provide valuable insights when addressing real-world constrained scenarios. Another promising direction involves improving the current ESC algorithm by integrating strengths from other meta-heuristic algorithms, such as hybridization with evolutionary operators or adaptive mechanisms, to enhance its performance and address any identified shortcomings. Furthermore, exploring the application of ESC in optimizing hyperparameters of machine learning algorithms and integrating it with machine learning frameworks represents a significant opportunity for advancing both the algorithm and its practical utility.

Reference

[1] S. Fu, K. Li, H. Huang, C. Ma, Q. Fan, and Y. Zhu, "Red-billed blue magpie optimizer: a novel metaheuristic algorithm for 2D/3D UAV path planning and engineering design problems," *Artificial Intelligence Review,* vol. 57, no. 6, pp. 1-89, 2024.

[2] J. Tang, H. Duan, and S. Lao, "Swarm intelligence algorithms for multiple unmanned aerial vehicles collaboration: A comprehensive review," *Artificial Intelligence Review,* vol. 56, no. 5, pp. 4295-4327, 2023.

[3] C. Zhang, W. Zhou, W. Qin, and W. Tang, "A novel UAV path planning approach: Heuristic crossing search and rescue optimization algorithm," *Expert Systems with Applications,* vol. 215, pp. 119243, 2023.

[4] A. R. Kashani, C. V. Camp, M. Rostamian, K. Azizi, and A. H. Gandomi, "Population-based optimization in structural engineering: a review," *Artificial Intelligence Review*, pp. 1-108, 2022.

[5] L. Galli, and C.-J. Lin, "A study on truncated newton methods for linear classification," *IEEE Transactions on Neural Networks and Learning Systems,* vol. 33, no. 7, pp. 2828-2841, 2021.

[6] Y.-F. Pu, J.-L. Zhou, Y. Zhang, N. Zhang, G. Huang, and P. Siarry, "Fractional extreme value adaptive training method: fractional steepest descent approach," *IEEE transactions on neural networks and learning systems,* vol. 26, no. 4, pp. 653-662, 2013.

[7] G. Wu, W. Pedrycz, P. N. Suganthan, and R. Mallipeddi, "A variable reduction strategy for evolutionary algorithms handling equality constraints," *Applied soft computing,* vol. 37, pp. 774-786, 2015.

[8] S. Yin, Q. Luo, G. Zhou, Y. Zhou, and B. Zhu, "An equilibrium optimizer slime mould algorithm for inverse kinematics of the 7-DOF robotic manipulator," *Scientific Reports,* vol. 12, no. 1, pp. 9421, 2022.

[9] Q. Luo, S. Yin, G. Zhou, W. Meng, Y. Zhao, and Y. Zhou, "Multi-objective equilibrium optimizer slime mould algorithm and its application in solving engineering problems," *Structural and Multidisciplinary Optimization,* vol. 66, no. 5, pp. 114, 2023.

[10] G. Sun, Z. Xu, H. Yu, X. Chen, V. Chang, and A. V. Vasilakos, "Low-latency and resource-efficient service function chaining orchestration in network function virtualization," *IEEE Internet of Things Journal,* vol. 7, no. 7, pp. 5760-5772, 2019.

[11] G. Ozdemir, and N. Karaboga, "A review on the cosine modulated filter bank studies using meta-heuristic optimization algorithms," *Artificial Intelligence Review,* vol. 52, pp. 1629-1653, 2019.

[12] J.-S. Pan, P. Hu, V. Snášel, and S.-C. Chu, "A survey on binary metaheuristic algorithms and their engineering applications," *Artificial Intelligence Review,* vol. 56, no. 7, pp. 6101-6167, 2023.

[13] M. Abdel-Basset, D. El-Shahat, M. Jameel, and M. Abouhawwash, "Young's double-slit

experiment optimizer: A novel metaheuristic optimization algorithm for global and constraint optimization problems," *Computer Methods in Applied Mechanics and Engineering,* vol. 403, pp. 115652, 2023.
[14] D. Zhu, S. Wang, C. Zhou, S. Yan, and J. Xue, "Human memory optimization algorithm: A memory-inspired optimizer for global optimization problems," *Expert Systems with Applications,* vol. 237, pp. 121597, 2024.
[15] S. Cheng, Q. Qin, J. Chen, and Y. Shi, "Brain storm optimization algorithm: a review," *Artificial Intelligence Review,* vol. 46, pp. 445-458, 2016.
[16] C. Qu, X. Peng, and Q. Zeng, "Learning search algorithm: framework and comprehensive performance for solving optimization problems," *Artificial Intelligence Review,* vol. 57, no. 6, pp. 139, 2024.
[17] J. Liao, Y. a. Ren, and W. Yan, "Kinetic modeling of a leader–follower system in crowd evacuation with collective learning," *Mathematical Models and Methods in Applied Sciences,* vol. 33, no. 05, pp. 1099-1117, 2023.
[18] L. Li, C. Lyu, H. Liu, and L. Lyu, "Safety indication signs-based crowd division and leader selection approach for evacuation guidance," *IEEE Sensors Journal*, 2024.
[19] D. H. Wolpert, and W. G. Macready, "No free lunch theorems for optimization," *IEEE transactions on evolutionary computation,* vol. 1, no. 1, pp. 67-82, 1997.
[20] J. H. Holland, "Genetic algorithms," *Scientific american,* vol. 267, no. 1, pp. 66-73, 1992.
[21] J. Kennedy, and R. Eberhart, "Particle swarm optimization." pp. 1942-1948.
[22] E. Rashedi, H. Nezamabadi-Pour, and S. Saryazdi, "GSA: a gravitational search algorithm," *Information sciences,* vol. 179, no. 13, pp. 2232-2248, 2009.
[23] R. V. Rao, V. J. Savsani, and D. Vakharia, "Teaching–learning-based optimization: an optimization method for continuous non-linear large scale problems," *Information sciences,* vol. 183, no. 1, pp. 1-15, 2012.
[24] Q. Gu, S. Li, W. Gong, B. Ning, C. Hu, and Z. Liao, "L-SHADE with parameter decomposition for photovoltaic modules parameter identification under different temperature and irradiance," *Applied Soft Computing,* vol. 143, pp. 110386, 2023.
[25] J. Brest, M. S. Maučec, and B. Bošković, "iL-SHADE: Improved L-SHADE algorithm for single objective real-parameter optimization." pp. 1188-1195.
[26] K. V. Price, "Differential evolution," *Handbook of optimization: From classical to modern approach*, pp. 187-214: Springer, 2013.
[27] B. H. Abed-alguni, and A. F. Klaib, "Hybrid whale optimisation and β-hill climbing algorithm for continuous optimisation problems," *International Journal of Computing Science and Mathematics,* vol. 12, no. 4, pp. 350-363, 2020.
[28] B. H. Abed-alguni, N. A. Alawad, M. Barhoush, and R. Hammad, "Exploratory cuckoo search for solving single-objective optimization problems," *Soft Computing,* vol. 25, no. 15, pp. 10167-10180, 2021.
[29] B. H. Abed-Alguni, D. Paul, and R. Hammad, "Improved Salp swarm algorithm for solving single-objective continuous optimization problems," *Applied Intelligence,* vol. 52, no. 15, pp. 17217-17236, 2022.
[30] N. A. Alawad, B. H. Abed-alguni, and M. El-ibini, "Hybrid Snake Optimizer Algorithm for Solving Economic Load Dispatch Problem with Valve Point Effect," *The Journal of Supercomputing*, pp. 1-50, 2024.
[31] J. S. Bo Sun, Ming Wei, "3D trajectory planning model of unmanned aerial vehicles (UAVs) in a dynamic complex environment based on an improved ant colony optimization algorithm," *Journal of Nonlinear and Convex Analysis,* vol. 25, no. 4, pp. 737-746, 2024.
[32] H. Kuo, and C. Lin, "Cultural evolution algorithm for global optimizations and its applications," *Journal of applied research and technology,* vol. 11, no. 4, pp. 510-522, 2013.
[33] N. Moosavian, and B. K. Roodsari, "Soccer league competition algorithm: A novel meta-heuristic algorithm for optimal design of water distribution networks," *Swarm and Evolutionary Computation,* vol. 17, pp. 14-24, 2014.
[34] N. Ghorbani, and E. Babaei, "Exchange market algorithm," *Applied soft computing,* vol. 19, pp. 177-187, 2014.
[35] H. Emami, and F. Derakhshan, "Election algorithm: A new socio-politically inspired strategy," *AI Communications,* vol. 28, no. 3, pp. 591-603, 2015.
[36] P. Savsani, and V. Savsani, "Passing vehicle search (PVS): A novel metaheuristic algorithm," *Applied Mathematical Modelling,* vol. 40, no. 5-6, pp. 3951-3978, 2016.
[37] Z.-Z. Liu, D.-H. Chu, C. Song, X. Xue, and B.-Y. Lu, "Social learning optimization (SLO) algorithm paradigm and its application in QoS-aware cloud service composition," *Information*

Sciences, vol. 326, pp. 315-333, 2016.
[38] E. Fadakar, and M. Ebrahimi, "A new metaheuristic football game inspired algorithm." pp. 6-11.
[39] S.-A. Ahmadi, "Human behavior-based optimization: a novel metaheuristic approach to solve complex optimization problems," *Neural Computing and Applications,* vol. 28, no. Suppl 1, pp. 233-244, 2017.
[40] A. M. Fathollahi-Fard, M. Hajiaghaei-Keshteli, and R. Tavakkoli-Moghaddam, "The social engineering optimizer (SEO)," *Engineering applications of artificial intelligence,* vol. 72, pp. 267-293, 2018.
[41] J. Zhang, M. Xiao, L. Gao, and Q. Pan, "Queuing search algorithm: A novel metaheuristic algorithm for solving engineering optimization problems," *Applied Mathematical Modelling,* vol. 63, pp. 464-490, 2018.
[42] M. Kumar, A. J. Kulkarni, and S. C. Satapathy, "Socio evolution & learning optimization algorithm: A socio-inspired optimization methodology," *Future Generation Computer Systems,* vol. 81, pp. 252-272, 2018.
[43] A. Shabani, B. Asgarian, S. A. Gharebaghi, M. A. Salido, and A. Giret, "A new optimization algorithm based on search and rescue operations," *Mathematical Problems in Engineering,* vol. 2019, pp. 1-23, 2019.
[44] A. Tharwat, and T. Gabel, "Parameters optimization of support vector machines for imbalanced data using social ski driver algorithm," *Neural computing and applications,* vol. 32, pp. 6925-6938, 2020.
[45] A. W. Mohamed, A. A. Hadi, and A. K. Mohamed, "Gaining-sharing knowledge based algorithm for solving optimization problems: a novel nature-inspired algorithm," *International Journal of Machine Learning and Cybernetics,* vol. 11, no. 7, pp. 1501-1529, 2020.
[46] Q. Askari, I. Younas, and M. Saeed, "Political Optimizer: A novel socio-inspired meta-heuristic for global optimization," *Knowledge-based systems,* vol. 195, pp. 105709, 2020.
[47] Q. Askari, M. Saeed, and I. Younas, "Heap-based optimizer inspired by corporate rank hierarchy for global optimization," *Expert Systems with Applications,* vol. 161, pp. 113702, 2020.
[48] H. Bouchekara, "Most Valuable Player Algorithm: a novel optimization algorithm inspired from sport," *Operational Research,* vol. 20, no. 1, pp. 139-195, 2020.
[49] M. A. Al-Betar, Z. A. A. Alyasseri, M. A. Awadallah, and I. Abu Doush, "Coronavirus herd immunity optimizer (CHIO)," *Neural Computing and Applications,* vol. 33, pp. 5011-5042, 2021.
[50] H. Emami, "Stock exchange trading optimization algorithm: a human-inspired method for global optimization," *The Journal of Supercomputing,* vol. 78, no. 2, pp. 2125-2174, 2022.
[51] H. Emami, "Anti-coronavirus optimization algorithm," *Soft Computing,* vol. 26, no. 11, pp. 4991-5023, 2022.
[52] H. Givi, and M. Hubalovska, "Skill Optimization Algorithm: A New Human-Based Metaheuristic Technique," *Computers, Materials & Continua,* vol. 74, no. 1, 2023.
[53] H. A. Shehadeh, "Chernobyl disaster optimizer (CDO): a novel meta-heuristic method for global optimization," *Neural Computing and Applications,* vol. 35, no. 15, pp. 10733-10749, 2023.
[54] M. Zhou, H. Dong, P. A. Ioannou, Y. Zhao, and F.-Y. Wang, "Guided crowd evacuation: approaches and challenges," *IEEE/CAA Journal of Automatica Sinica,* vol. 6, no. 5, pp. 1081-1094, 2019.
[55] J. Zhang, J. Zhu, P. Dang, J. Wu, Y. Zhou, W. Li, L. Fu, Y. Guo, and J. You, "An improved social force model (ISFM)-based crowd evacuation simulation method in virtual reality with a subway fire as a case study," *International Journal of Digital Earth,* vol. 16, no. 1, pp. 1186-1204, 2023.
[56] Z. Li, H. Huang, N. Li, M. L. C. Zan, and K. Law, "An agent-based simulator for indoor crowd evacuation considering fire impacts," *Automation in Construction,* vol. 120, pp. 103395, 2020.
[57] M. Haghani, E. Cristiani, N. W. Bode, M. Boltes, and A. Corbetta, "Panic, irrationality, and herding: three ambiguous terms in crowd dynamics research," *Journal of advanced transportation,* vol. 2019, 2019.
[58] M. A. Lopez-Carmona, and A. P. Garcia, "Adaptive cell-based evacuation systems for leader-follower crowd evacuation," *Transportation research part C: emerging technologies,* vol. 140, pp. 103699, 2022.
[59] W. Xie, E. W. M. Lee, and Y. Y. Lee, "Simulation of spontaneous leader–follower behaviour in crowd evacuation," *Automation in Construction,* vol. 134, pp. 104100, 2022.
[60] J. Wang, M. Chen, W. Yan, Y. Zhi, and Z. Wang, "A utility threshold model of herding–panic behavior in evacuation under emergencies based on complex network theory," *Simulation,* vol. 93, no. 2, pp. 123-133, 2017.

[61] A. A. Heidari, S. Mirjalili, H. Faris, I. Aljarah, M. Mafarja, and H. Chen, “Harris hawks optimization: Algorithm and applications,” *Future Generation Computer Systems,* vol. 97, pp. 849-872, 2019/08/01/, 2019.
[62] S. Li, H. Chen, M. Wang, A. A. Heidari, and S. Mirjalili, “Slime mould algorithm: A new method for stochastic optimization,” *Future Generation Computer Systems,* vol. 111, pp. 300-323, 2020/04/03/, 2020.
[63] G. Wu, R. Mallipeddi, and P. Suganthan, “Problem definitions and evaluation criteria for the CEC 2017 competition and special session on constrained single objective real-parameter optimization,” *Nanyang Technol. Univ., Singapore, Tech. Rep*, pp. 1-18, 2016.
[64] R. Biedrzycki, J. Arabas, and E. Warchulski, "A version of NL-SHADE-RSP algorithm with midpoint for CEC 2022 single objective bound constrained problems." pp. 1-8.
[65] R. Ahmed, G. P. Rangaiah, S. Mahadzir, S. Mirjalili, M. H. Hassan, and S. Kamel, “Memory, evolutionary operator, and local search based improved Grey Wolf Optimizer with linear population size reduction technique,” *Knowledge-Based Systems,* vol. 264, pp. 110297, 2023.
[66] L. dos Santos Coelho, “Gaussian quantum-behaved particle swarm optimization approaches for constrained engineering design problems,” *Expert Systems with Applications,* vol. 37, no. 2, pp. 1676-1683, 2010.
[67] Y. Li, K. Sun, Q. Yao, and L. Wang, “A dual-optimization wind speed forecasting model based on deep learning and improved dung beetle optimization algorithm,” *Energy,* vol. 286, pp. 129604, 2024.
[68] S. Yin, Q. Luo, Y. Du, and Y. Zhou, “DTSMA: Dominant swarm with adaptive t-distribution mutation-based slime mould algorithm,” *Mathematical Biosciences and Engineering,* vol. 19, no. 3, pp. 2240-2285, 2022.
[69] S. A. Rather, and P. S. Bala, “A hybrid constriction coefficient-based particle swarm optimization and gravitational search algorithm for training multi-layer perceptron,” *International Journal of Intelligent Computing and Cybernetics,* vol. 13, no. 2, pp. 129-165, 2020.
[70] S. Mirjalili, and A. Lewis, “The whale optimization algorithm,” *Advances in engineering software,* vol. 95, pp. 51-67, 2016.
[71] R. M. Rizk-Allah, and A. E. Hassanien, “A comprehensive survey on the sine–cosine optimization algorithm,” *Artificial Intelligence Review,* vol. 56, no. 6, pp. 4801-4858, 2023.
[72] H. Jia, H. Rao, C. Wen, and S. Mirjalili, “Crayfish optimization algorithm,” *Artificial Intelligence Review,* vol. 56, no. Suppl 2, pp. 1919-1979, 2023.
[73] M.-Y. Cheng, and M. N. Sholeh, “Optical microscope algorithm: A new metaheuristic inspired by microscope magnification for solving engineering optimization problems,” *Knowledge-Based Systems,* vol. 279, pp. 110939, 2023.
[74] M. Abdel-Basset, R. Mohamed, M. Jameel, and M. Abouhawwash, “Spider wasp optimizer: A novel meta-heuristic optimization algorithm,” *Artificial Intelligence Review*, pp. 1-64, 2023.
[75] F. Wilcoxon, "Individual comparisons by ranking methods," *Breakthroughs in Statistics: Methodology and Distribution*, pp. 196-202: Springer, 1992.
[76] Y. Ç. Kuyu, and F. Vatansever, “GOZDE: A novel metaheuristic algorithm for global optimization,” *Future Generation Computer Systems,* vol. 136, pp. 128-152, 2022.
[77] M. Pant, R. Thangaraj, and V. Singh, “Optimization of mechanical design problems using improved differential evolution algorithm,” *International Journal of Recent Trends in Engineering,* vol. 1, no. 5, pp. 21, 2009.
[78] Z. Wang, Q. Luo, and Y. Zhou, “Hybrid metaheuristic algorithm using butterfly and flower pollination base on mutualism mechanism for global optimization problems,” *Engineering with Computers,* vol. 37, pp. 3665-3698, 2021.
[79] L. Deng, and S. Liu, “A multi-strategy improved slime mould algorithm for global optimization and engineering design problems,” *Computer Methods in Applied Mechanics and Engineering,* vol. 404, pp. 115764, 2023.
[80] R. V. Rao, V. J. Savsani, and D. P. Vakharia, “Teaching–learning-based optimization: a novel method for constrained mechanical design optimization problems,” *Computer-aided design,* vol. 43, no. 3, pp. 303-315, 2011.
[81] C. Zhu, “Intelligent robot path planning and navigation based on reinforcement learning and adaptive control,” *J. Logist. Inform. Serv. Sci,* vol. 10, no. 3, pp. 235-248, 2023.
[82] M. D. Phung, and Q. P. Ha, “Safety-enhanced UAV path planning with spherical vector-based particle swarm optimization,” *Applied Soft Computing,* vol. 107, pp. 107376, 2021.
[83] V. Roberge, M. Tarbouchi, and G. Labonté, “Comparison of parallel genetic algorithm and particle swarm optimization for real-time UAV path planning,” *IEEE Transactions on industrial*

informatics, vol. 9, no. 1, pp. 132-141, 2012.